



**БЪЛГАРСКА АКАДЕМИЯ НА НАУКИТЕ
ИНСТИТУТ ПО ПОЛИМЕРИ**



**СТРУКТУРНИ ФОНДОВЕ Оперативна програма
"Развитие на човешките ресурси"**

Договор № BG051PO001/07/3.3-02/51 "Подкрепа за развитие и реализация
на докторанти, пост-докторанти и млади учени в областта на
полимерната химия, физика и инженерство"

**ВТОРА ПОСТЕРНА СЕСИЯ
"МЛАДИТЕ УЧЕНИ В СВЕТА
НА ПОЛИМЕРИТЕ"**

3 юни 2010 г.

ABSTRACT

The synthesis of three novel α -aminophosphonic acid diesters *N,N*-dimethyl-[*N*-methyl(diethoxyphosphonyl)-(2-furyl)]-1,3-diaminopropane, *p*-[*N*-methyl(diethoxyphosphonyl)-(2-furyl)]toluidine and *p*-[*N*-methyl(diethoxyphosphonyl)-(4-dimethylaminophenyl)]toluidine through an addition of diethyl phosphite to *N,N*-dimethyl-*N*-furfurylidene-1,3-diaminopropane, *N*-furfurylidene-*p*-toluidine and *N*-(4-dimethylaminobenzylidene)-*p*-toluidine, respectively, are reported.[1] The α -aminophosphonates have been characterized by elemental analysis, IR and NMR (^1H , ^{13}C and ^{31}P) spectra. [2] The pharmacological importance and utility of aminophosphonate derivatives have stimulated extensive studies on various aspects of their chemistry and biochemistry: synthetic routes, structural and spectral characterization and evaluation of their biological property.[3] The compounds were tested for antiproliferative effects against 4 human leukemic cell lines, namely LAMA-84, K-562 (chronic myeloid leukemias), HL-60 (acute promyelocyte leukemia) and HL-60/Dox (multi-drug resistant sub-line, characterized by overexpression of MRP-1 (ABC-C1)) and were found to exert concentration dependent cytotoxic effects. A representative aminophosphonate compound was shown to induce oligonucleosomal DNA fragmentation which implies that the induction of cell death through apoptosis plays important role for its cytotoxicity mode of action.

INTRODUCTION

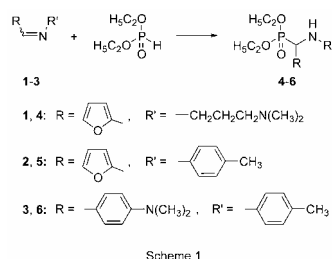
Aminophosphonic acid derivatives constitute an important class of organophosphorus compounds on account of their versatile biological activity. The generally low mammalian toxicity of these compounds makes them attractive for use in agriculture and medicine. Numerous of them possess antifungal, pesticidal, herbicidal and plant growth regulatory activity and are of particular interest for agrochemistry. Aminophosphonic acids are structural analogues of natural α -aminocarboxylic acids, and have been found to act as inhibitors of specific enzymes as HIV protease, thrombin and human collagenase, and to suppress the growth of various tumors and viruses.[4] Moreover, some aminophosphonic acids inhibit bone resorption, delay the progression of bone metastases, exert direct cytostatic effects on a variety of human tumor cells and have found clinical application in the treatment of bone disorders and cancer.[5] Polymeric aminophosphonate analogues are used as bone seeking radiopharmaceuticals.

Among the numerous synthetic approaches to aminophosphonates, the addition of dialkyl phosphites to Schiff bases in the presence of sodium alkoxide and Lewis acids is the most convenient procedure.

Chemistry

The novel α -aminophosphonic acid diesters - *N,N*-dimethyl-[*N*-methyl(diethoxyphosphonyl)-(2-furyl)]-1,3-diaminopropane (**4**), *p*-[*N*-methyl(diethoxyphosphonyl)-(2-furyl)]toluidine (**5**) and *p*-[*N*-methyl(diethoxyphosphonyl)-(4-dimethylaminophenyl)]toluidine (**6**), were synthesized through addition of diethyl phosphite to the azomethine bond of the Schiff bases *N,N*-dimethyl-*N*-furfurylidene-1,3-diaminopropane (**1**), *N*-furfurylidene-*p*-toluidine (**2**) and *N*-(4-dimethylaminobenzylidene)-*p*-toluidine (**3**), according to the Scheme 1.

The reaction was carried out using NaOC_2H_5 and CdI_2 as catalysts, as well as without catalyst. The addition of the phosphite to the Schiff bases was controlled by IR spectroscopy. In the presence of the catalysts the aminophosphonates **4** - **6** were obtained in good yields for 3 h, while in the absence of catalyst the reaction time was longer - up to 8 h. The products **4** and **5** are oils and **6** is crystalline solid. They are soluble in methanol, ethanol, benzene, chloroform.



The synthesized compounds **4** - **6** gave satisfactory elemental analyses, and their molecular structure was confirmed by IR and ^1H , ^{13}C and ^{31}P NMR spectroscopy

The IR spectra of **4** - **6** showed the expected absorption bands at 3375-3306 and 1250 - 1239 cm^{-1} , which are attributed to NH and P=O stretching vibrations, respectively

Scheme 1

Pharmacology

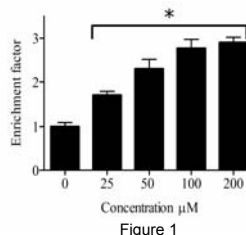
The Schiff bases **2** and **3** and the aminophosphonates **4-6** were assessed for cytotoxicity against a panel of cell lines representative for some important types of human leukemia including the multidrug-resistant model HL-60/Dox. All compounds exerted concentration - dependent antiproliferative effects after 72 h exposure which enabled the construction of concentration-response curves and the calculation of the corresponding IC_{50} values summarized in Table 1.

Cells line	IC_{50} value (μM) ^a					
	1	2	3	4	5	Cisplatin
LAMA-84 ^b	39.9	251.9	> 400.0	71.2	119.4	18.2
K-562 ^b	29.9	212.9	352.9	22.9	42.4	25.7
HL-60 ^c	> 400.0	> 400.0	163.4	74.8	> 400.0	7.8
HL-60/Dox ^{c,d}	68.6	226.1	190.0	115.2	107.2	14.5

Table 1. Comparative cytotoxic activity of compounds **2-6** vs. cis - DDP in a panel of tumor cell lines after 72 h (MTT-dye reduction assay).

As evident from the cytotoxicity data the Schiff base **2** and the corresponding aminophosphonate derivative **5** proved to be the most potent cytotoxic agents, which implies that the presence of both furyl- and *N*-tolyl moieties is an important prerequisite for optimal activity for these compounds. All tested compounds were generally less active as compared to the referent anticancer drug cisplatin, although compound **5** showed superior activity against K-562 cells.

The level of internucleosomal DNA fragmentation, a key feature of apoptotic cell death after 24 h treatment with varying concentrations of the newly synthesized aminophosphonate compound **5** is presented in Figure 1.



As evident from the results obtained, the exposure of LAMA-84 with the tested agent evoked concentration-dependent increase of the proportion of apoptotic cells as evidenced by the enrichment of cytosol with oligonucleosomal DNA-fragments. These data unambiguously indicate that the induction of apoptosis plays crucial role in the cytotoxic mode of action of the aminophosphonates under investigation.

CONCLUSION

✓ The starting Schiff bases **2** and **3** and the α -aminophosphonates **4** - **6** were evaluated for cytotoxicity against 4 human leukemic cell lines, including the multi-drug resistant model HL-60/Dox.

✓ The cytotoxicity data obtained revealed that the Schiff base **2** and the corresponding aminophosphonate **5** provided to be the most potent cytotoxic agents among the tested compounds.

✓ It implies that the presence of both furyl and *N*-tolyl moieties is an important prerequisite for optimal activity in these substances.

✓ The studied compounds were far less active as compared to the referent anticancer drug cisplatin, except the aminophosphonate **5**, which effect towards K-562 cell line was comparable with the referent.

✓ The Schiff bases **2** and **3** and aminophosphonate **6** failed to exert any significant antiproliferative effects against the sensitive cell line HL-60.

✓ The ability of these compounds to selectively inhibit MRP-1 expressing HL-60/Dox indicates that they could be considered as promising leads for further development of agents active in chemotherapy refractory malignant diseases.

✓ The compound was shown to induce oligonucleosomal DNA fragmentation which implies that the induction of cell death through apoptosis plays an important role for its cytotoxicity mode of action.

✓ Taken together the biological data give us reason to consider the presented Schiff bases and α -aminophosphonates as a novel class of antiproliferative agents. The observed collateral sensitivity of multi-drug resistant cancer cell lines and the established activity of a representative compound to trigger apoptosis at sub-cytotoxic levels suggest that these compounds necessitate further more detailed pharmacological evaluation.

References:

- [1] I. Kraicheva, Iv. Tsacheva, K. Troev, *Bulg. Chem. Commun.*, **2008**, 40, 54.
- [2] I. Kraicheva, P. Finocchiaro, S. Failla, *Phosphorus, Sulfur, and Silicon*, **2004**, 179, 2345.
- [3] E. Naydenova, M. Topashka-Ancheva, P. Todorov, Ts. Yordanova, K. Troev, *Bioorganic & Medicinal Chemistry*, **2006**, 14, 2190.
- [4] E. Naydenova, K. Troev, M. Topashka-Ancheva, G. Hägele, I. Ivanov, A. Krill, *Amino Acids*, **2007**, 33, 695.
- [5] D. M. Mizrahi, T. Waner, Y. Segall, *Phosphorus, Sulfur and Silicon*, 2001, 173, 1.



Acknowledgements: A. Bogomilova and I. Tsacheva thank the European Social Fund, Structural Funds, Operational Programme "Human Resources Development" for financial support in the frame of Grant No. BG051PO01/07/3.3-02/51.

СИМУЛАЦИИ НА ЕЛЕКТРИЧНИ ПОЛЕТА И ДИЗАЙН НА КОЛЕКТОРИ ЗА ЕЛЕКТРООВЛАКНЯВАНЕ

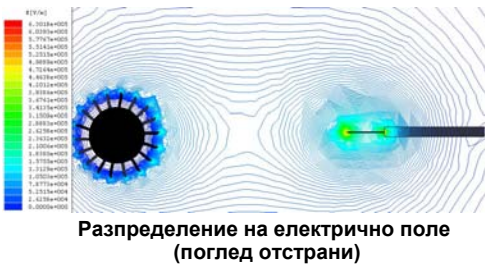
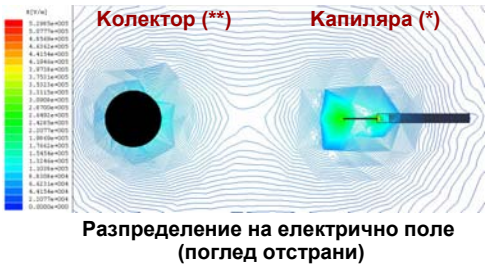


А. Тончева, И. Рашков*, Д. Панева, Н. Манолова,
 Лаборатория биологично активни полимери, Институт по полимери,
 Българска Академия на Науките, 1113 София

Електроовлакняването е върхова технология за получаване на микро- и нановлакнести материали. Класическата лабораторна апаратура включва три основни елемента: източник на високо напрежение, резервоар (спринцовка с капиляра^(*)) и колектор^(**), върху който се отлагат получените влакна. Разпределението на приложеното електрично поле е ключов фактор за насоченото отлагане на влакната, за тяхната самоорганизацията в снопове или прежди. **Целта на изследването** е теоретичното предсказване на електричното поле в апаратури с различен дизайн и сравнението с експерименталните резултати, за да се намерят условията за получаване на нановлакнести материали с желана морфология и организация.

Видове въртящи се колектори

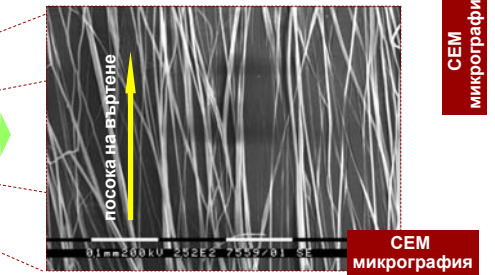
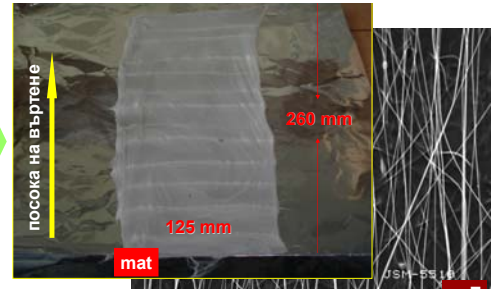
Теоретично симулиране на електрично поле. Програма - Ansoft Maxwell SV 2D (USA)



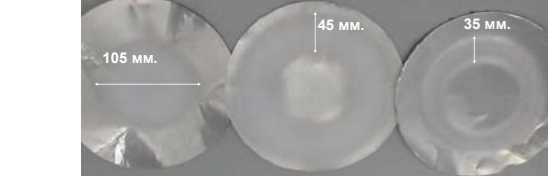
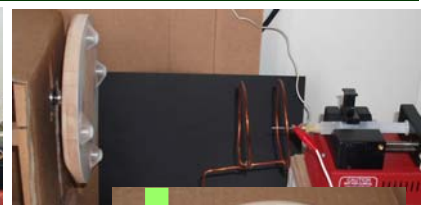
Дизайн на колектора



Нановлакнести материали и изделия



Допълнителни устройства към апаратурата за електроовлакняване



Получаване на нановлакнести изделия с желана форма и размери. Превръзка за око (с формата на контактна леща)

Игленият електрод спомага самоорганизацията на влакната в снопове

Включването на фокусиращо устройство, позволява да се контролира площта, върху която се отлагат нановлакнестите материали

Авторите благодарят за финансовата помощ на ФНИ (Договор "Идеи", DO 02-237/08). А.Т. и Д.П. благодарят на Европейският социален фонд, Структурни фондове, Оперативна програма "Развитие на човешките ресурси" за финансовата помощ (Договор BG051P0001/07/3.3-02/51)

За контакти: rashkov@polymer.bas.bg



Имобилизиране на уреаса в хибридни гелове конструирани от ядро от поли (2-хидрокси-етилден метакрилат) и обвивка от поли (етиленов оксид)

Д. Желева¹, П. Петров¹, Х. Цветанов¹, Я. Топалова², Р. Димков²

1. Лаборатория Полимеризационни процеси, Институт по полимери, БАН
2. Катедра "Обща и приложна хидробиология", Биологически факултет, СУ "Св. Климент Охридски"

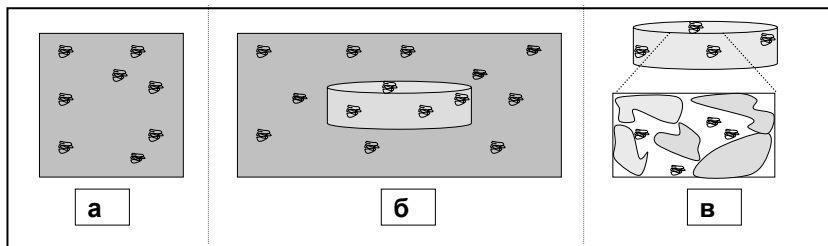
1. Увод

Уреазите са широко разпространени в природата ензими, които катализират хидролизата на урея до амониак и въглеродна киселина. Тези ензими намират приложение като биосензори в медицината, хранително-вкусовата промишленост, строителство и др. За да се оптимизира използването им е необходимо да бъдат имобилизирани.

Настоящото изследване представя изработването на оригинален метод за нековалентно имобилизиране на уреазата и ефективността му на задържане.

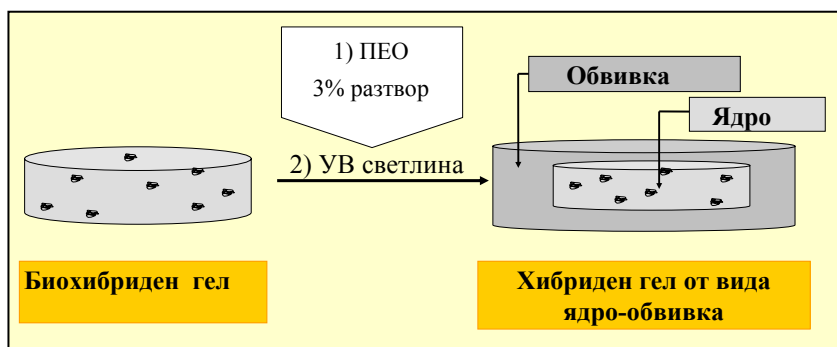
2. Стратегия

2.1. Получаване на биохибридни гелове



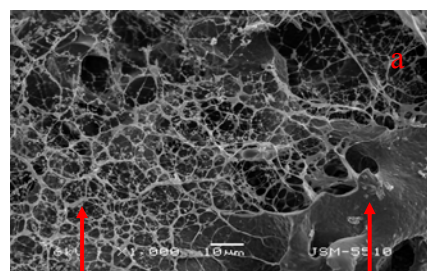
Фигура 1. Схематично представяне на процеса на имобилизиране на уреазата в носители от поли (2-хидроксиетил метакрилат) (пХЕМА): а – разтвор на уреазата (1,5 мг/мл); б – имобилизиране на ензимните молекули в пХЕМА криогел; в – биохибриден гел.

2.2. Получаване на хибриден гел от вида ядро-обвивка



Фигура 2. Схематично представяне на процеса на обвиване на биохибридните ядра от пХЕМА криогел с обвивка от поли (етиленов оксид) (ПЕО) хидрогел.

2.3. Морфология на получените гелове



ПЕО обвивка

Ядро от пХЕМА

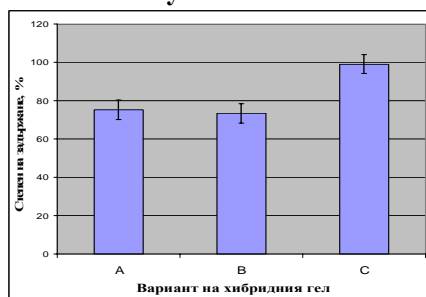


Фигура 3. SEM снимка (а) и фотографска снимка (б) на хибриден гел от вида ядро-обвивка.

3. Резултати

Таблица № 1. Експериментални условия за получаване на ПЕО обвивка

Вариант	тегловно съотношение ПЕО : омрежващ агент	ПЕО	Фото-инициатор [спрямо теглото на ПЕО]
A	без омрежващ агент	3%	5%
B	1 : 0,75	3%	5%
C	1 : 1	3%	5%



Фигура 4. Ефективност на задържане на уреазата.

Определяне степента на задържане на уреазата

За да се определи количеството на уреазата, който е преминал през обвивката се използва метода на Кочетов за белтъчно съдържание. Предварително към всяка проба се прибавя реактив на Бенедикт, в резултат на което се получава синьо оцветяване. Измерва се абсорбцията на всяка проба при дължина на вълната 330 nm с Beckman Coulter DU 800 спектрофотометър. От интензитета на абсорбцията с помощта на стандартна права определяме количеството на уреазата.

4. Изводи

- Макропорестите криогелове са подходящи за имобилизиране на биообекти, благодарение на тяхната инертност, висока порьозност и големината на кухините.
- Намерени са условия, при които обвивката от ПЕО-хидрогел успешно задържа ензимните молекули имобилизирани в ядрата от пХЕМА криогел, като осигурява свободно дифундиране на субстрата и крайния продукт на реакцията.
- Получените хибридни гелове могат да се използват като индикатори за замърсяване на водни проби с тежки метали.

Благодарности

Настоящото изследване беше реализирано с финансовата подкрепа на :

- BG051PO001/07/3.3-02/51, "Подкрепа за развитие и реализация на докторанти, пост-докторанти и млади учени в областта на полимерната химия, физика и инженерство"
- Фонд Научни Изследвания : Договор ВУ-Х-302



PROTON CONDUCTING SEMI-INTERPENETRATING NETWORKS BASED ON POLYBENZIMIDAZOLE AND CROSSLINKED POLYACIDS

D. Budurova, V. Sinigersky, St. Shenkov
Institute of Polymers, Bulgarian Academy of Sciences, 1113 Sofia, Bulgaria

Introduction

Interpenetrating polymer network (IPN) is an assembly of interpenetrating networks of two crosslinked polymers, which could have or not chemical interaction, but at least one of them is synthesized and crosslinked in presence of the other [1]. If only one component of the assembly is crosslinked, the system is termed as a semi IPN. Depending on the synthetic approach, nature of the components and many other factors, IPN can be classified into different categories. Generally this is a suitable combination of crosslinked polymer with another polymer in linear or crosslinked (network) form. These materials exhibit specific properties as improved solvent resistance, high water uptake, good thermal and mechanical properties, etc.

The direct methanol fuel cells (DMFCs) are promising energy conversion devices due to their high energy efficiency, stable and simple operating conditions at a relatively low temperature, and no requirement of fuel reforming process [2-3]. The proton exchange membrane (PEM) is one of the most important components in DMFC. The PEMs with high proton conductivity have huge potential in DMFC applications. The main aim of this study is to obtain the PEMs with high proton conductivity and low methanol diffusion coefficient for DMFC applications. To achieve this objective two acids - the cheap and easily available 2-acrylamido-2-methyl-1-propanesulfonic acid (AMPS) and vinylphosphonic acid (VPhA) were introduced into the PBI matrix. By introducing AMPS/VPhA the proton conductivity of membrane would be improved greatly due to the superior ability of sulfonic acid /phosphonic acid groups originated from AMPS /VPhA in supporting proton conduction. By crosslinking, the water swelling and methanol diffusion could be restricted and stability of membranes can be enhanced owing to the formation of compact network structure.

Preparation of porous PBI films

Preparation of porous PBI films from a dry PBI foil

A dry PBI foil (cast from dimethylacetamide solution) was swollen in a bath containing 70-85% phosphoric acid. After achieving the desired degree of swelling, the film was washed in deionized water. In this way a porous PBI membrane, containing up to 60 wt.-% water can be prepared.

Parameters varied:

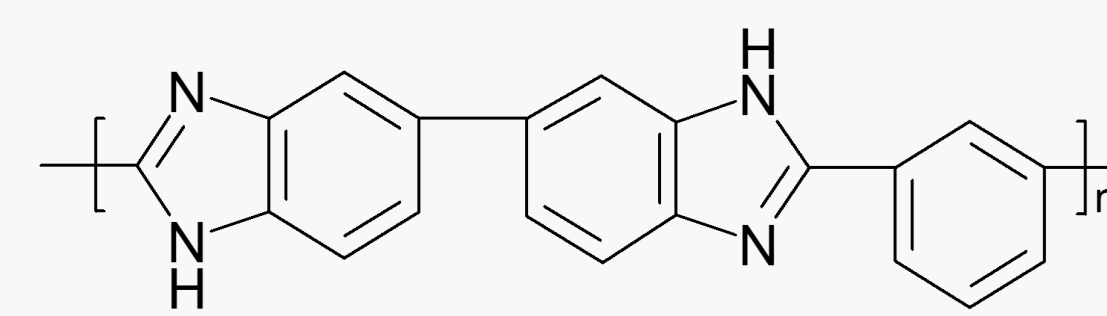
- Bath composition
- Conditions of swelling (time, temperature)
- Weight uptake - up to 1000% (usually 300-900%)

Preparation of porous PBI films from phosphoric acid doped PBI (Celitek P® membrane- trade mark of BASF FC)

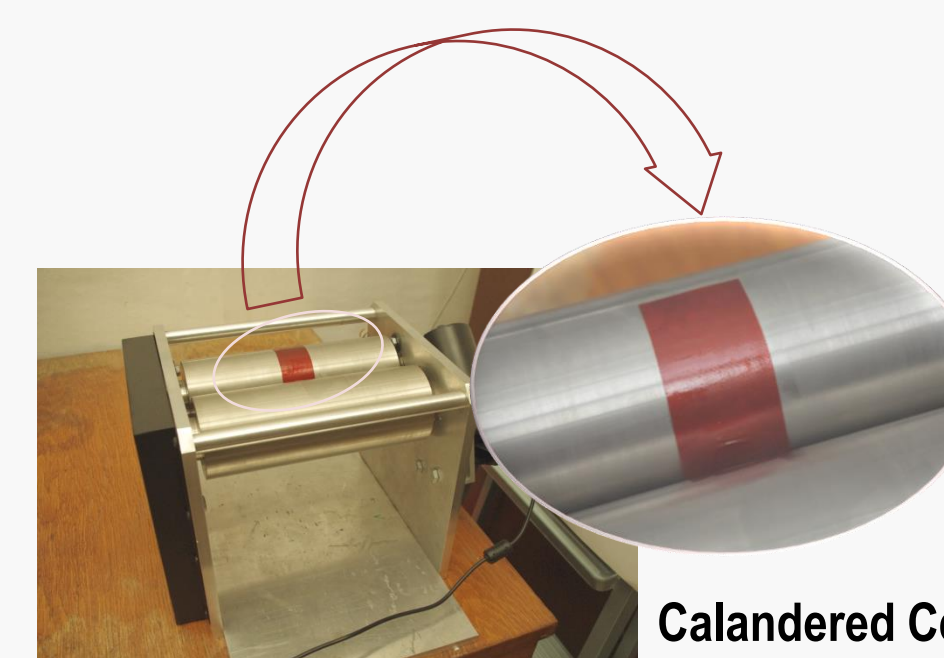
The membrane is calandered to the desired thickness (100-200 µm) and was washed in deionized water. The result is porous film containing up to 80 wt.-% water.

Parameters varied:

- Film thickness
- Water content



Polybenzimidazole (PBI)

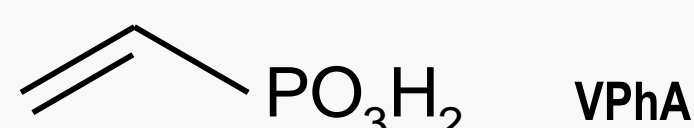


Calandered CelteckP® membrane

Preparation of s-IPNs- membranes containing water insoluble phosphonic and sulfonic acid groups

The present s-IPNs are prepared using a two step simultaneous technique: the polyacids are synthesized in situ from the monomers (VPhA, AMPS) and simultaneously crosslinked within the PBI matrix.

1. Membranes, prepared by polymerization /crosslinking of VPhA in a porous PBI film



Mixture containing VPhA, 2,2'-Azobis(methylpropionamide) as initiator system, triallyl-s-triazine-2,4,6 as crosslinking agent and water were stirred continuously until a transparent solution was obtained. Then porous PBI film was immersed in the solution for 2 hs.

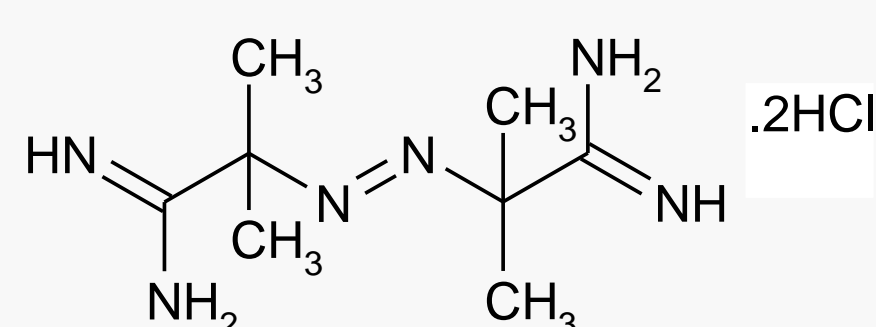
In this way the water in the porous film was replaced by the reagents of the mixture.

The resulting film was placed on a glass substrate and dried in vacuum. The polymerization was carried out by UV irradiation.

Parameters varied:

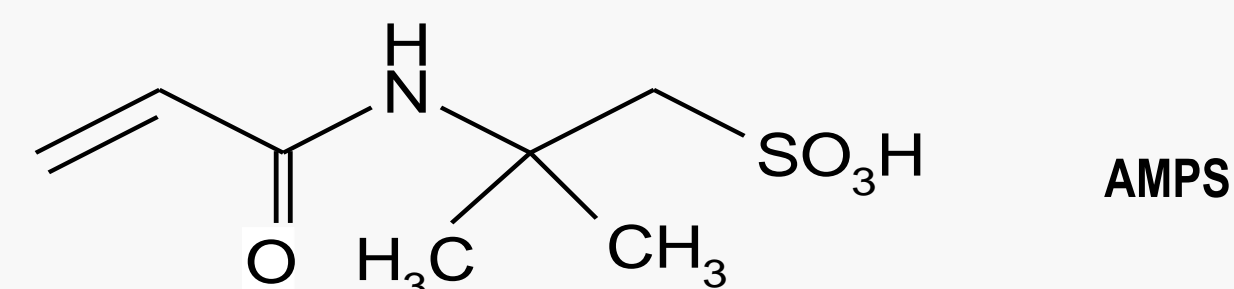
- Bath composition: (monomer- 60-90 wt.-%; initiator-0,5-3 wt.-%; crosslinking agent- 2-5 wt.-%)
- Polymerization/Crosslinking conditions-(irradiation time and temperature)

Applying this procedure dense and homogeneous membranes of good quality with PBI/water insoluble crosslinked acid ratio from 1:2 to 1:3,5 were prepared.



2,2'-Azobis(methylpropionamide)

2. Membranes, prepared by polymerization/crosslinking of VPhA/ AMPS in a porous PBI film



Mixture containing 2-acrylamido-2-methyl-1-propanesulfonic acid (AMPS), 2,2'-Azobis(methylpropionamide) as initiator system, trimethylolpropan-tri(vinylphosphonic acid)ester as crosslinking agent and water were stirred continuously until a transparent solution was obtained. Then porous PBI film was immersed in the solution for 2 hs.

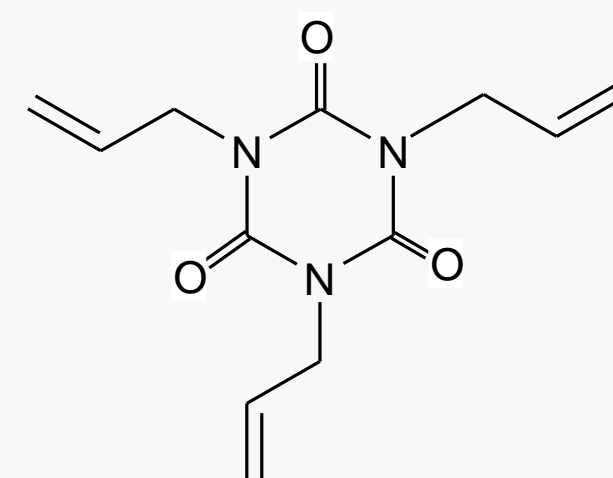
In this way the water in the porous film is replaced by the reagents of the mixture.

The resulting film was placed on a glass substrate and dried in vacuum. The polymerization was carried out thermally for several hours.

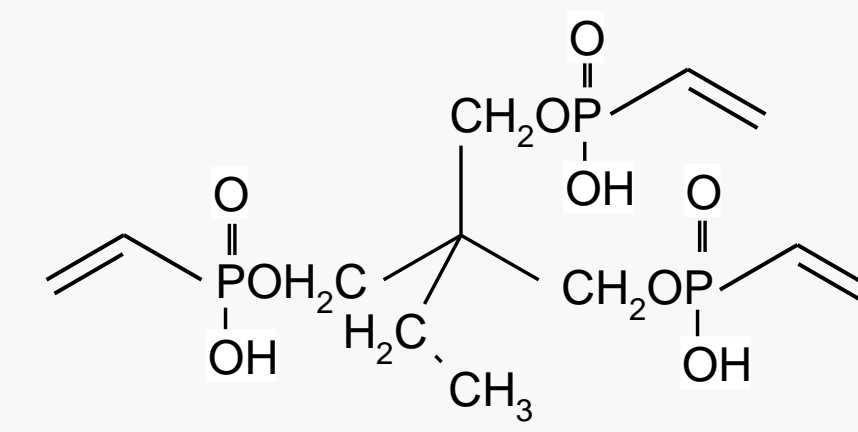
Parameters varied:

- Bath composition: (monomer- 10-25 wt.-%; initiator-0,5-1,5 wt.-%; crosslinking agent- 1-3 wt.-%)
- Polymerization/crosslinking conditions-(time and temperature)

Applying this procedure dense and homogeneous membranes of good quality with PBI/water insoluble crosslinked acid weight ratio from 1:1,2 to 1:3,2 were prepared.



triallyl-s-triazine-2,4,6)



trimethylolpropan-tri(vinylphosphonic acid)ester

Proton conductivity and mechanical properties measurements as well as long term stability determination are in progress.

Conclusion: Membranes based on PBI were modified by the introduction of crosslinked PVPhA and crosslinked PVPhA/PAMPS which were prepared by in situ polymerization. The additional acid groups into the PBI should increase the proton conductivity and decrease the methanol permeability. It is believed that semi-IPNs could be a good material for DMFC.

References

- [1] L.H.Sperling, Interpenetrating Polymer Networks and Related Materials, Plenum. Press, New York, 1981, pp 1-30
- [2] S.Zhong, K.Cui, K.Cai, T.Fu, K.Shao, H. Na, Journal of Power Sources, 168(2007) 154-161
- [3] L.Gubler, D.Kramer, J.Belack, O.Unsal, T.Schmidt, G.Scherera, A Polybenzimidazole-Based Membrane for the Direct Methanol Fuel Cell, J.Electrochem.Soc. 154(2007) 981-987

Acknowledgment

D. B. thanks the Structural Funds and Educational Programs Directorate of Ministry of Education, Youth and Science for financial support in the frame of the Project "Support for the development and realization of PhD-students, post-docs and young researchers in the field of polymer chemistry, physics and engineering", Grant № BG051PO001/07/3.3-02/51 51.





STATE OF CURE MEASUREMENTS BY DIFFERENT TECHNIQUES IN ELASTOMERIC MATRIX COMPOSITES

ОПРЕДЕЛЯНЕ НА СТЕПЕНТА НА ВУЛКАНИЗАЦИЯ НА ЕЛАСТОМЕРНИ КОМПОЗИТИ ЧРЕЗ РАЗЛИЧНИ МЕТОДИ И ПРИЛОЖЕНИЕТО ИМ ПРИ МАСИВНИ ИЗДЕЛИЯ

Diana Zaimova¹, Emin Bayraktar², Nikolay Dishovsky¹

¹University of Chemical Technology and Metallurgy – Sofia
8, Kliment Ohridski blvd., Sofia 1756, Bulgaria

²Supmeca/LISMMA-Paris,
3 rue Fernand Hainaut, 93407 St Ouen Cedex - France

Abstract

In this study we look for: quantify the state of cure by different techniques (chemical; mechanical; thermal; spectroscopic); Comparison among the used experimental methods for measuring state of cure is made by choosing the following criteria: destructivity, need of specific sample geometry, reversion detection, error and timing; validating the numerical simulation with experimental results.; validating the numerical simulation with experimental results. As a first step test sheets were obtained from tested rubber-based compound. Different methods (DSC, NMR, mass swelling, tensile test, compression set test, relaxation, hardness, shear stress) were used to quantify the state of cure experimentally. The same techniques were applied for obtaining the state of cure in a thick part obtained from the tested compound. Then the results for the thick part were correlated with the results for the test sheets obtained by rheometer. Finally is made a comparison among the used methods by several criteria. Also numerical data obtained for evolution of state of cure in the thick part is compared by special software with the experimental data.

Introduction

The state of cure at the end of rubber parts moulding determines the essential of the parts properties [1]. Rubber material mainly consists of long polymer chains. In the uncured state, under mechanical stress, relative chains sliding is possible: the material has a plastic behaviour. After vulcanization, in the cured state, a three-dimensional chains network is created. Chemical cross-links between the chains prevent them from relative sliding: the material has an elastic behaviour [2]. There is, therefore, a strong dependence of the mechanical properties with the cross-link density during the vulcanization process [2].

B. Blumich [3] uses NMR and swelling methods for determining the cross-link density. In his study he observes that with increasing curing time, cross-link density increases as the cross-linking reaction proceeds leading to a decrease in T_2 and the degree of swelling. Some rubber types show reversion, i.e. a decrease in the shear modulus at high curing times due to chain scission starting to dominate cross-linking. For measuring the state of cure Richard J. Pazur [4] uses in his study several methods- NMR, tension test, swelling method, compression set and hardness tests. In our study we use a great number of methods (DSC, NMR, mass swelling, tensile test, compression set test, relaxation, hardness, shear stress) for measuring the state of cure distribution in elastomeric matrix composites. El Labban et al [5] have developed a simulation tool that predicts and controls the temperature and the state of cure distribution within thin-section rubber parts. The heat transfer model was experimentally validated. The curing kinetic model was validated qualitatively by the location of vulcanization front (dividing the surface between vulcanized and unvulcanized materials). The purpose of the present paper is: to quantify the state of cure by different techniques (chemical; mechanical; thermal; spectroscopic); to compare the used experimental methods for measuring state of cure by choosing the following criteria: destructivity, need of specific sample geometry, reversion detection, error and timing; to validate the numerical simulation with experimental results.

Experimental

The tested compound is natural rubber based reinforced with carbon black and sulfur vulcanized. From the compound were vulcanized two thick parts (sample A and sample B) with two different curing times giving two different state of cure distributions in the part's thickness. For characterization of the composite vulcanization properties is used rheometer type RPA2000 with moving die. The frequency is 1,66Hz and angle $0,5^\circ$ (standard setup conditions). Rheometer specimens were prepared at different temperatures (130°C, 140°C, 150°C, 160°C, 170°C). Test sheets were cured for different curing times (test sheets thickness 2mm) in order to obtain different state of cure for temperatures set of 140°C and 170°C. The sheets were immediately put in ice cold water in order to freeze the state of cure. The curing temperature was measured and saved by using thermo-couples on the press form boundaries. The state of cure values of the test sheets expected by the rheometer measurements were calculated and correlated by a finite element software in order to take to consideration the increasing of state of cure during cooling. Mass swelling was carried out for 72h until equilibrium using ambient temperature according to ISO 1817. As a solvent is used cyclohexane. The chemical cross-link density (1/2Mc) was calculated using the Flory-Rehner [5] equation. Simple stress-strain tests were made by using dynamometer and rate of 500mm/min. Compression set is measured in agreement with ISO 815-1 for 72h and 25% deformation. For measuring shear stress is used apparatus MetraviB for ambient temperature and frequency 5Hz for different level of deformation. Hardness is measured by using two different methods- Shore A and IRHD. Relaxation test data was carried out in accordance with ISO 2285 for 24h and 200% deformation for ambient temperature and temperature of 70°C. A wide line NMR-MOUSE (MOBILE Universal Surface Explorer) spectrometer was used to collect the relaxation data. For performing DSC-test is used apparatus DSC METTLER TOLEDO. To obtain the simulation of state of cure distribution in thickness of sample A and sample B is used special software called COMSOL.

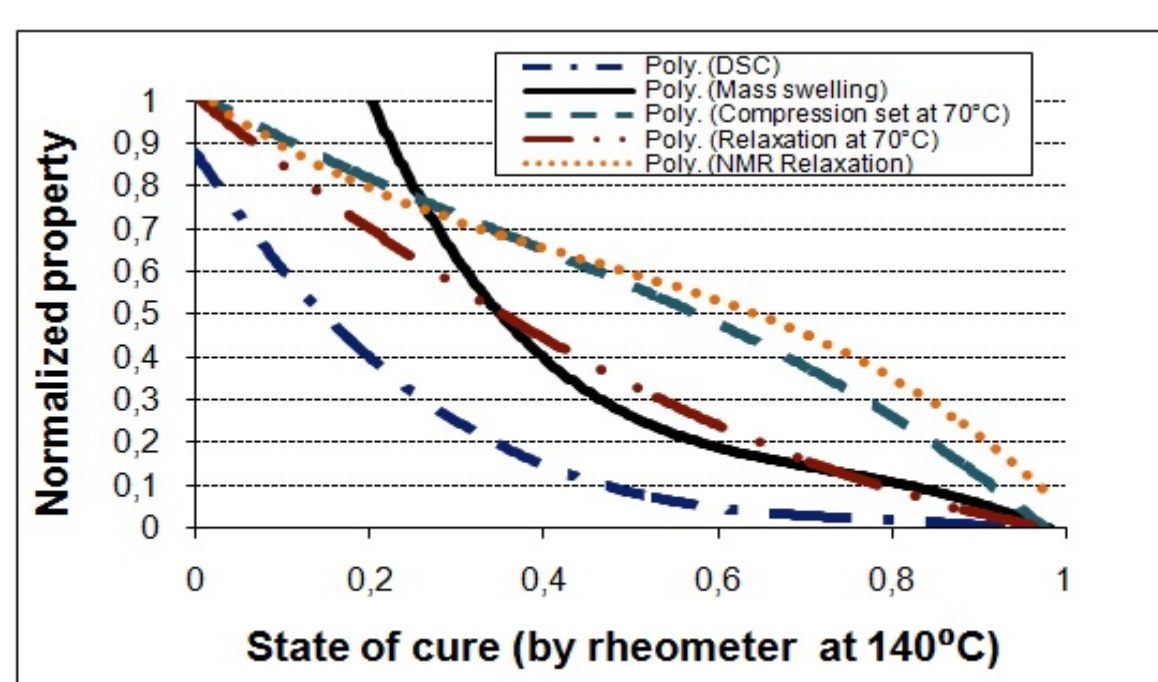


Figure 1. Normalized properties as a function of state of cure measured by: DSC, mass swelling, relaxation, compression set and NMR tests

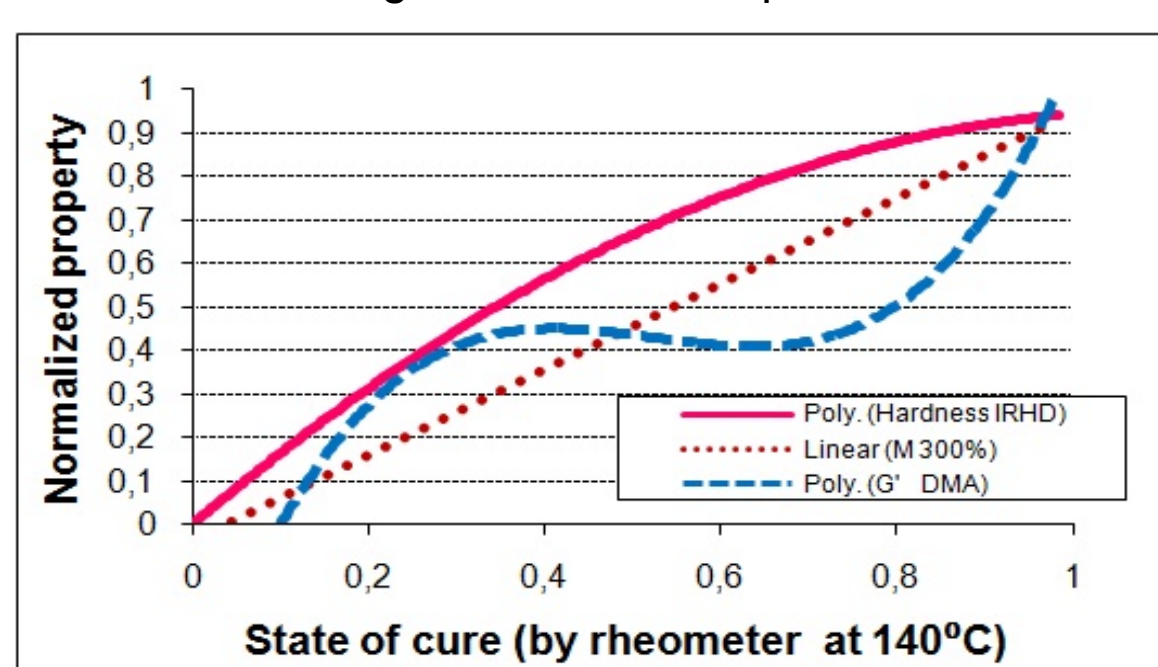


Figure 2. Normalized properties as a function of state of cure measured by: Hardness, shear stress and tensile tests.

Results and discussion

1. Comparison between different experimental methods

The normalized properties as a function of state of cure, measured by the different methods (for the test sheets) are shown in fig. 1 and fig. 2. The property values are increasing with the state of cure measured by the methods of hardness and elongation modulus. Exactly the opposite is the dependence for the values measured by the methods of NMR, DSC, compression set, relaxation and swelling. DSC and compression set are decreasing linearly. For shear modulus can be observed 3 stages- first the values of the property are rising slowly with the state of cure, after we have section with constant values an third rapid increasing of the property values, the measurements were made only for one sample for each state of cure. This must be completed with more measurements in order to have accurate results. Table 1 shows the comparison of the used methods by several criteria.

Table 1 Comparison of the used methods

Method	Destructivity	Specific sample geometry needed	Reversion detection	Error	Timing
DSC	Destructive	Not needed	Don't detects	↗	30 min
NMR	Not destructive	Not needed	Detects	↘	1min
Mass swelling	Destructive	Not needed	Detects	↘	72h
Tensile test	Destructive	Needed	Detects	↘	1 min
Compression set test	Destructive	Not needed	Don't detects	↘	72h
Relaxation	Destructive	Needed	Don't detects	↘	24h
Hardness	Destructive	Not needed	Detects	↘	1min
Shear stress	Destructive	Not needed	Don't detects	↗	3h

2. Comparison between numerical and experimental results

The results from the comparison of the measurements obtained by using different techniques for the thick part are displayed in fig. 3 and fig.4. There was also made a numerical simulation of distribution of the state of cure in the tested thick part. We have always the same evolution of the curves – from the borders to the center the level of vulcanization is decreasing and unvulcanized center. In one of the borders we have reversion. In fig. 3 and fig.4 is also observed that numerical and experimental data have close values which makes the numerical prediction of distribution of state of cure reliable. The curve obtained by using swelling method has the closest values with the numerical results compared to the other used methods. Unfortunately the results are obtained with different error for the different methods and it is hard to be determined which one is the most precise. But in general can be said that we have good correlation between numerical and experimental results.

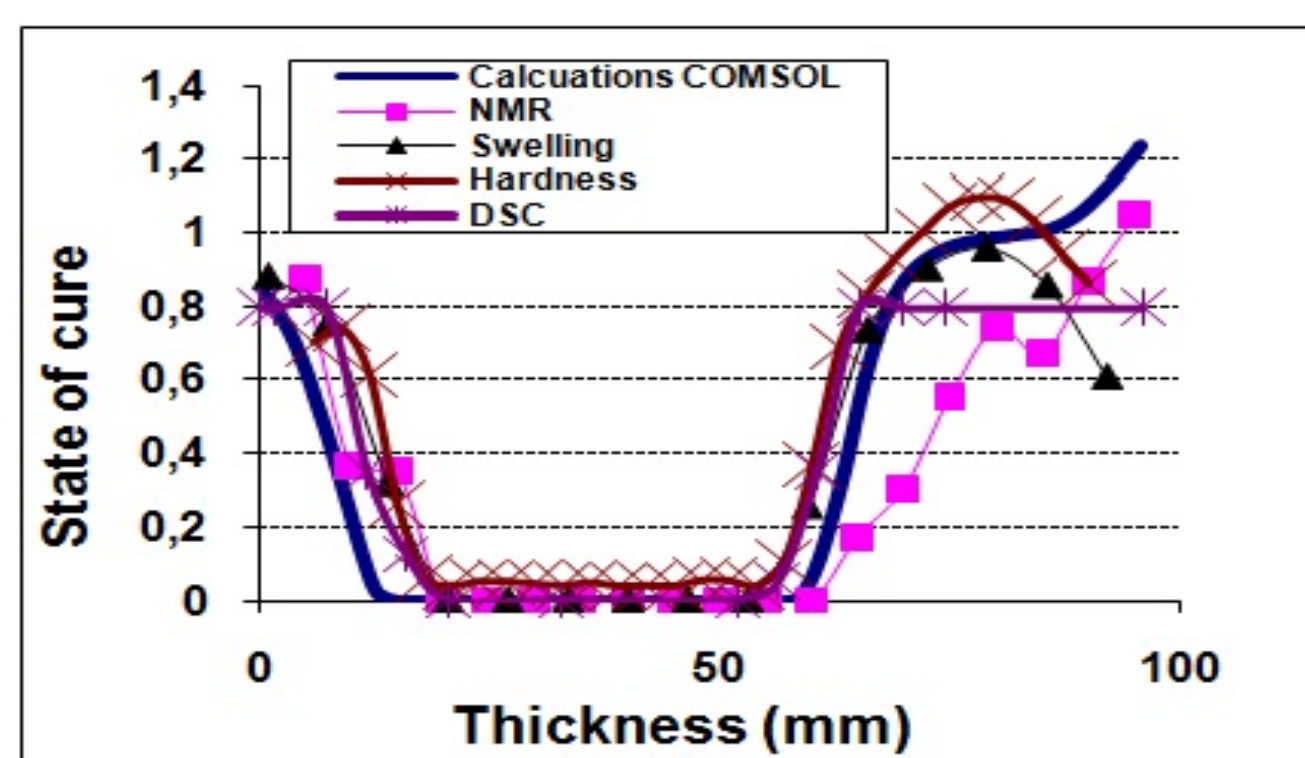


Figure 3. Comparison between numerical and experimental results for the thick part (sample A)

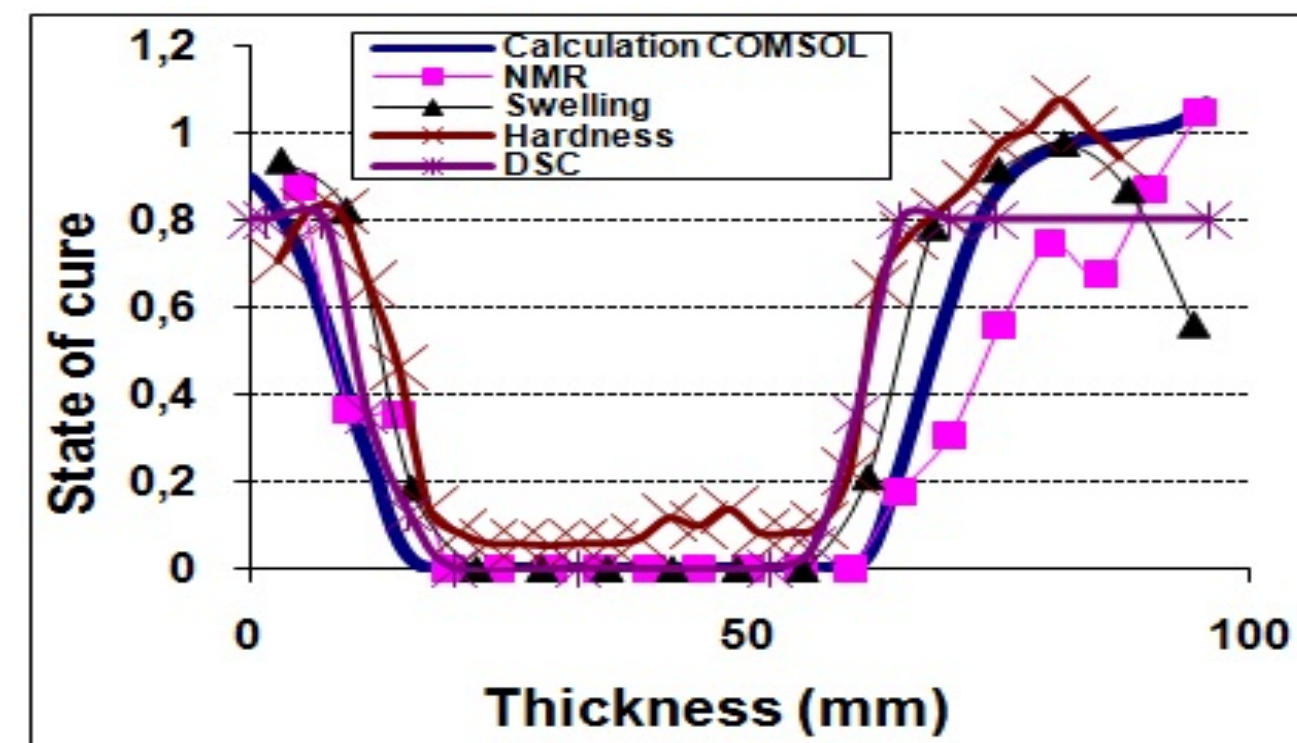


Figure 4. Comparison between numerical and experimental results for the thick part (Sample B)

Conclusion

- Different methods (chemical, mechanical, thermal and spectroscopic) were applied successfully for measuring the state of cure in the test sheets.
- Some of the mechanical methods (shear stress, stress-strain, compression set and relaxation) are not suitable for measuring the state of cure in thick parts.
- From the comparison of the methods used in this study according to some criteria, it can be concluded that:
 - all of used methods are destructive except for NMR;
 - DMA(shear stress) and DSC gives high values of error and don't detect reversion;
 - for relaxation and tensile test is needed a specific geometry of the specimen;
 - NMR, mass swelling, tensile and hardness test gives reliable results for measuring the state of cure in rubber parts.
- A good correlation has been found between numerical and experimental results which give the possibility to make a reliable prediction on the distribution of state of cure in thick parts. Mass swelling method gives better results than other methods.

References

- [1] A. Cheymol, Processing of elastomers (Mise en oeuvre des élastomères 2), Traité MIM, série polymères, Hermès Lavoisier, 2006.
- [2] F. Dimier, Injection of reactive systems: kinetic and rheological properties (Injection des systèmes réactifs: détermination de lois cinétiques et rhéologiques et modélisation), ENSMP, Ph.D. Report 2003.
- [3] Abdulrahman El Labban, Pierre Mousseau, Remi Deterre, Jean-Luc Bailleul, Alain Sarda, "Temperature measurements and control within molded rubber during vulcanization process", 2009 Elsevier Ltd.
- [4] B. Blumich, J. Perlo, F. Casanova, "Mobile single-sided NMR", Progress in Nuclear Magnetic Resonance Spectroscopy 52 (2008) 197–269
- [5] Richard J. Pazur* and F.J. Walker, "State of cure measurements in peroxide and sulfur cured ", presented at the Fall 174th Technical Meeting of the Rubber Division of the American Chemical Society, Inc. Louisville, KY October 14-16, 2008 ISSN: 1547-1977
- [6] P.J. Flory, J.J. Rehner, Chem. Phys 11, 1943



Acknowledgement: The presentation of the following results was supported by the project "Support for the development and realization of PhD-students, post-docs and young researchers in the field of polymer chemistry, physics and engineering", Grant № BG051PO001/07/3.3-02/51 and the authors want to thank sincerely for the opportunity to participate in this event.

Tuning of the Surface Biological Behavior of Poly(L-Lactide)-Based Electrospun Materials by Polyelectrolyte Complex Formation

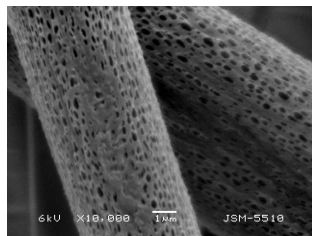
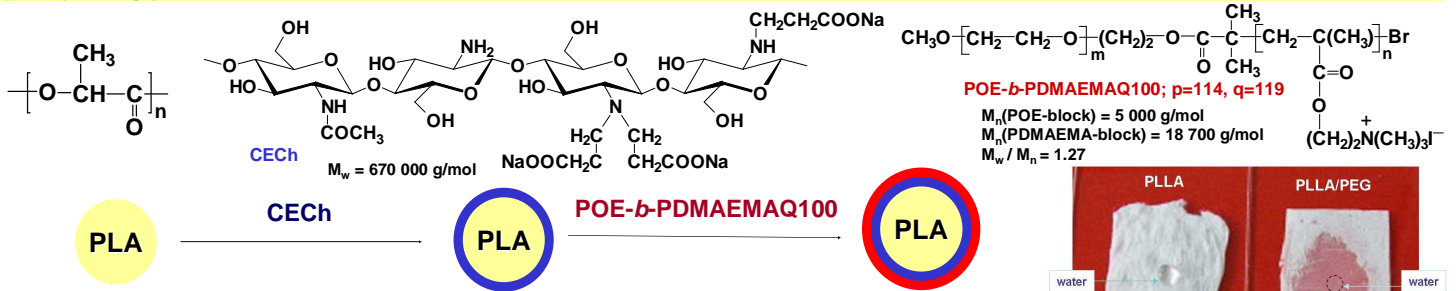
E. Yancheva,¹ D. Paneva,¹ N. Manolova,¹ R. Mincheva,² D. Danchev,³

Ph. Dubois,² I. Rashkov¹

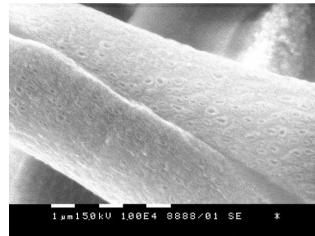


¹Laboratory of Bioactive Polymers, Institute of Polymers, BAS, Bulgaria; ²Laboratory of Polymeric and Composite Materials, University of Mons-UMONS, Belgium; ³Department of Haemostasis, Military Medical Academy, Sofia, Bulgaria.

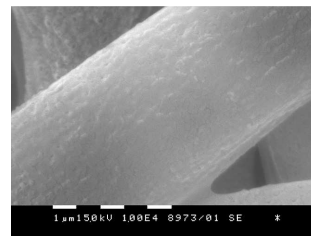
THE AIM of the study is modification of the surface biological behavior of electrospun textiles based on poly(L-lactide) (PLLA) using the polyelectrolyte complex formation tool. This is achieved by consecutive deposition of *N*-carboxyethylchitosan (CECh) and poly(ethylene oxide)-*b*-quaternized poly[2-(dimethylamino)ethyl methacrylate] (PEO-*b*-PDMAEMAQ100) on PLLA or PLLA/poly(ethylene glycol) micro- and nanofibrous materials.



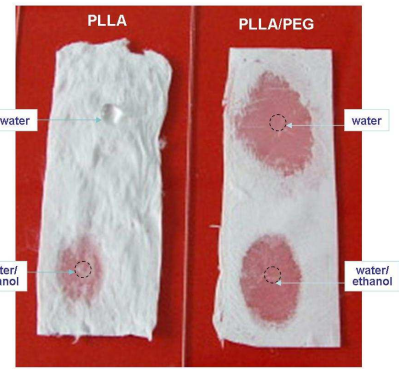
$L_{\text{pore}} = 370 \pm 70 \text{ nm}$
 $D_{\text{pore}} = 160 \pm 40 \text{ nm}$
 48 pores/9 μm^2



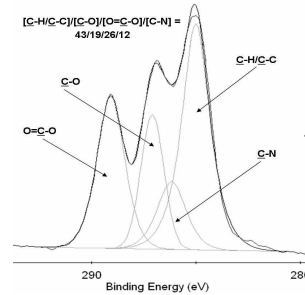
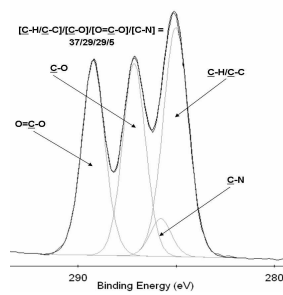
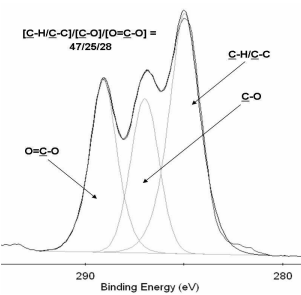
$L_{\text{pore}} = 240 \pm 50 \text{ nm}$
 $D_{\text{pore}} = 120 \pm 30 \text{ nm}$
 22 pores/9 μm^2



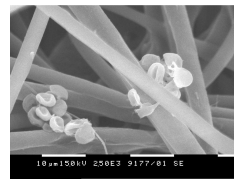
$L_{\text{pore}} = 120 \pm 30 \text{ nm}$
 $D_{\text{pore}} = 100 \pm 20 \text{ nm}$
 15 pores/9 μm^2



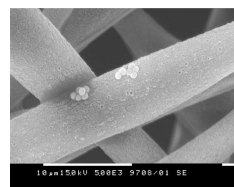
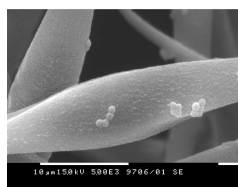
Because of the high hydrophobicity of PLLA mats water/ethanol mixed solvent (1/1 v/v) was used for preparation of the coating solutions.



The developed approach for coating of PLLA-based materials is a suitable one as evidenced by the presence of a C-N peak in the C 1s XPS spectra of the coated mats.



Behavior of the (non)coated mats in contact with blood cells.



Behavior of the (non)coated mats in contact with *S. aureus*.

CONCLUSION: The preparation of a coating from CECh(crosslinked) or CECh(crosslinked)/PEO-*b*-PDMAEMAQ100 complex is a feasible route for modification of the surface properties of PLLA and PLLA/PEG electrospun materials. Coating with CECh(crosslinked) leads to the preparation of novel materials, which are characterized by good compatibility with the blood cells and reduce the adhesion of pathogenic microorganisms. These materials can find potential applications in tissue regeneration. The preparation of a CECh(crosslinked)/PEO-*b*-PDMAEMAQ100 complex coating imparts haemostatic properties to the PLLA and PLLA/PEG mats. In addition, the PEC coating reduces the adhesion of pathogenic microorganisms. Thus, the PEC-coated PLLA and PLLA/PEG mats are potential candidates for wound healing applications.

Refs: Yancheva E., Paneva D., Manolova N., Mincheva R., Danchev D., Dubois Ph., Rashkov I. Tuning of the Surface Biological Behavior of Poly(L-Lactide)-Based Electrospun Materials by Polyelectrolyte Complex Formation. *Biomacromolecules* 11: 521-532 2010.

Acknowledgements: The authors thank the bilateral cooperation between the Bulgarian Academy of Sciences and Wallonie-Bruxelles International (WBI, ex-CGRI, Brussels) and the National Science Fund of Bulgaria (Grant No. DO-02-333/2008) for the financial support. E.Y. and D.P. are very grateful to the Structural Funds and Educational Programs Directorate for the financial support (Grant No. BG051PO001/07/3.3-02/51).

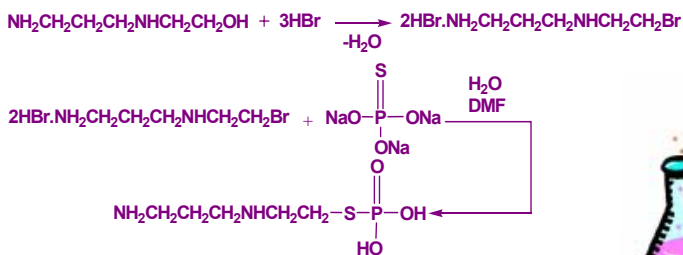


Introduction: Poly(oxyethylene H- phosphonate)s are especially attractive materials because of the relative easiness of their preparation from commercially available building blocks, the variety of molecular weights attainable, and the relatively narrow molecular weight distributions of the polymers formed. Poly(oxyethylene H- phosphonate)s are quite promising for biomedical application because of their biodegradation and low cytotoxicity. Amifostine (S – 2- [(3- aminopropyl)amino]ethane - thiol dihydrogen phosphate ester; WR2721) is a radioprotective agent used clinically to minimize damage from radiation therapy and to protect normal tissues. WR2721 is, in fact, a pro- drug which must be dephosphorylated by membrane- bound alkaline phosphatase to the active metabolite, 1- (3- aminopropyl)aminoethanethiol (WR1065).

The purpose of this study: The synthesis and characterization of polymer complexes constructed from the radioprotective agent WR2721 and biodegradable poly(oxyethylene H- phosphonate), poly(hydroxyoxyethylene phosphate), or poly(methyloxyethylene phosphate) via an ionic bond, and physical complexation, respectively. The structure of the complexes formed is elucidated by ¹H, ¹³C, ³¹P NMR and FTIR spectroscopy.

Synthesis of radioprotective agent:

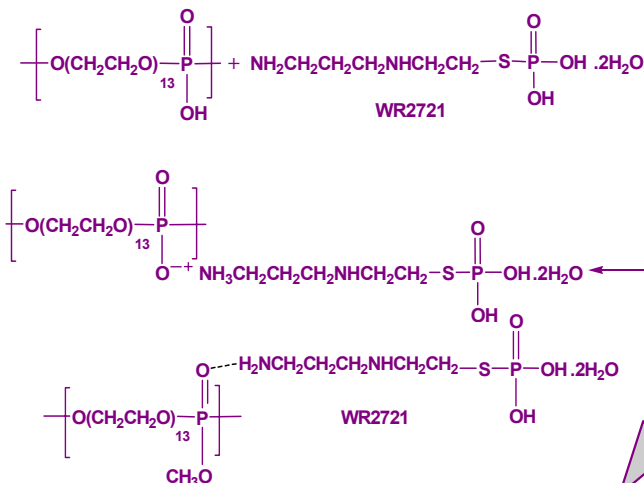
Amifostine (S – 2- [(3- aminopropyl)amino]ethane- thiol dihydrogen phosphate ester; WR2721)



Immobilization of WR2721 onto polyphosphoesters:

Product P5 - WR-2721 was immobilized onto polymer 1 via hydrogen bonding.

Product P6 - WR-2721 was immobilized onto polymer 2 via electrostatic interactions.

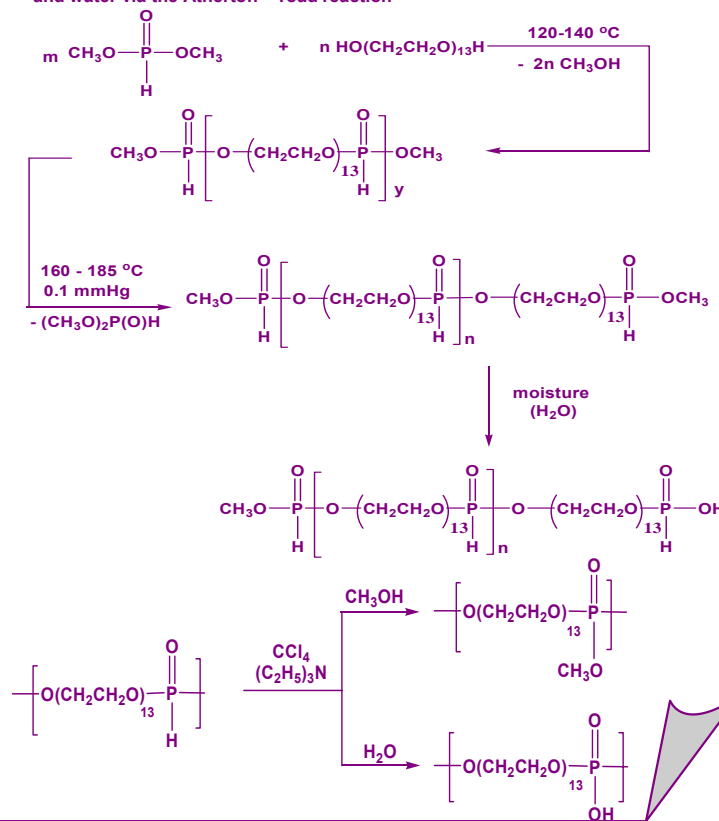


Synthesis of polymer carriers:

Polymer P1 – the precursor poly(oxyethylene H- phosphonate) was obtained via polytransesterification of dimethyl H phosphonate with PEG 600

Polymer P2 - poly(methoxyoxyethylene phosphate) was obtained from Polymer 1 and methanol via the Atherton- Todd reaction

Polymer P3- poly(hydroxyoxyethylene phosphate) was obtained from Polymer 1 and water via the Atherton- Todd reaction

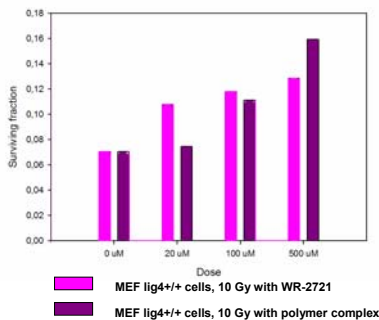


Preliminary Evaluation of Radioprotective Efficiency

Table 1. Radioprotective Efficiency of WR-2721 Polymer Complexes in Mice Exposed to 8.5 Gy (LD100/14) Gamma Radiation

Compound	Equivalent dose of WR-2721		30-day survival, %	MST ⁺ days	PF	TI	PI
	mg/kg	mmol/kg					
POEP(OCH ₃)–WR-2721	50	0.20	30	16.3	1.30	-	7.34
	100	0.40	80	19.5	1.80	5.65 ^a	10.17
	200	0.80	70	21.3	1.70	-	9.60
POEP(OH)–WR-2721	50	0.20	50	14.8	1.50	-	14.04
	100	0.40	50	18.3	1.50	9.36	14.04
	200	0.80	90	26.0	1.90	-	17.78
WR-2721	50	0.20	30	12.1	1.30	-	5.37
	100	0.40	40	16.3	1.40	4.13	5.78
	200	0.80	50	22.0	1.50	-	6.20
Control group (20 mice)	-	-	0	10.7	-	-	-

Scheme 1. Survival of 10 Gy irradiated MEF lig4+/+ cells in the presence of WR-2721 and its polymer complex



Conclusions

- ◆ The product of practical interest is the immobilized of WR2721 onto poly (hydroxyoxyethylene phosphate) via ionic bond, which possesses the highest protective activity (PI – 17.78) and low toxicity (TI- 9.36).
- ◆ The clinically approved radioprotectors WR 2721 could be successfully immobilized on poly(hydroxyoxyethylene phosphate).
- ◆ The polymer dig complexes show significant radioprotection efficiency by comparison with the basic components.



Acknowledgements: E. Vodenicharova and I. Tsacheva thank the European Social Fund, Structural Funds, Operational Programme “Human Resources Development” for financial support in the frame of Grant No. BG051PO001/07/3.3-02/51

Получаване на полимерни наночастици от вида ядро/корона от поли(стирен-съ-диен)-бл-полиетер съполимери с желана морфология

Е. Халаджова¹; Н. Дишовски¹; Хр. Цветанов²; Хр. Новаков²
emihaladjova@abv.bg



¹ХимикоТехнологичен и Металургичен Университет, бул. Кл. Охридски №8, 1756 София, България
²Институт по полимери, БАН, ул. Акад. Г. Бончев, бл. 103, 1113 София, България



Цел

Получаване на полимерни наночастици от амфифилни поли(стирен-съ-диен)-бл-полиетер блокови съполимери със стабилизирана морфология. Изследване на възможностите за промяна в структурата (ядро/корона) на частиците в желана посока.

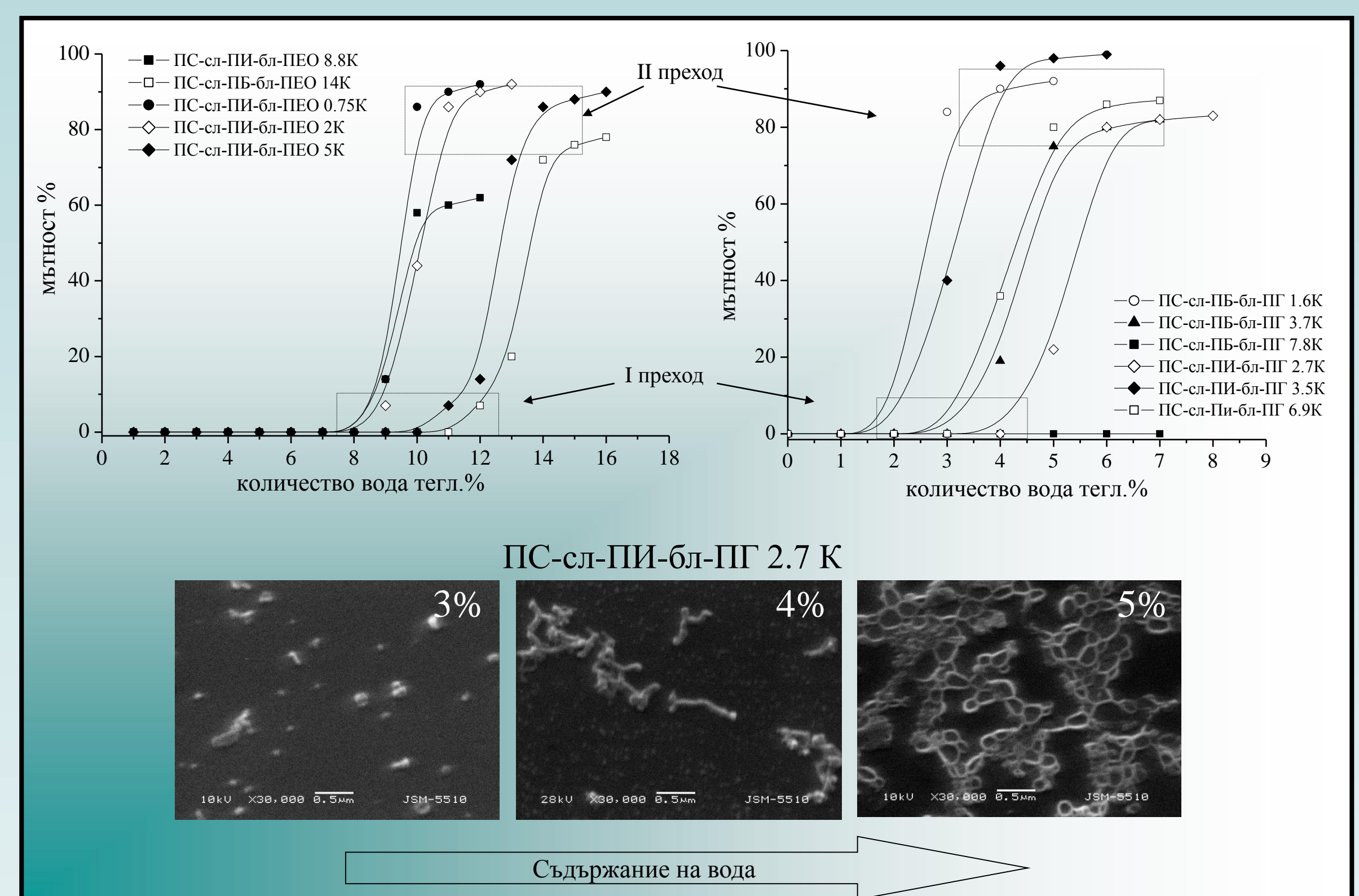
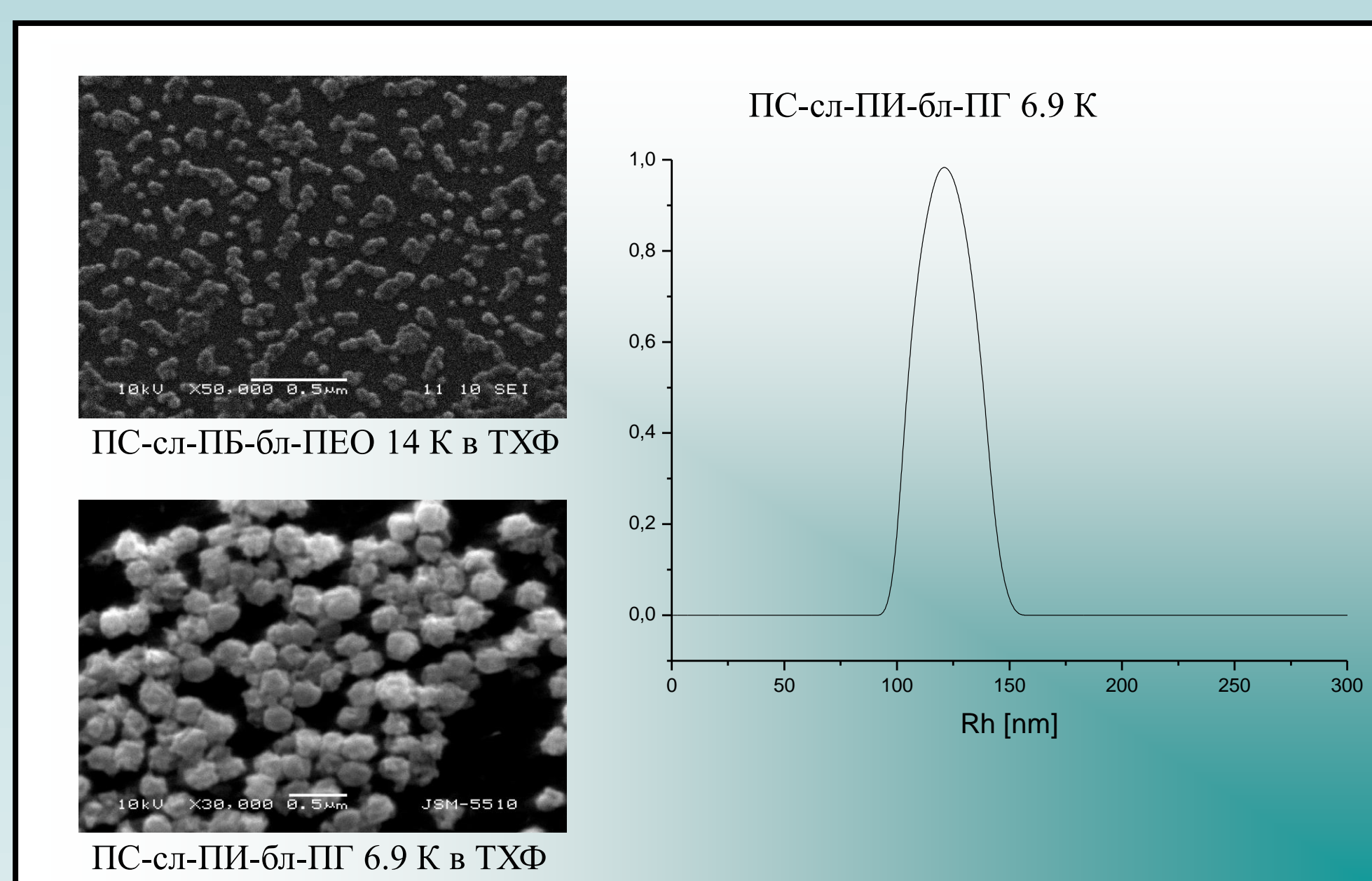
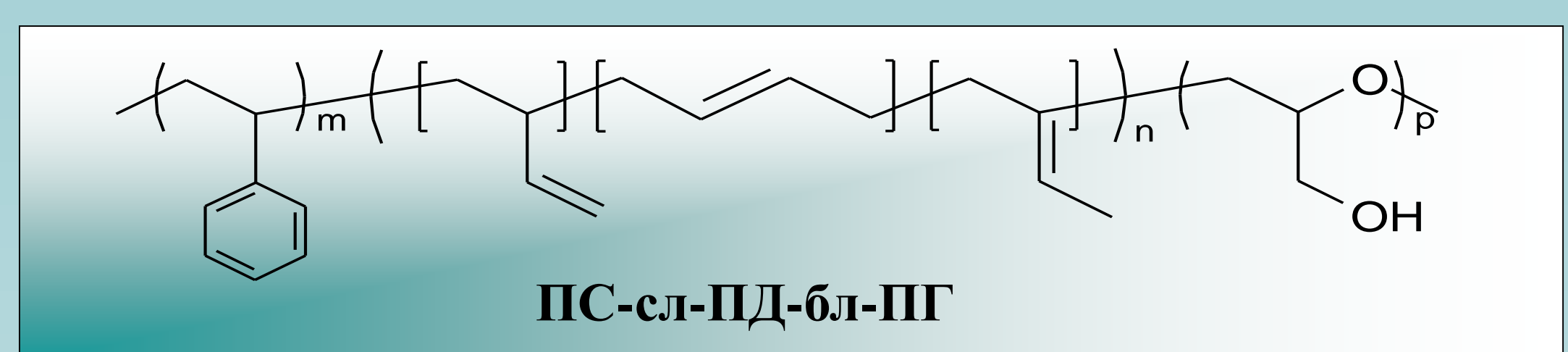
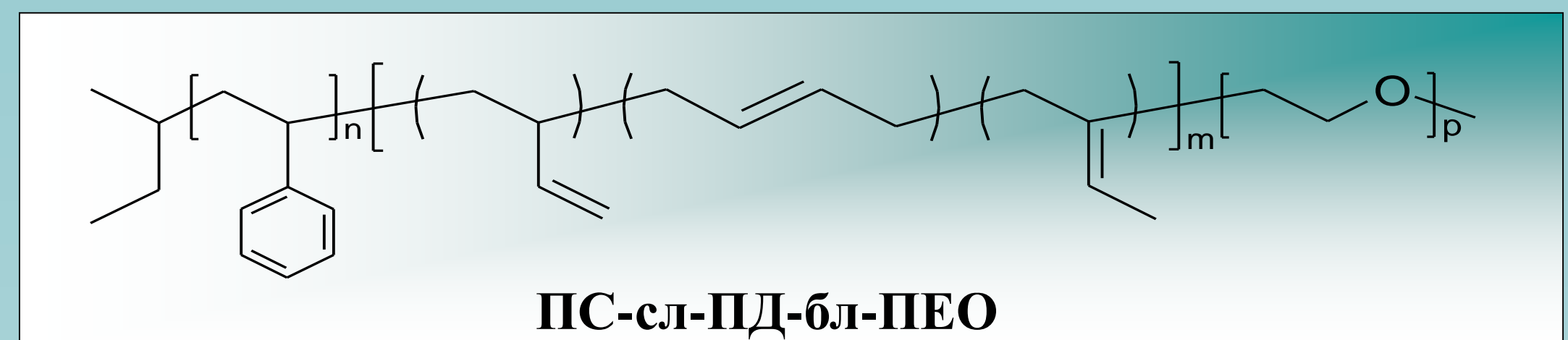
Получаване

1. Синтез на съполимерите

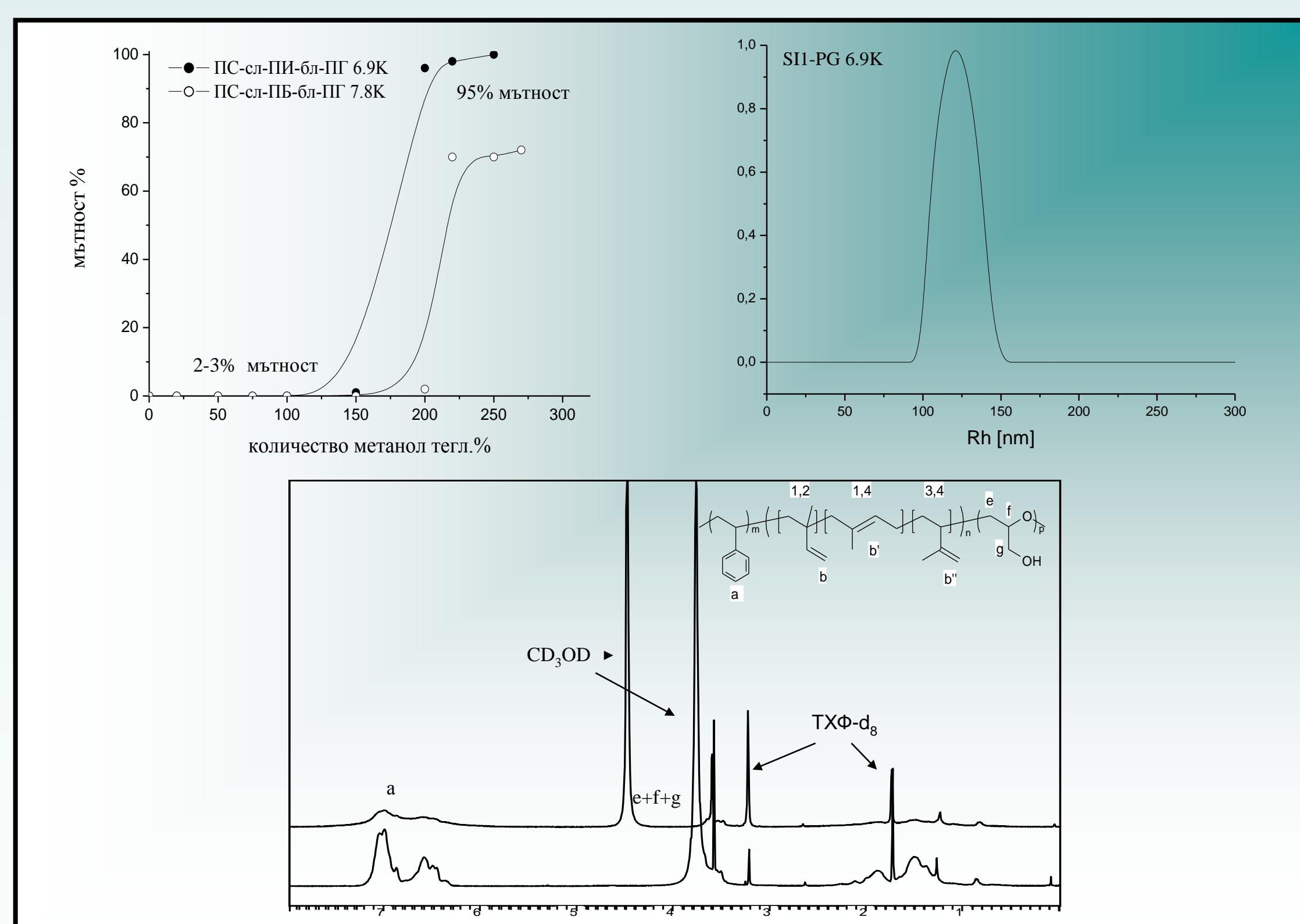
Синтезирани са амфифилни блокови съполимери, изградени от постоянен хидрофобен блок от полистирен (ПС) с включени по случаен начин диенови звена (Д) (изопрен (И) или бутadiен (Б)) и различен по дължина хидрофилен блок от полиетер - полиоксиетилен (ПЕО) или полиглицидол (ПГ).

2. Получаване на частиците

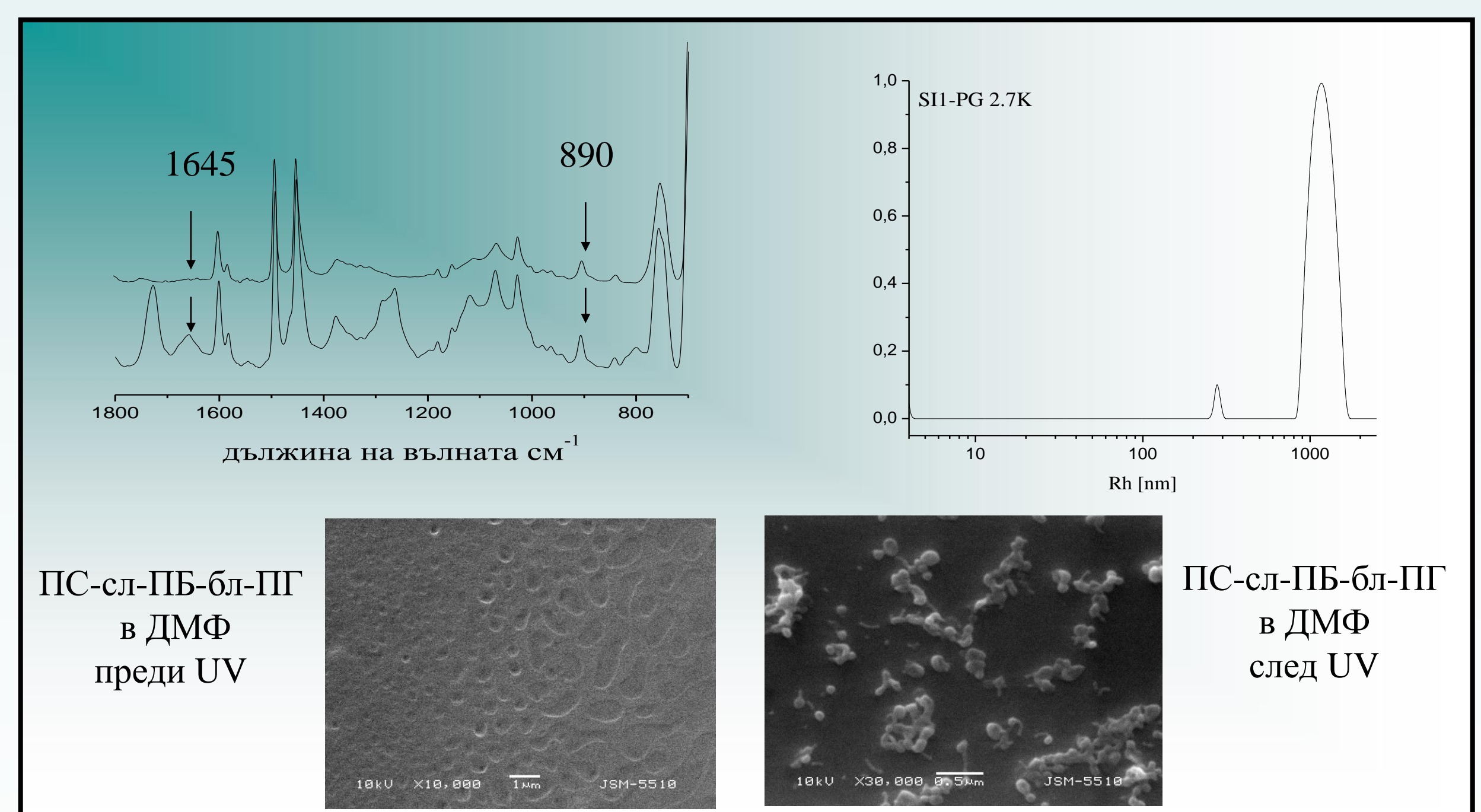
Нано- и микрочастиците са получени от амфифилните блокови съполимери при разтваряне в органични разтворители или в смесени разтвори по метода на Tuzar и Kratochvil.



Промяна в структурата ядро/корона на частиците



Стабилизиране на морфологията



Изводи

Изследвана е зависимостта на формата и размерите на частиците от начина на получаването им, вида на използвания разтворител както и състава на съполимера. Демонстрирани са възможностите за обръщане структурата (ядро/корона) на частиците в желана посока, чрез добавяне на подходящ селективен разтворител. Стабилизиране на получените структури е осъществено чрез облъчване на полимерните разтвори с UV светлина в присъствие на фотоинициатор или γ-лъчи.

Включването на ПГ блок в състава на блоковите съполимери предоставя възможност за тяхното допълнително модифициране в зависимост от конкретната цел на приложение. Лесната разградимост в кисела среда на частици с ядро изградено от ПГ предоставя и възможности за образуването на кухи структури с ценни приложения.

Изказваме искрени благодарности на:

• Министерство на образованието, младежта и науката, Дирекция структурни фондове, Оперативна програма "Развитие на човешките ресурси", Договор № BG051PO001/07/3.3-02/51 "Подкрепа за развитие и реализация на докторанти, пост-докторанти и млади учени в областта на полимерната химия, физика и инженерство".
• Национален център за нови материали UNION, Договор №02-82/2008.



NANOMECHANICAL CHARACTERIZATION OF MULTIWALL CARBON NANOTUBE REINFORCED EPOXY COMPOSITES



E. Ivanov, R. Kotsilkova, E. Krusteve

Central Laboratory of Physico-Chemical Mechanics, Bulgarian Academy of Sciences, Acad. G. Bonchev, St., Bl 1, 1113 Sofia, Bulgaria; e-mail: ivanov_evgeni@yahoo.com

INTRODUCTION

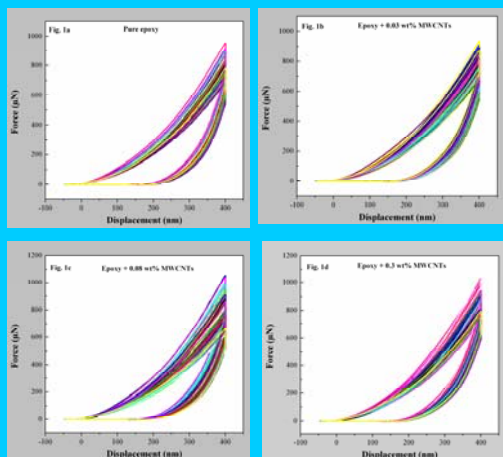
The exceptional physical properties and high aspect ratio of carbon nanotubes (CNTs) have made them ideal candidates for developing the next generation of polymer composites. Thus, the CNTs are expected to be ideal mechanical reinforcements for lightweight composite systems. There are some problems with obtaining of this kind of materials. First, the ability to disperse the CNTs is of critical importance for the formation of a reinforced polymer composite. Homogeneous dispersion of CNTs in the polymer matrix is not easily achieved. Second, the poor bonding between the nanotubes and polymer matrix restricts load transfer from the matrix to the nanotubes. In this study, the hardness and elastic modulus of MWCNT reinforced epoxy composites were measured using a nanoindenter.

MATERIALS AND METHODS

The materials used in this study are multiwall carbon nanotubes (MWCNTs) containing about 8 wt% magnetic ferroxides (supplied by IFW, Dresden). Epoxy resin D.E.R.TM 321 was selected as the polymer matrix, since it is known that carbon nanotubes are well dispersed in epoxies, compared to other oligomers. Polyethylene polyamine (PEPA) was used as a curing agent. The MWCNTs were mixed directly with the epoxy oligomer and then the amine hardener was added. Sample homogenization was realized by high speed mechanical mixing followed by ultrasonic cavitation disintegration. Samples within the concentration range of 0 to 0.3 wt% were prepared and further investigated.

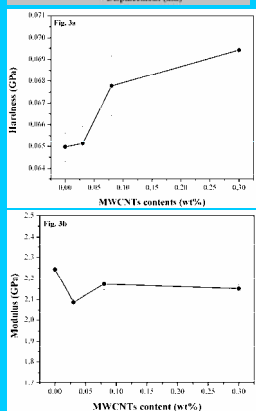
The surface of the samples was polished using a Power Tome XL microtome. The roughness of the samples was measured using Nanofocus profilometer in the range between 4 and 33 nm for the different samples. Nanoindentation tests were performed using a Triboindenter[®] nanomechanical test instrument (Hysitron). The hardness and elastic modulus were calculated from the recorded load-displacement curves. The indentation impressions were then imaged using scanning electron microscopy (SEM). Indenter Bercovich tip 50nm was used for indentations in displacement control mode of 400 nm. A series of seventy (10x7; spacing between indents 5 μm) indentations were performed for each sample. A typical indentation experiment consist of four subsequent steps: approaching the surface; loading to peak load for 5 s; holding the indenter at peak load for 10 s; final complete unloading for 5 s (load function 5s-10s-5s trapezoid). The hold step was included to avoid the influence of creep on the unloading characteristics since the unloading curve was used to obtain the elastic modulus of a material.

RESULTS AND DISCUSSION

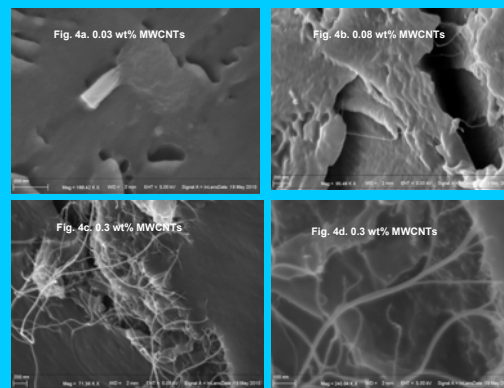
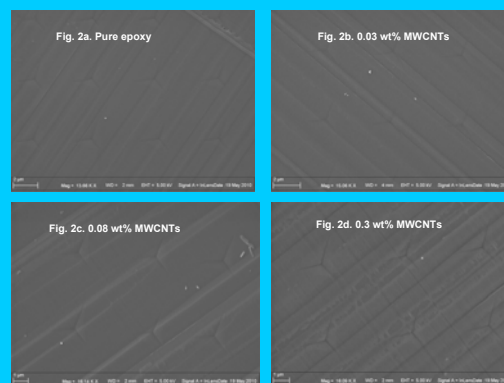


Representative load-displacement curves and SEM images of indentations on epoxy and its MWCNT reinforced samples are compared in Figures 1(a-d) and 2(a-d). No discontinuities or steps were found on the loading curves, indicating that no cracks were formed during indentation.

The elastic modulus was calculated using the Oliver-Pharr data analysis procedure. The unloading stiffness can be obtained from the slope of the initial portion of the unloading curve, $S = dP / dh$.



The hardness and elastic modulus values as a function of MWCNTs content for the epoxy and its composites were obtained on the basis of 70 nanoindentation tests for each concentration (Figures 3(a,b)). The experimental errors are within the range ± 0.01 to ± 0.03 GPa for the modulus and $\pm 6.65 \cdot 10^{-4}$ to $\pm 13.7 \cdot 10^{-4}$ GPa for the hardness. The MWCNT reinforced samples exhibit higher hardness (~7%) and slight decrease (within the range of the experimental error) of elastic modulus compared to the neat epoxy composites. This indicates the existence of adhesion between carbon nanotubes and the epoxy matrix and this is shown on SEM images of the composite fracture surfaces (Figures 4(a-d)).



ACKNOWLEDGMENT

The study is supported by several projects: ESF, OP-HRD №BG051PO001/07/3.3-02, NSF-Bulgaria, 2008; D01-469/06 and NT4-0205 849/09, NSF-Bulgaria; the FP7-CSA-NaPolyNet. We acknowledge our gratitude to IFW Dresden for the supply of MWCNT and Max-Planck-Institut für Eisenforschung GmbH, Dusseldorf, Germany for nanoindentation measurements.

REFERENCES

- 1.R. Kotsilkova, (Ed.). Thermosetting nanocomposites for engineering application. Rapra Smiths Group, UK (2007) 325 p.
- 2.R. Kotsilkova, E. Ivanov. Nanoscience & Nanotechnology 4, Heron Press, Sofia (2004), 123
- 3.R. Kotsilkova et al. J. Appl. Pol. Sci. 92 (2004), 2220

Georgi L. Georgiev, Petar Petrov, Christo B. Tsvetanov

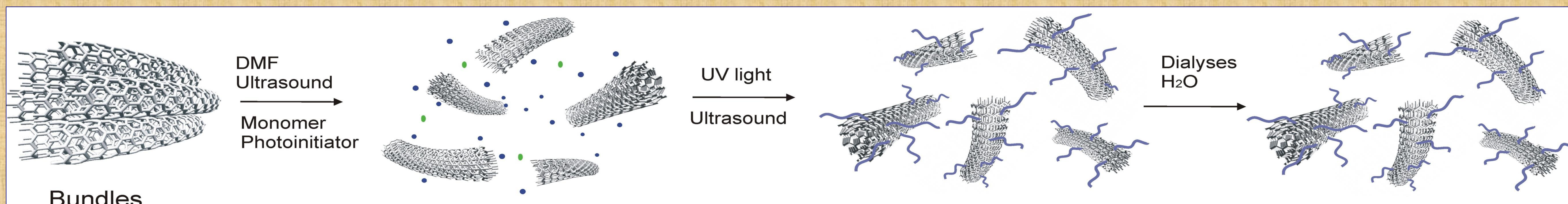
Laboratory of Polymerization Processes, Institute of Polymers, Bulgarian Academy of Sciences "Akad. G. Bonchev" str., bl.103A, 1113 Sofia, Bulgaria; e-mail: neoblade@abv.bg

Introduction

Pristine carbon nanotubes (CNTs) interact mutually by van der Waals forces which makes difficult their dispersibility in liquids and processing. The modification of carbon nanotubes enables preparation of stable aqueous dispersions and can overcome the apparent cytotoxicity of non-modified CNTs that makes these materials of special interest for biochemical and biomedical applications. Various hydrophilic and temperature-responsive polymers were covalently attached onto full-length multi-walled carbon nanotubes via UV-initiated free-radical polymerization.

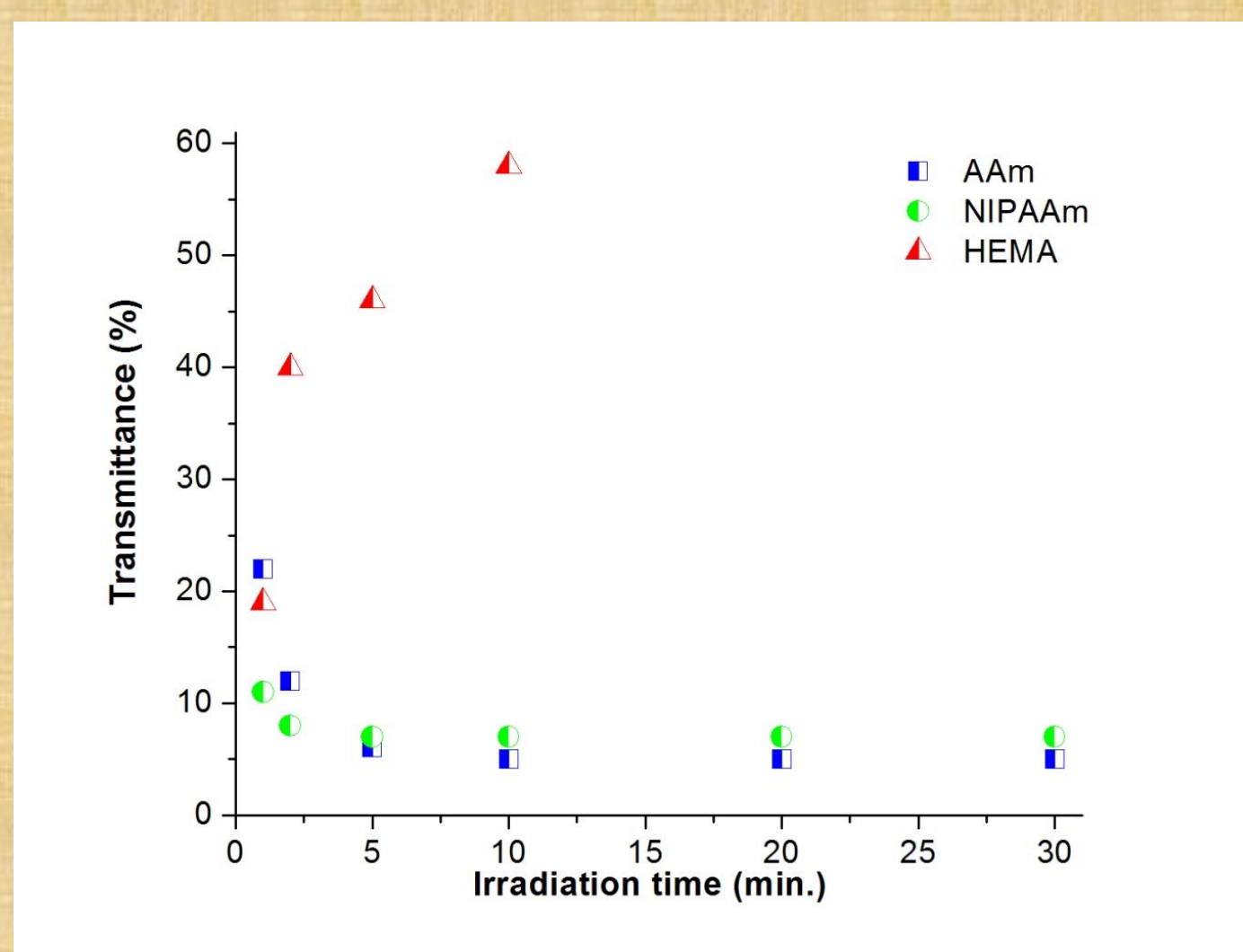
Strategy

Grafting of polymers onto MWNTs via UV-induced free radical polymerization

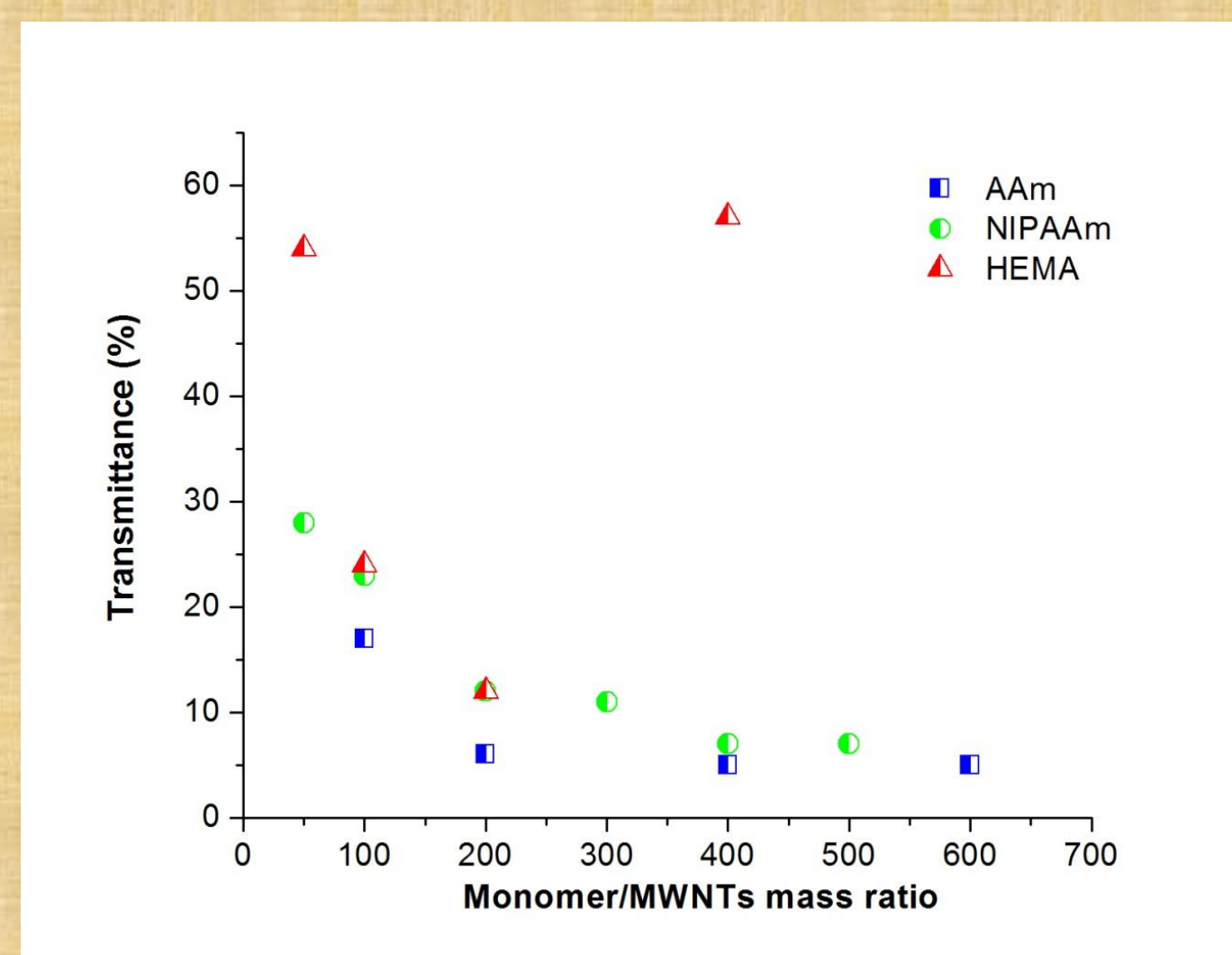


Results and Discussions

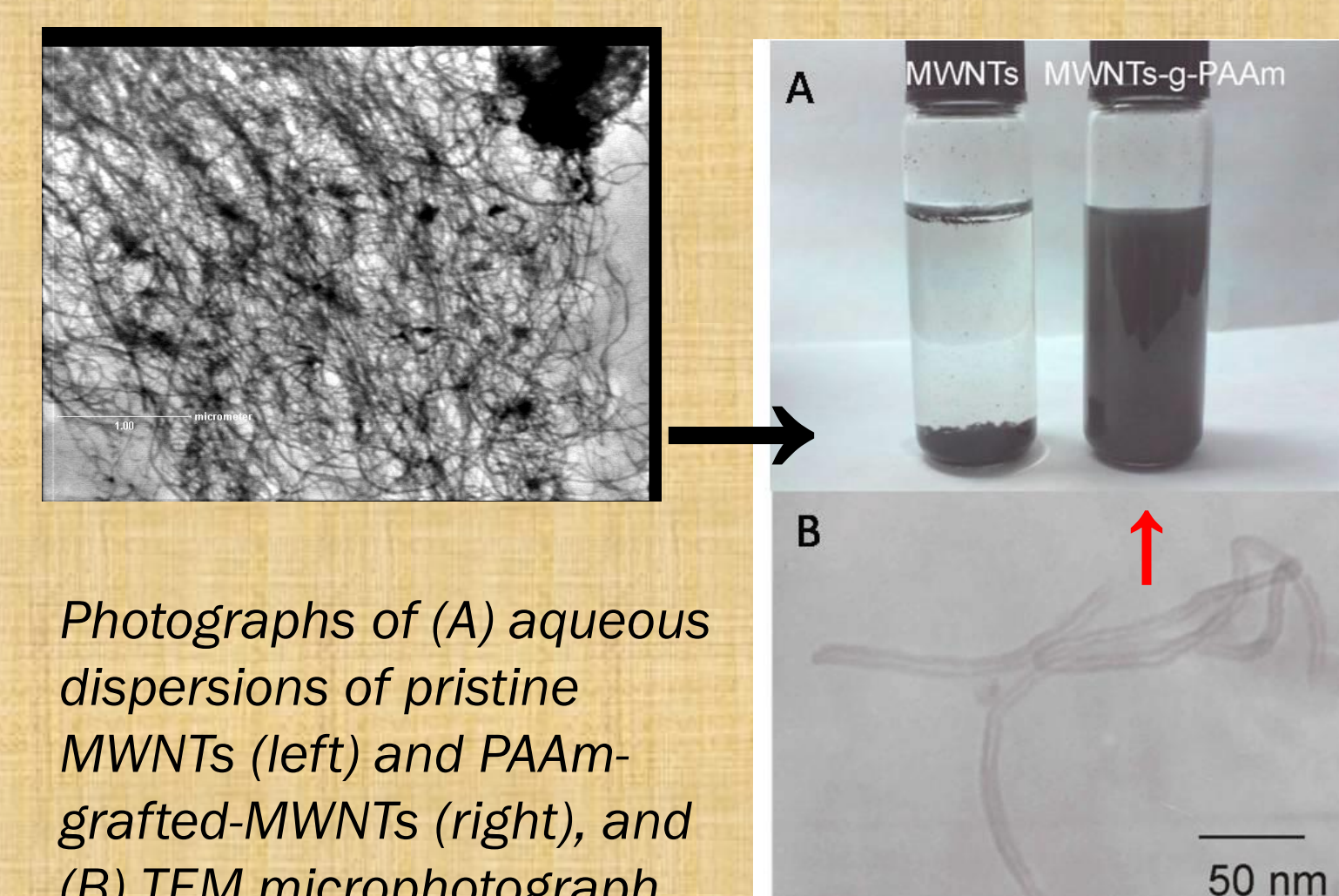
In our work we used Multi-walled carbon nanotubes: produced by the CVD method (carbon content >95%; OD×ID×L:20-30nm × 5-10nm × 0.5-200 μm)



Effect of the irradiation time(dose) on the turbidity of aqueous dispersions of MWNTs-g-polymer (monomer:MWNTs mass ratio 400:1)



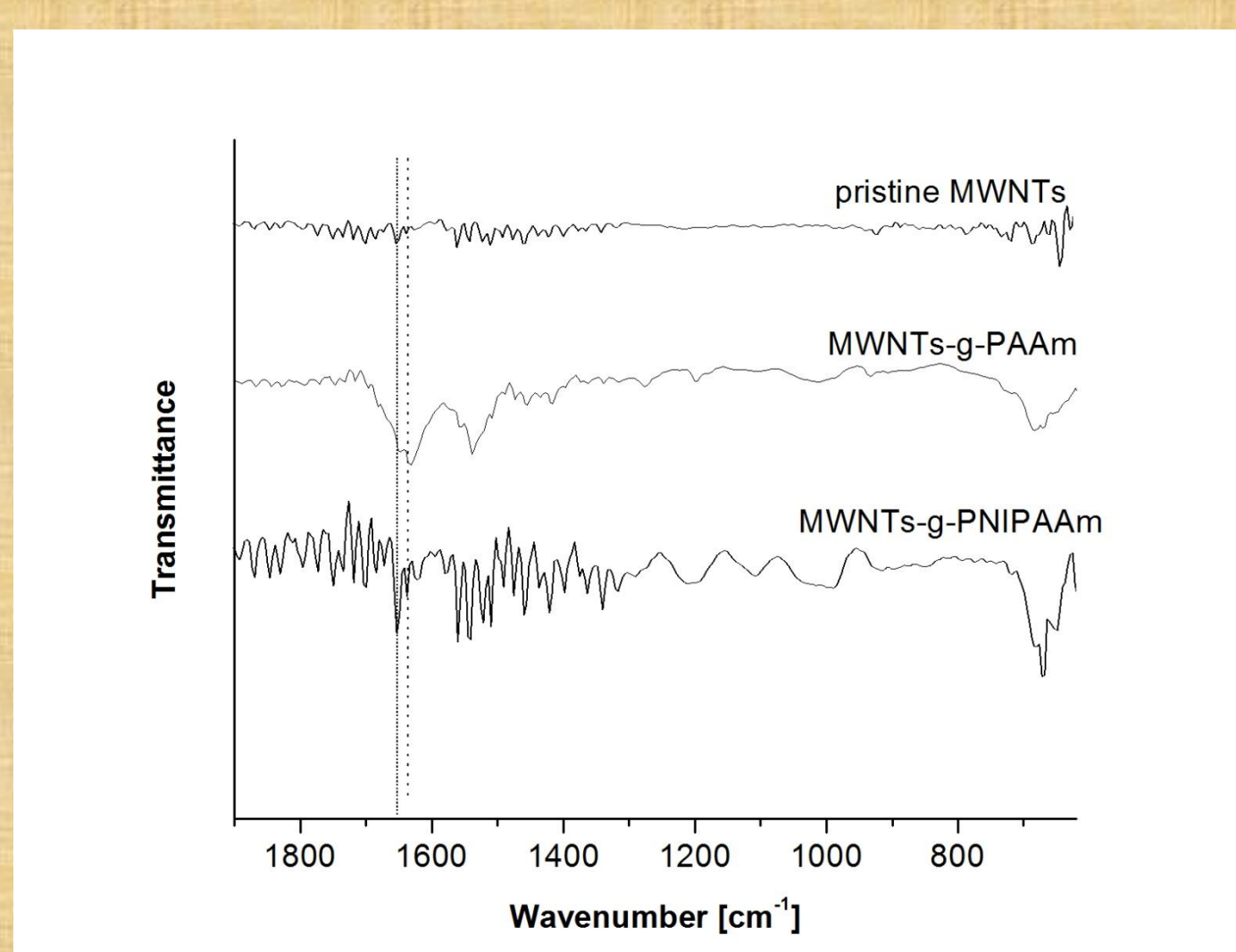
Effect of monomer:MWNTs mass ratio on the turbidity of aqueous dispersions of MWNTs-g-polymer (10 min irradiation with UV light)



Photographs of (A) aqueous dispersions of pristine MWNTs (left) and PAAm-grafted-MWNTs (right), and (B) TEM microphotograph of individually dispersed MWNTs-g-PAAm

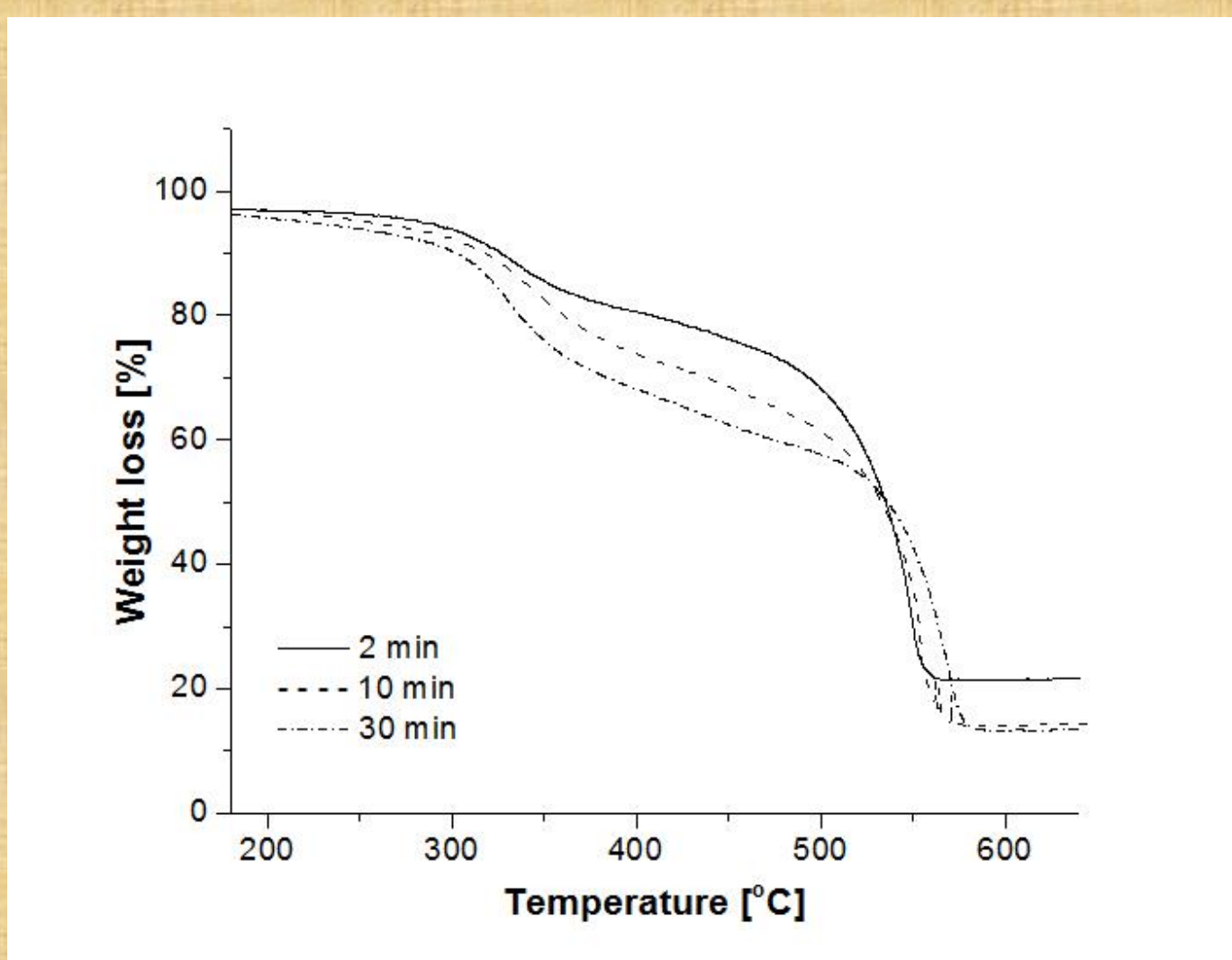
It was found that 5 min irradiation with UV light at a dose rate of 5.7 J/cm² min is adequate for preparation of stable aqueous dispersions of PAAm- and PNIPAAm-grafted MWNTs at monomer/MWNTs mass ratio > 200:1

The visual inspection of MWNTs dispersions provides roughly an evidence whether sufficient polymer chains are grafted



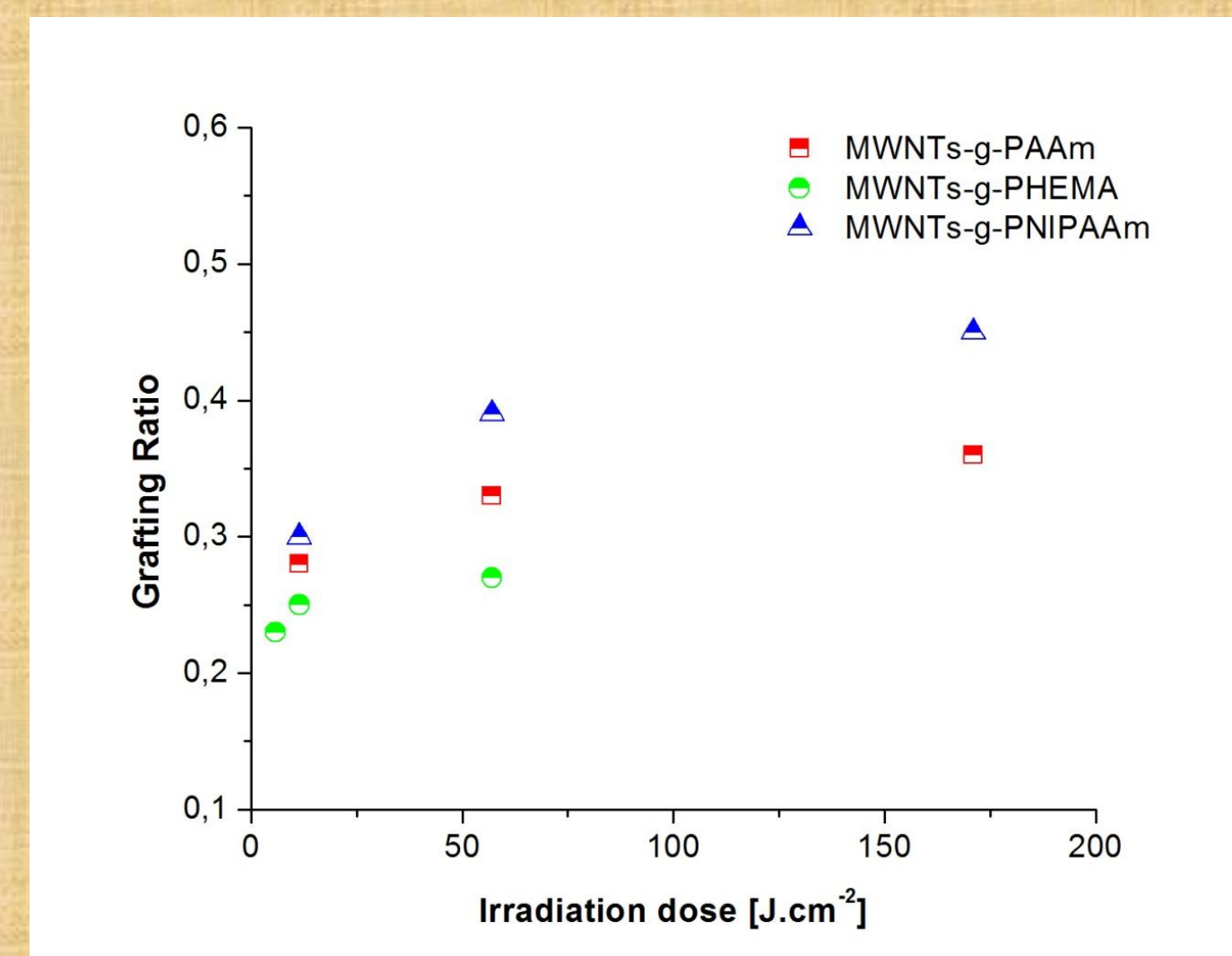
FTIR spectra of the pristine MWNTs, MWNTs-g-PAAm and MWNTs-g-PNIPAAm

The most characteristic absorption peaks of PAAm and PNIPAAm (C=O stretching vibration of the amide group at 1660 cm⁻¹; the bending vibration of the amide group at 1630 cm⁻¹) were detected

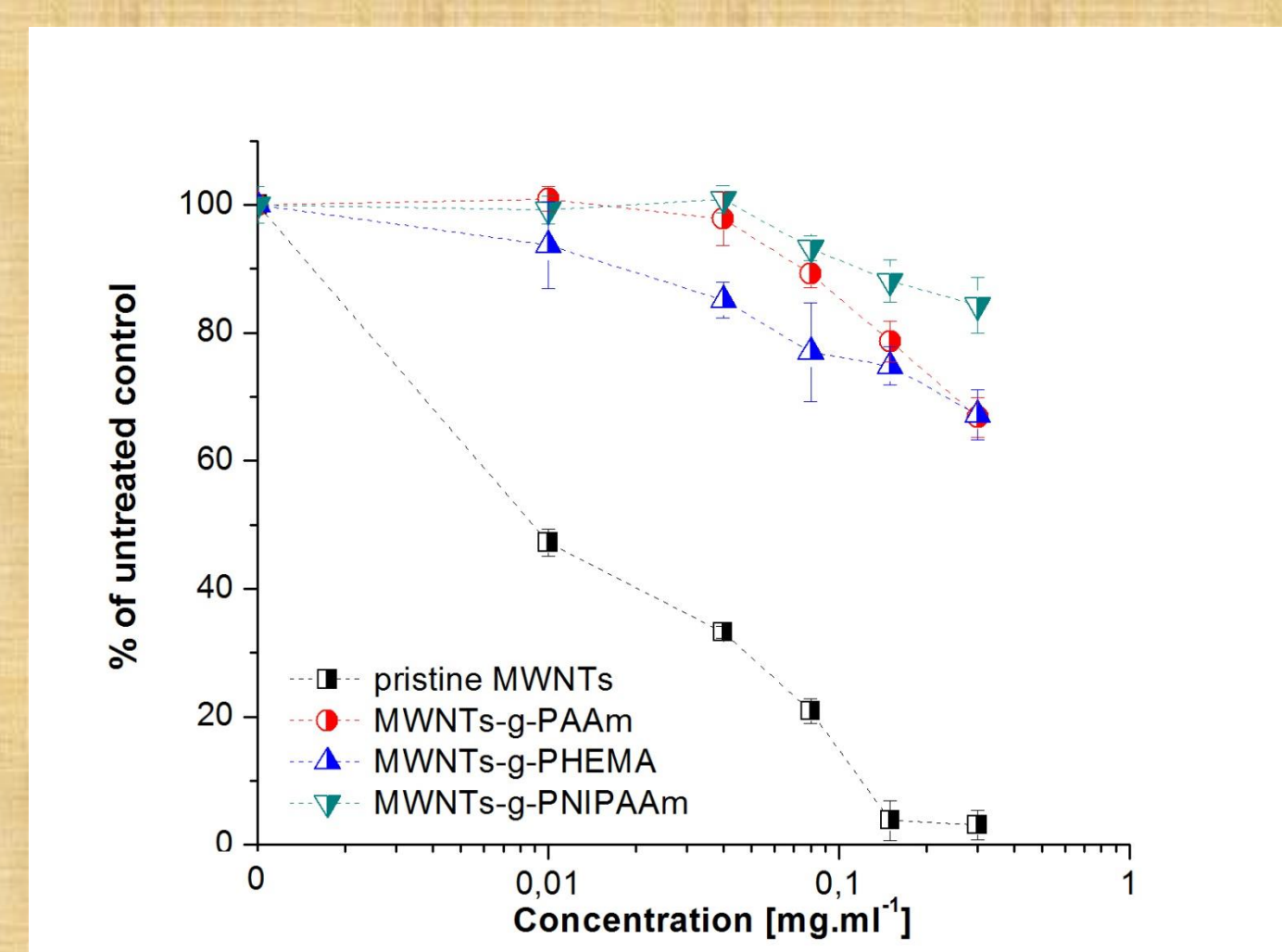


TGA curves of MWNTs-g-PNIPAAm obtained at different irradiation time

Evidence for the relative amount of polymers grafted on to MWNTs was provided by TGA analysis

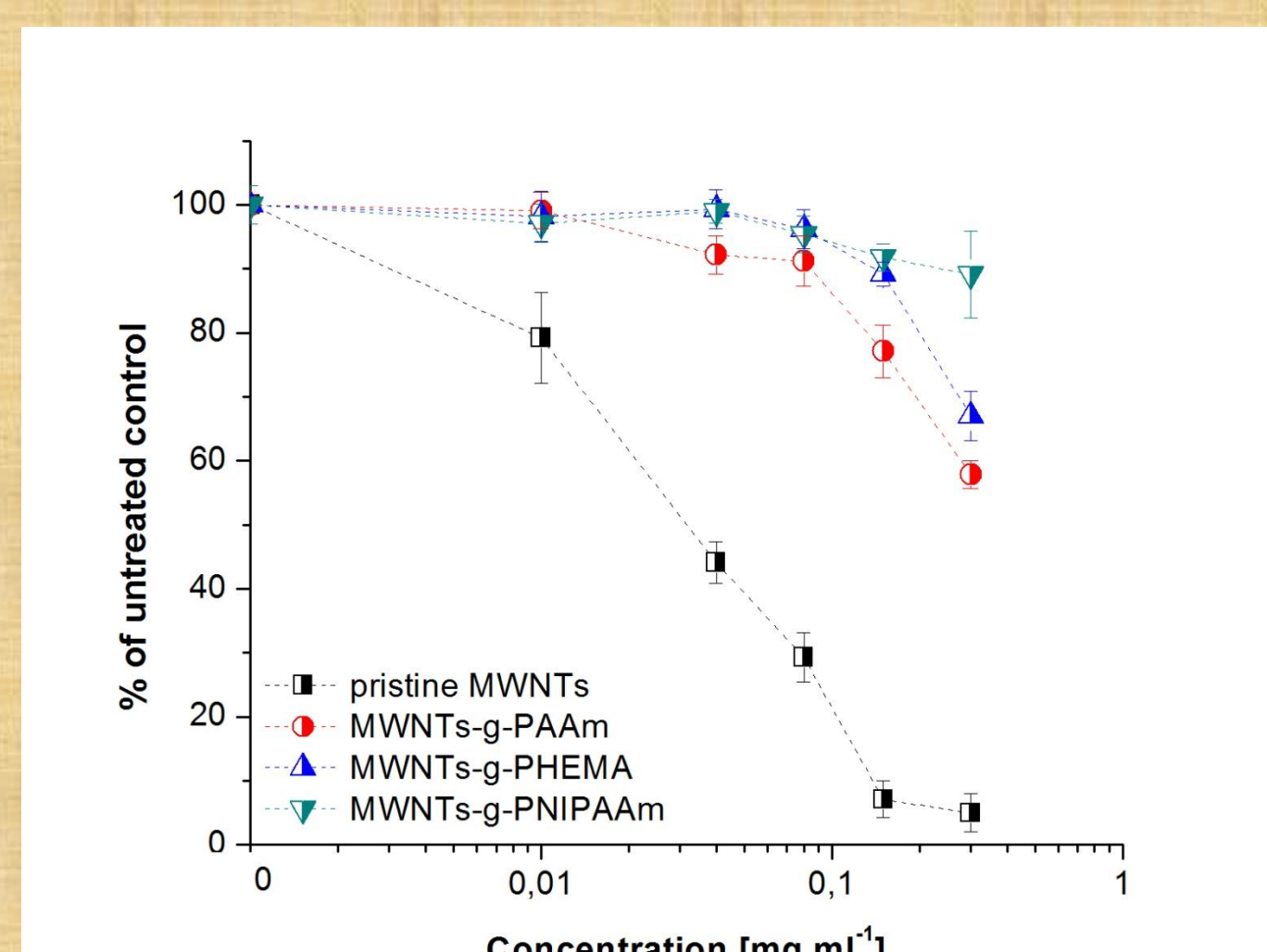


Effect of the irradiation dose on the grafting ratio of different polymer-grafted MWNTs

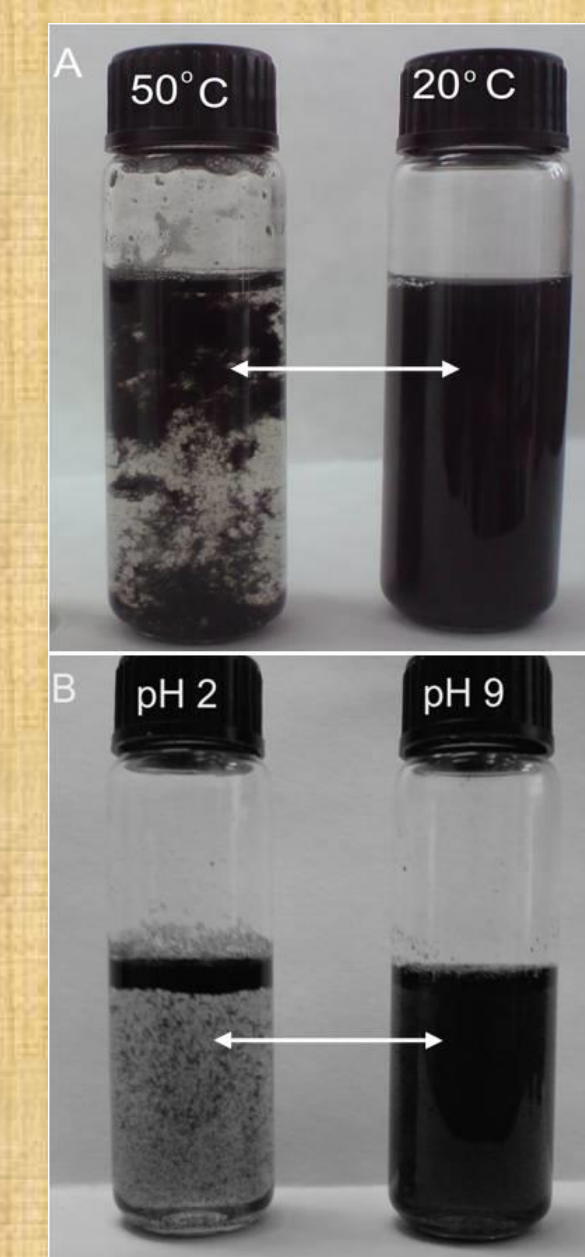


Cytotoxic effects of: pristine MWNTs, MWNTs-g-PAAm, MWNTs-g-PHEMA and MWNTs-g-PNIPAAm against the human multiple myeloma-derived cell line

The modified MWNTs exhibit remarkably improved biocompatibility, especially PNIPAAm-grafted MWNTs which are non-cytotoxic even at concentration of 300 mg/mL



Cytotoxic effects of: pristine MWNTs, MWNTs-g-PAAm, MWNTs-g-PHEMA and MWNTs-g-PNIPAAm against the human colon carcinoma-derived cell line



Photographs of aqueous dispersions of (A) MWNTs-g-PNIPAAm at different temperature and (B) MWNTs-g-poly(sodium methacrylate) at different pH

Grafting of stimuli-sensitive polymers onto MWNTs allows a reversible precipitation upon external stimuli

Gelatin micro- and nanocapsules preparation via sonochemical method

I. Yankova, E. Vassileva

Laboratory on Structure and Properties of Polymers, Faculty of Chemistry, Sofia University
1, James Bourchier blvd., 1164 Sofia, Bulgaria

Nanocapsules are submicronic colloidal drug carriers with a solid shell around an oily core. Morphologically, they are ranged between nanoemulsions and nanospheres. In nanoemulsions and nanocapsules the drug is located in the oily moiety which in the case of nanocapsules is surrounded by a polymeric shell. In order to improve the delivery of hydrophobic drugs, growth factors, proteins and other biologically active compounds, we are exploring the potential of nano-scaled carriers made from biodegradable polymers for controlled and targeted delivery to specific organs, tissues, and cells.

Sonochemical method for micro and nanocapsules preparation

Empty gelatin nanocapsules

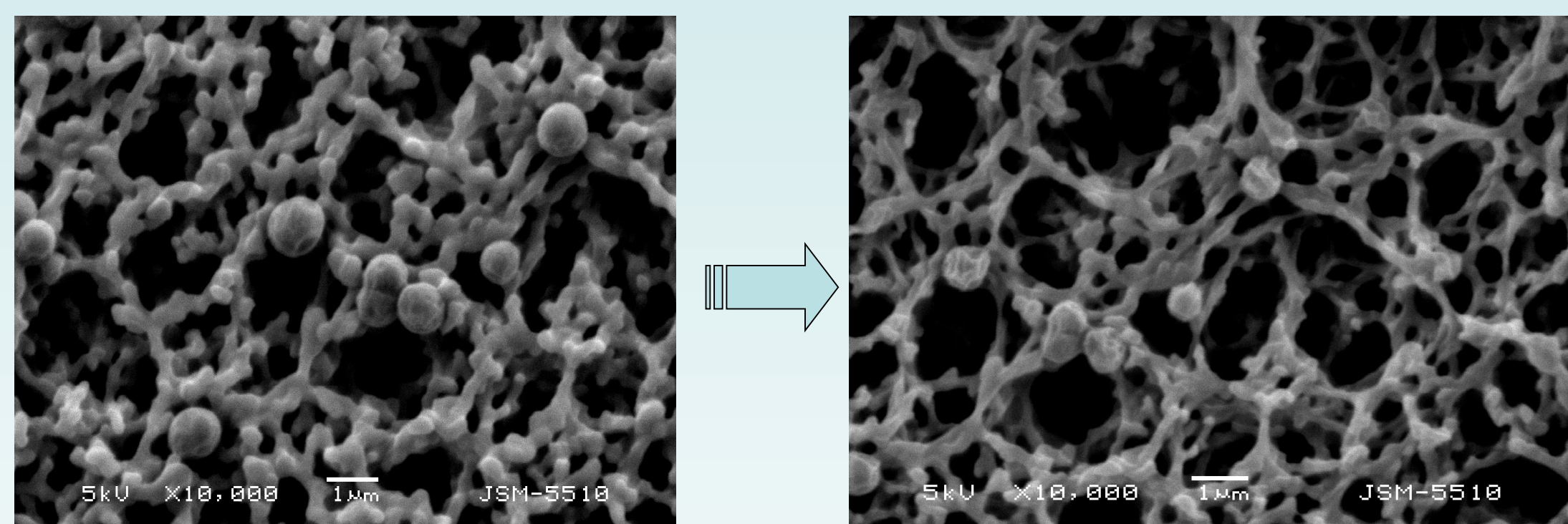


Figure 1. SEM of empty gelatin nanocapsules.

Empty gelatin nanocapsules have been shown to be very unstable under electron irradiation in the SEM camera and after 2 scans they collapsed as shown in the Figure.

Aspirin loaded gelatin particles

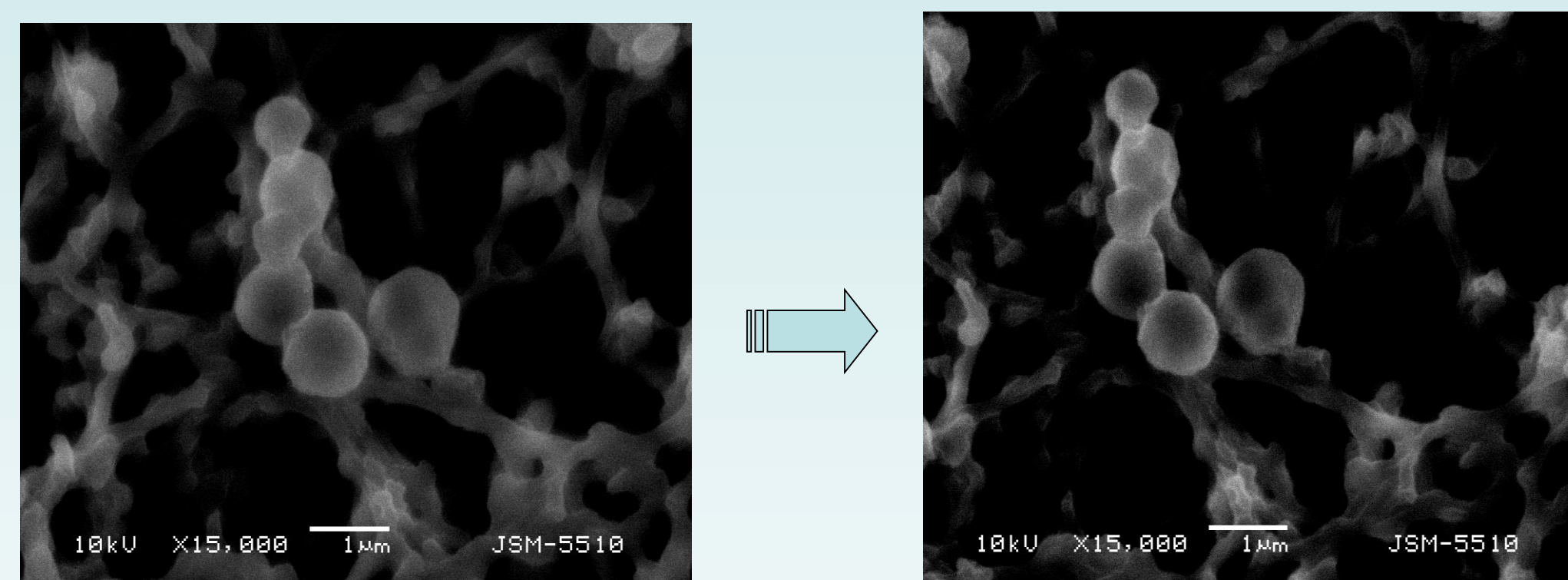


Figure 2. SEM of aspirin loaded gelatin nanocapsules.

Gelatin nanocapsules loaded with aspirin remain almost with their initial shape and size (Figure 2) due to the inclusion of aspirin in their core.

Transmission electron microscopy of gelatin capsules

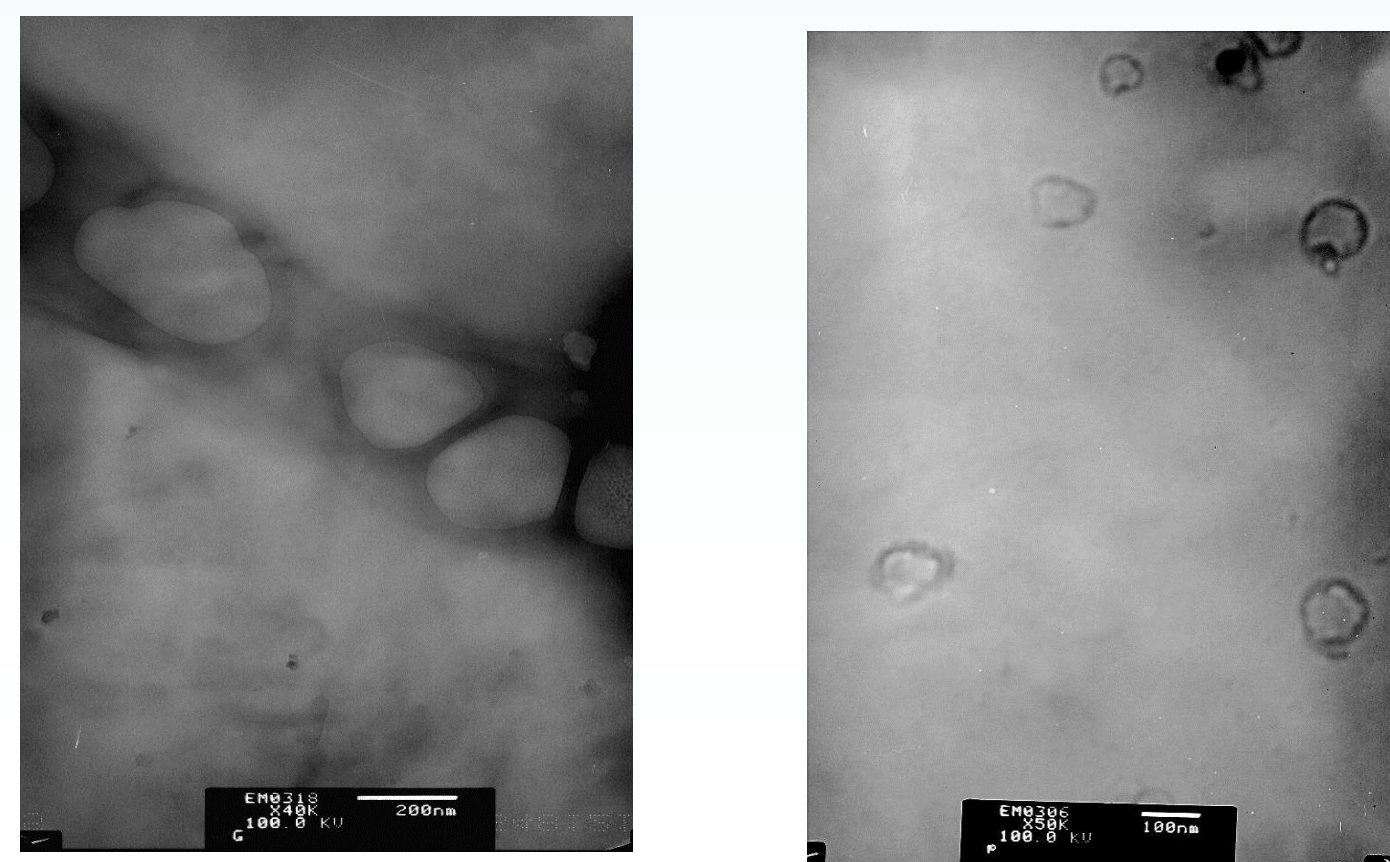


Figure 3. The study of gelatin capsules by transmission electron microscopy (TEM) clearly shows the hollow core of the particles.

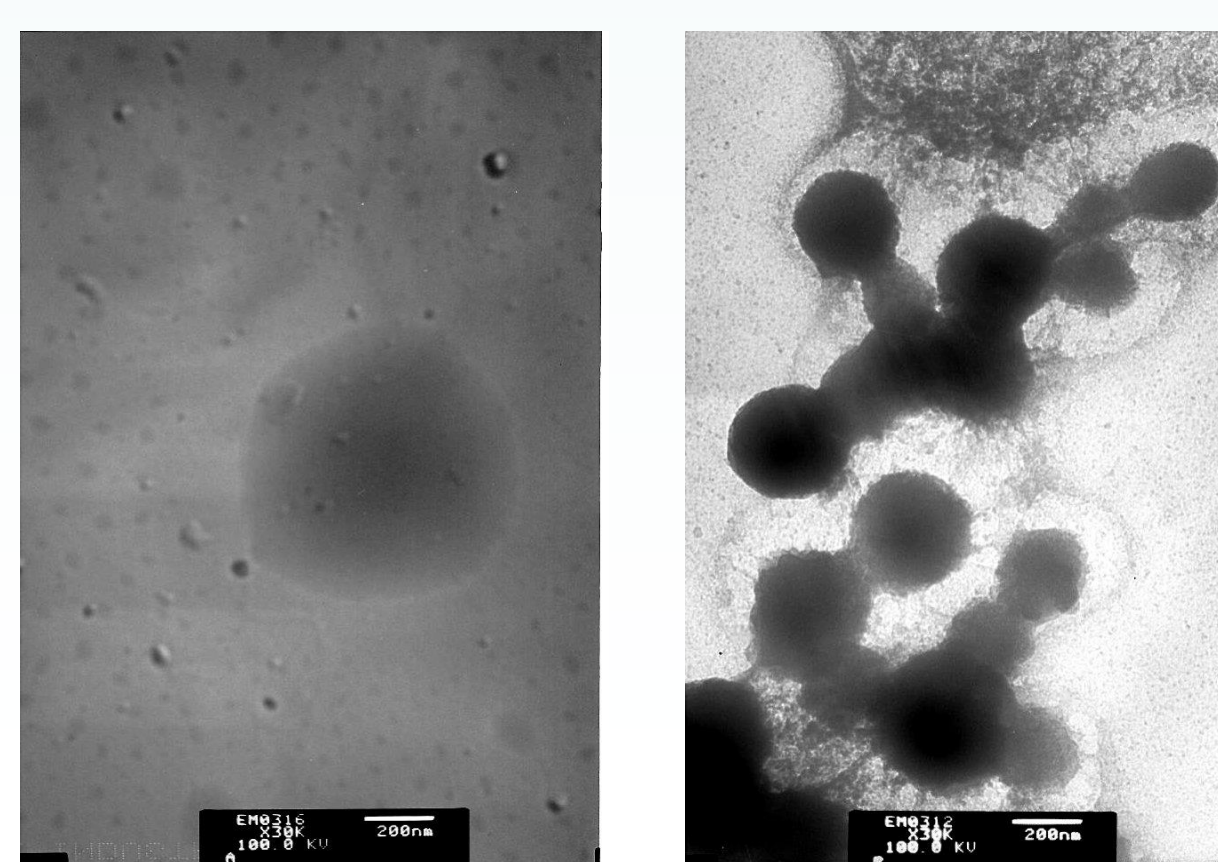


Figure 4. TEM of gelatin nanocapsules loaded with aspirin, obtained at pH=5.22 at 30°C for 3.5 min sonication time.

Dynamic light scattering of gelatin capsules

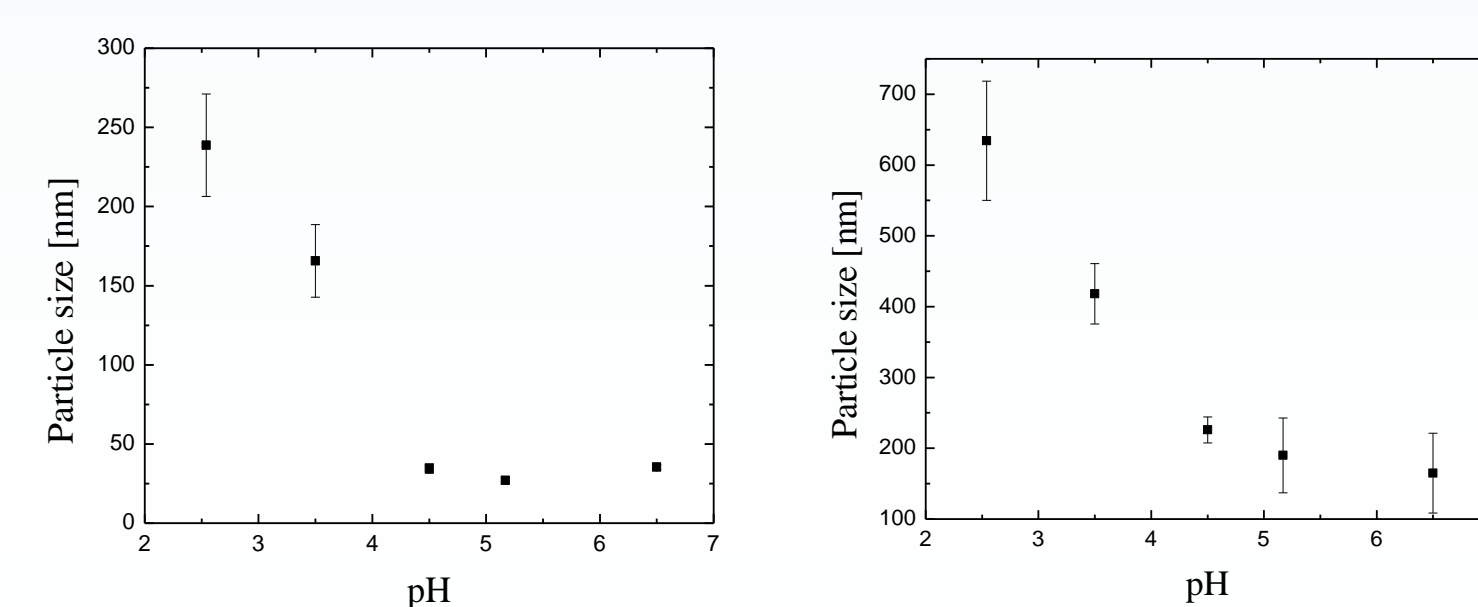


Figure 5. pH dependence of gelatin nanocapsules size as measured by dynamic light scattering for the both peaks from the bimodal particles size distribution (respectively A and B).

Preparation of gelatin nanocapsules loaded with α -tocopherol:

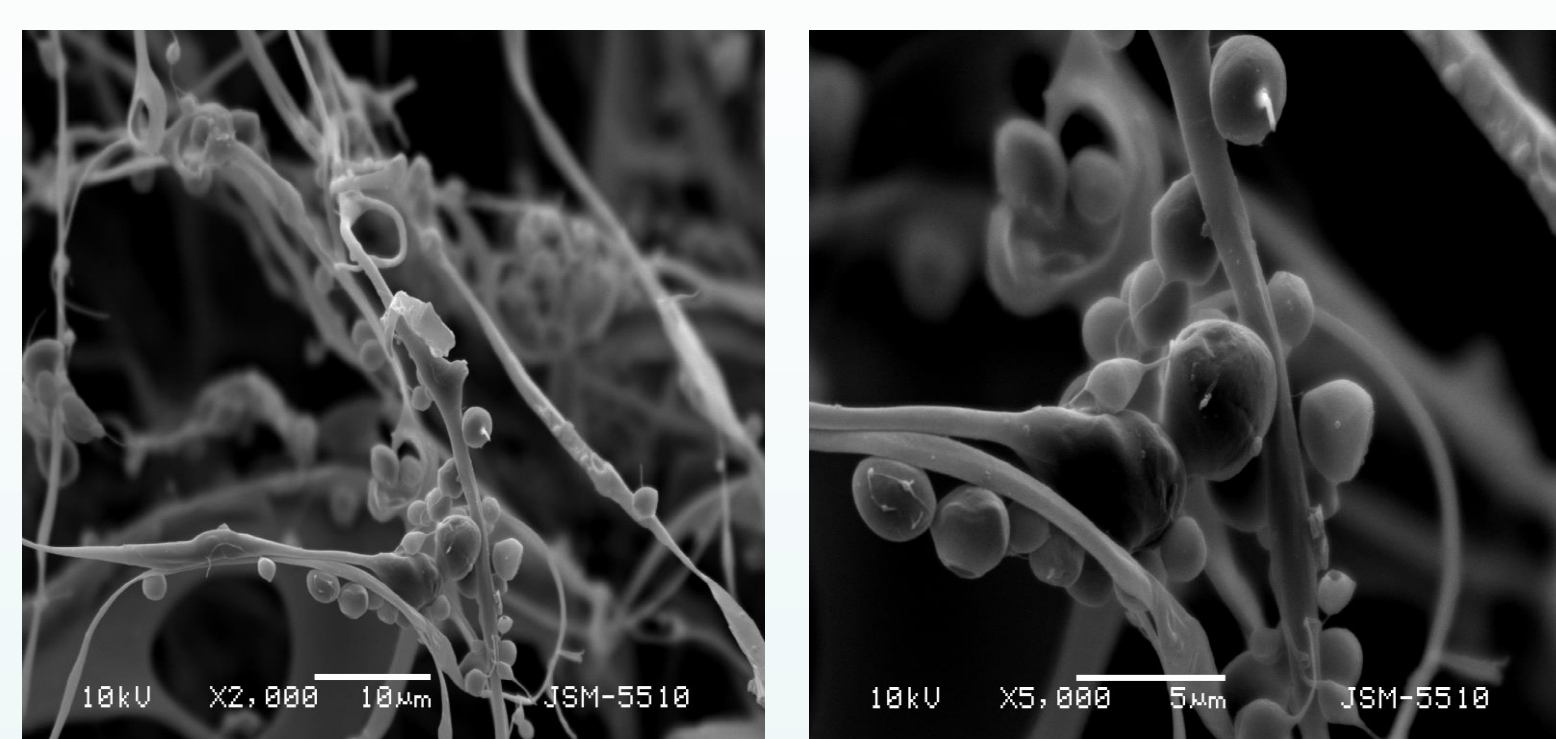


Figure 6. SEM of α -tocopherol loaded gelatin nanocapsules.

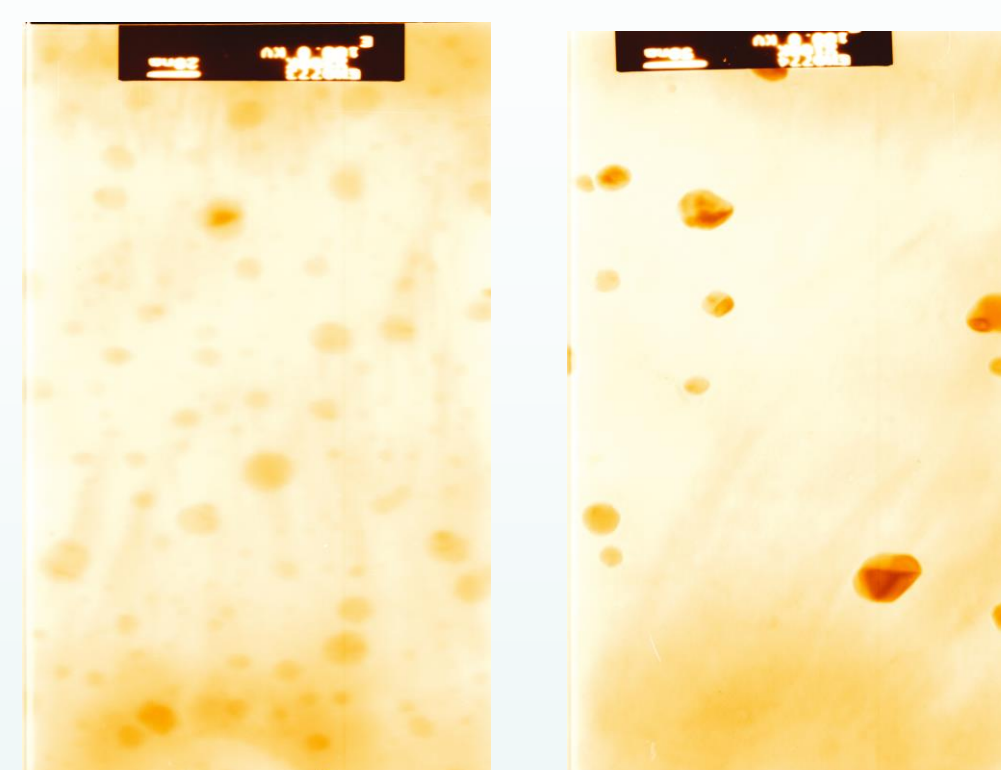


Figure 7. TEM of gelatin nanoparticles loaded with α -tocopherol.

Table 1. Influence of sonication time on particle size.

Time [min]	1 st peak	2 nd peak
3.5	27.8 ± 4.3	190 ± 53
7	36.0 ± 2.6	222 ± 25

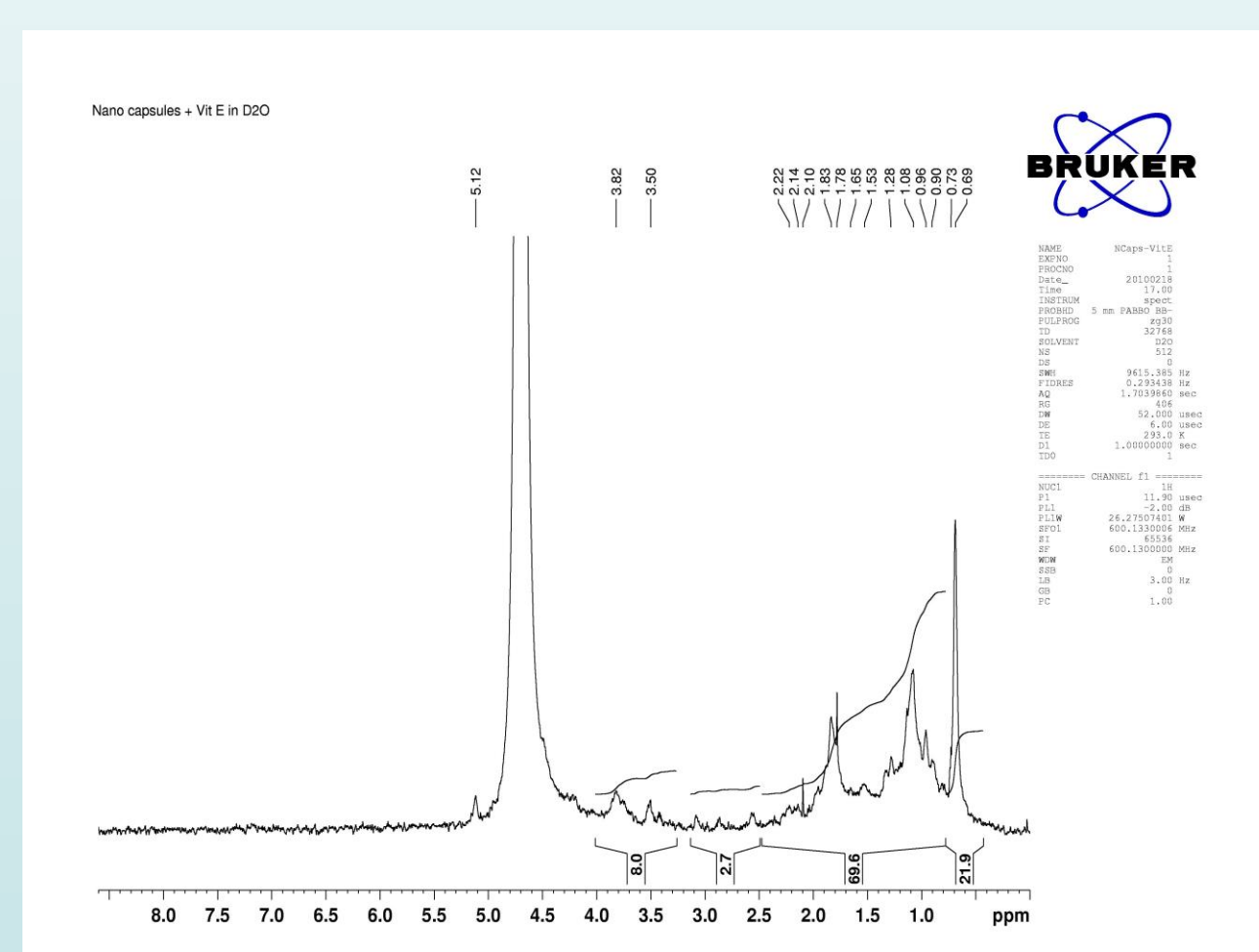


Figure 8. NMR of α -tocopherol loaded gelatin nanocapsules.

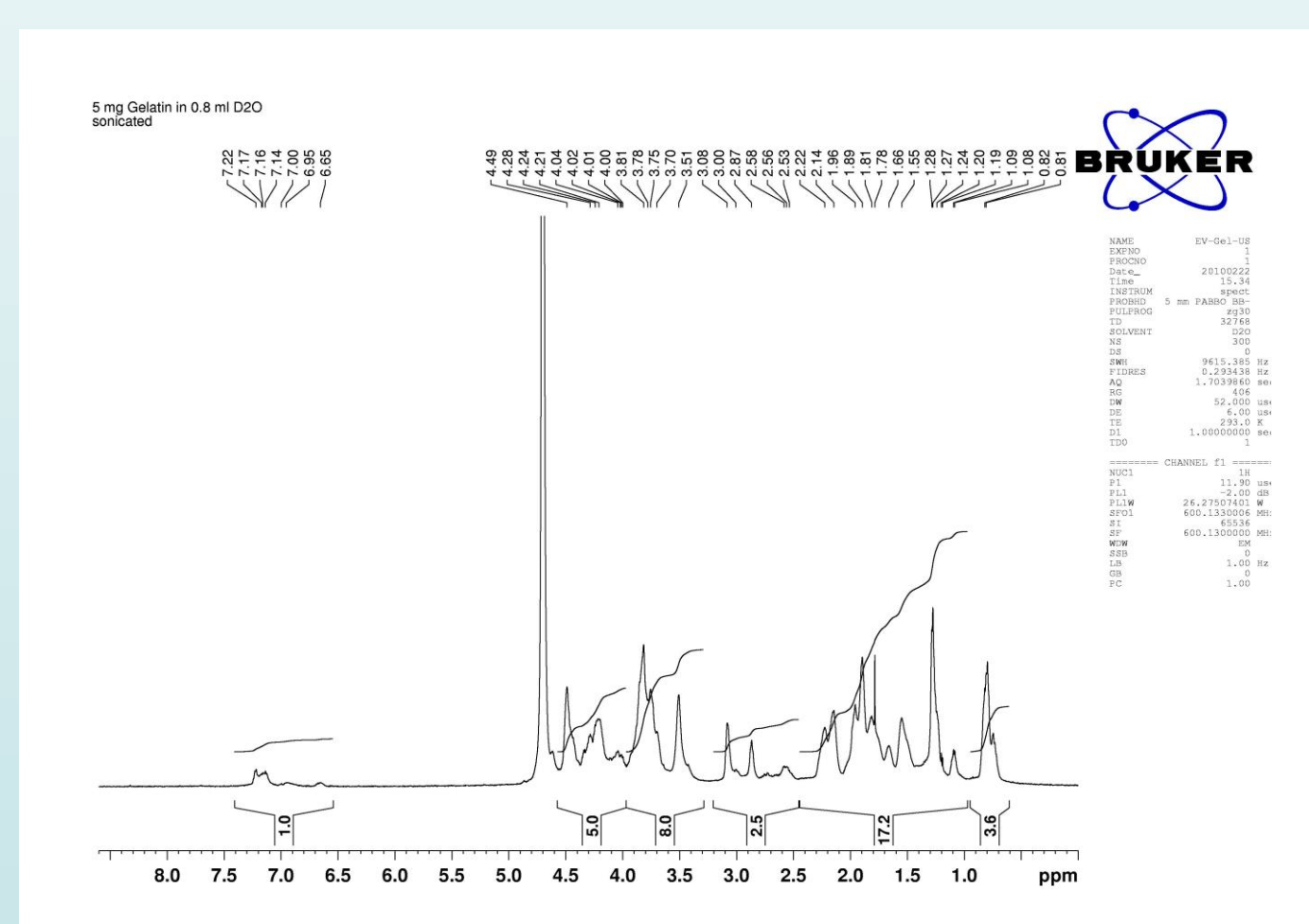


Figure 9. NMR of empty gelatin particles.

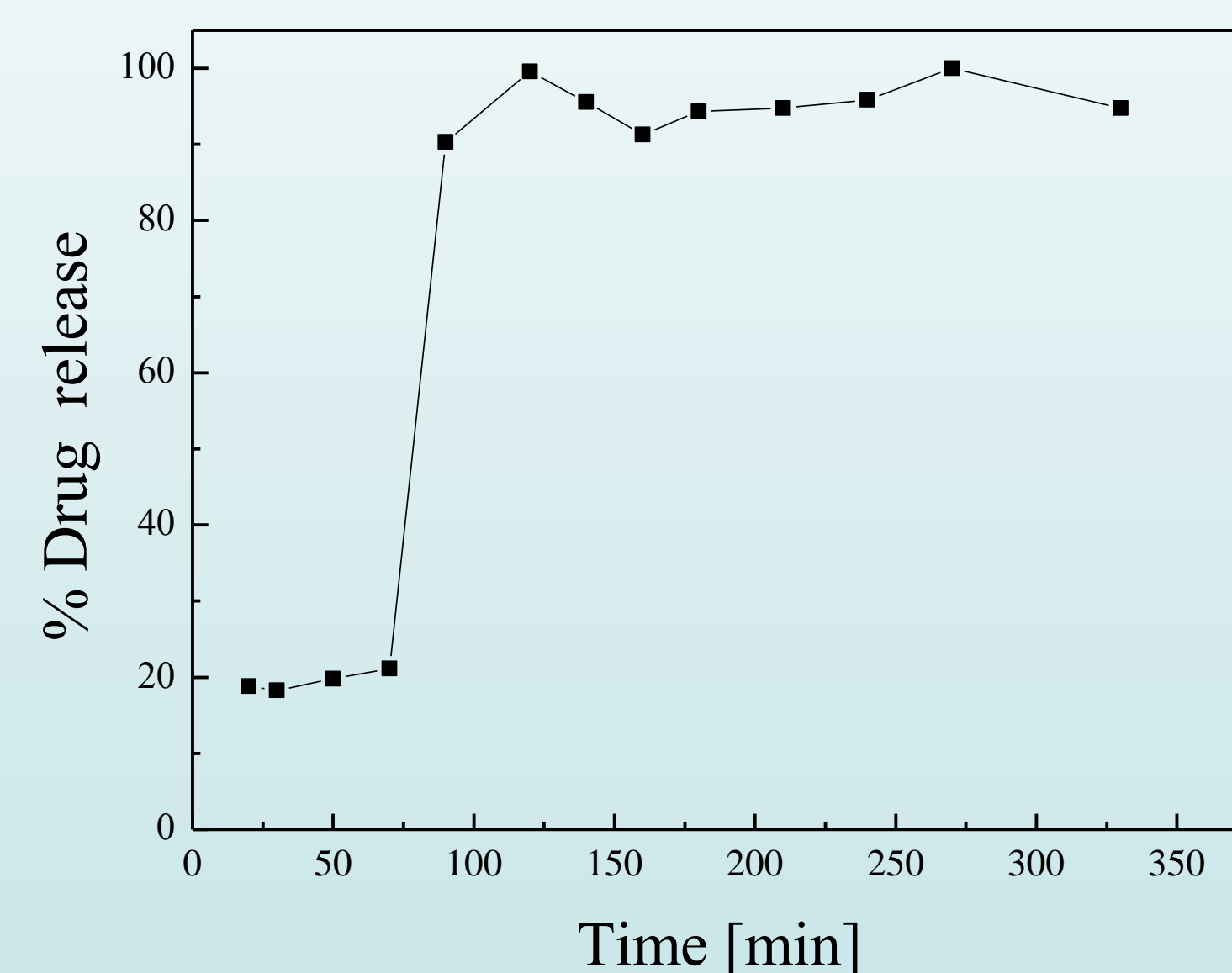


Figure 10. Release UV profile of α -tocopherol from gelatin nanocapsules.

Conclusions

Sonochemical method has been applied to gelatin and for the first time gelatin nanocapsules are obtained and proved to be with hollow core. The influence of parameters as pH and ultrasound irradiation time on the gelatin nanocapsules size has been studied. Thus obtained nanocapsules have been loaded with aspirin and α -tocopherol and *in vitro* release of the second has been followed by UV spectroscopy.

Acknowledgements: This research is financed through the National Fund for Scientific Investigations, Project No DO02-198/17.12.2009. The presentation of current investigation is financed by Project No BG051PO001/07/3.3.-02/51.



QUALITY STUDY OF RECYCLED ELASTICIZED LDPE/PP BLENDS FROM TECHNOLOGICAL SCRAP

Irena Borovanska¹, Rosario Benavente², Strashimir Djoumalisky¹, George Kotzev¹

¹Central Laboratory of Physico-Chemical Mechanics, Bulgarian Academy of Sciences, Acad. G. Bonchev St., Block 1, 1113 Sofia, Bulgaria; e-mail: reniboro@abv.bg

²Instituto de Ciencia y Tecnología de Polímeros CSIC, Juan de la Cierva 3, 28006-Madrid, Spain.

I. INTRODUCTION

The statistics show that in the polymer wastes the most essential part is the volume of polyethylene and polypropylene [1]. Because of the facts that the both polymer are mixed in the plastic waste and their separation gravimetrically is difficult, they have to be utilized as blend. When a polymer blend consists of two or more polymers they tend to separate each other because of their mutual incompatibility. Compatibilization is a process of modification of the interfacial properties in immiscible polymer blend resulting in reduction of the interfacial tension, formation and stabilization of the desired morphology [2,3].

The objective of this poster is to characterize the industrial scraps: LDPE and PP and their blends modified with different amount of ethylene propylene rubber (EPR) by usage of DSC, FTIR, WAXS and DMTA.

II. EXPERIMENTAL

Double and triple blends were prepared from industrial scrap from packaging - LDPE and PP in the form of granulate, supplied from "Asenova Krepost" Ltd (Asenograd- Bulgaria). The triple blends were prepared by adding the non-polar terpolymer: ethylene-propylene diene rubber (EPR) "Keltan 512". The polymers were blended in a twin-screw extruder type DSE 35/17D "BRABENDER" at following conditions: screw rate 20 rpm, temperatures in the barrel zones: I - 175°C; II -190°C III -200 and IV - 210°C. The used composition of polyolefin blends were shown in Table 1.

DSC was carried out with a TA Q100 differential scanning calorimeter at a scanning rate of 10°C min⁻¹.

Fourier Transform Infrared Spectroscopy was carried out on a Perkin Elmer FTIR spectrometer using the attenuated total reflection (ATR) technique.

Wide-Angle X-Ray Diffraction (WAXD) patterns were recorded in the reflection mode by using a Bruker D8 Advance diffractometer. Cu K α radiation (0.1542 nm) was used.

Table1. Compositions

№	LDPE (wt%)	PP (wt%)	EPR (wt%)	Melt flow Index(2,16kr)-230°(g/10min)
1	100	-	-	1,37
2	-	100	-	4,33
3	50	50	-	3,38
4	46,5	46,5	7	2,30
5	45	45	10	2,00
6	42,5	42,5	15	1,74
7	40	40	20	2,10

Morphology of composites was studied by Scanning Electron Microscopy (SEM) on JEOL instrument.

The loss factor ($\tan \delta$) was measured as a function of temperature by using a Polymer Laboratories MK II Dynamic Mechanical Thermal Analyser (DMTA) working in the tensile mode.

III. RESULTS AND DISCUSSION

Recycled materials from one type often show a double or triple peak in DSC measurements, while a clean virgin material shows just one peak. The existence of double and/or wider peak of melting can appear in a sample that consists more than one plastic, a sample that consists of only one plastic but with different imperfections and magnitude of crystallinities, a sample with mechanical contaminants or in a degraded sample [4].

The broad peak at 60°C of LDPE is due to not so perfect crystals (Figure 1). PP is not pure material and presents some quantity of LDPE.

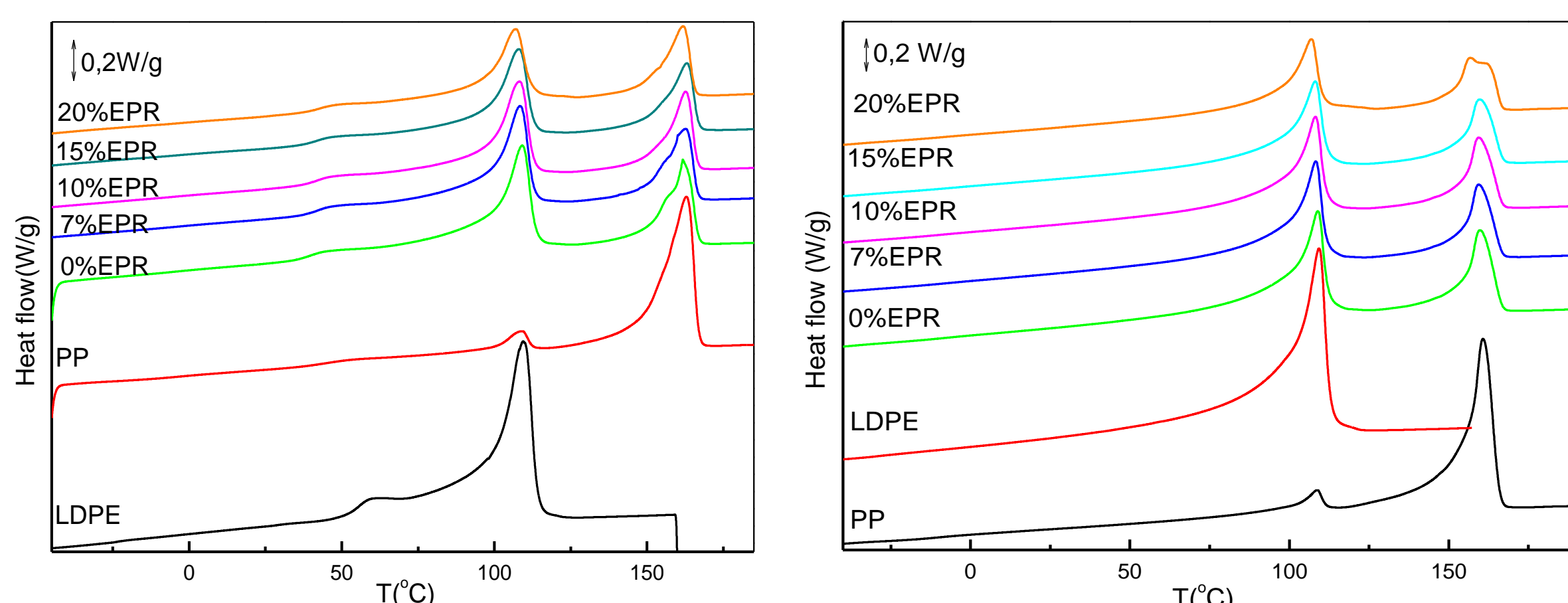


Figure 1: DSC curves of First melting temperatures of industrial scrap blends of LDPE and PP with different quantity of EPR.

Figure 2: DSC curves of Second melting temperatures of industrial scrap blends of LDPE and PP with different quantity of EPR.

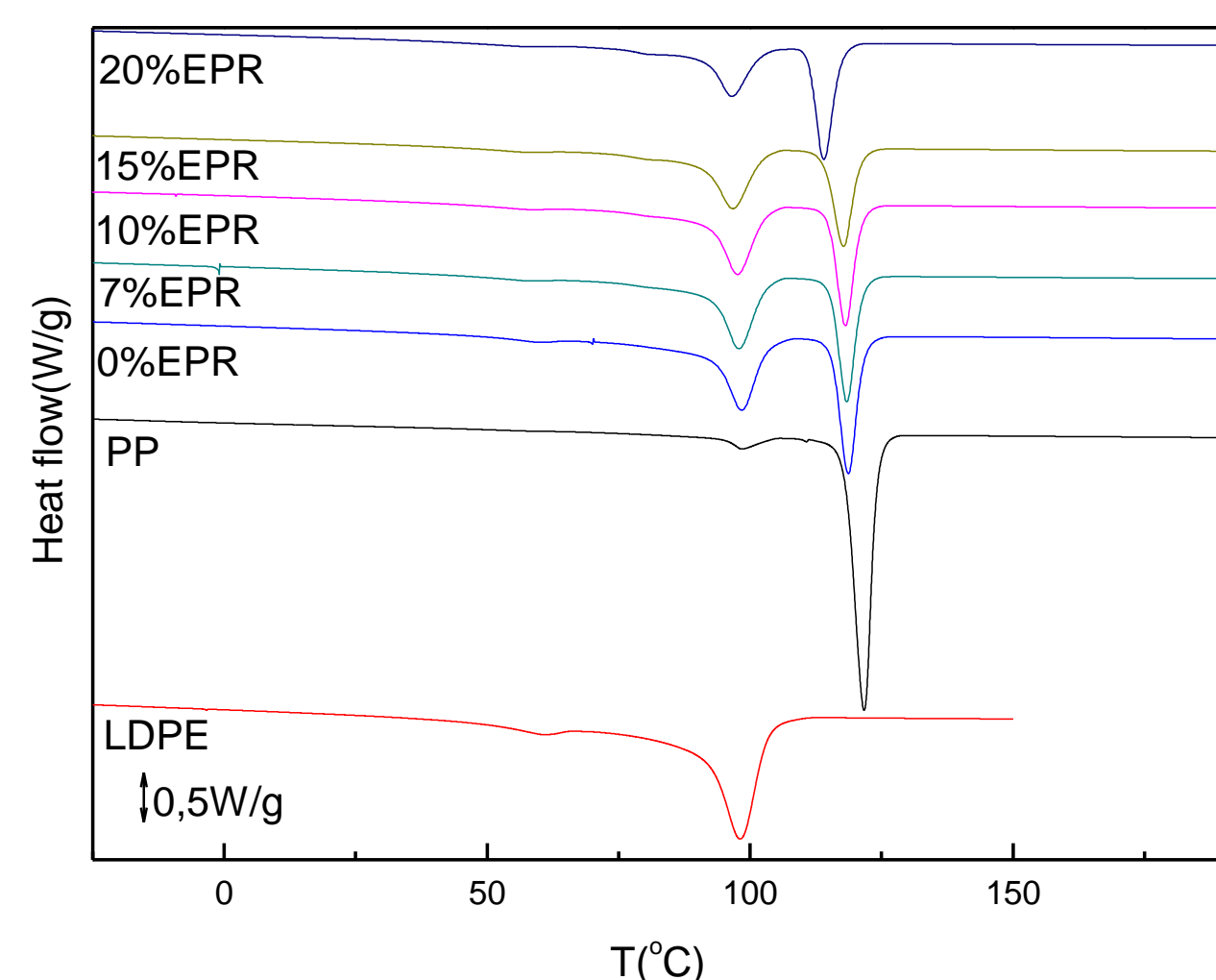


Figure 3: DSC Crystallisation of industrial scrap blends of LDPE and PP with different quantity of EPR.

The second melting confirms a small quantity of LDPE into the PP sample. The addition of EPR, leads to polymorphism in PP or more imperfected crystals, especially for the blend with 20% EPR.

With addition of rubber the heights of crystallization peaks of the both polymers decrease (Fig.3) and the crystallization peaks of PP move to smaller temperatures.

TABLE 2. Melting Temperatures (T_m) and Degree of Crystallinity at second melting at DSC and Degree of Crystallinity from WAXS of the compositions.

Concentrations of compatibilizer EPR(wt %)(№)	T_m^{LDPE} (°C)	T_m^{PP} (°C)	α_{cDSC}^{LDPE} (%)	α_{cDSC}^{PP} (%)	α_{cDSC} (%)	α_{cWAXS} (%)
100%LDPE(1)	109,35		35		35	44
100%PP(2)		160,65		33	33	47
0%EPR(3)	108,91	159,78	40	34	37	43
7%EPR(4)	108,2	159,39	38	34	34	41
10%EPR(5)	108,08	159,35	37	34	32	40
15%EPR(6)	108,11	159,65	36	36	31	40
20%EPR(7)	106,94	156,68	32	35	27	39

The addition of rubber moves the melting temperatures of the both polymers to the smaller values. The crystallinity of the blends decreases with increasing of quantity of modifier.

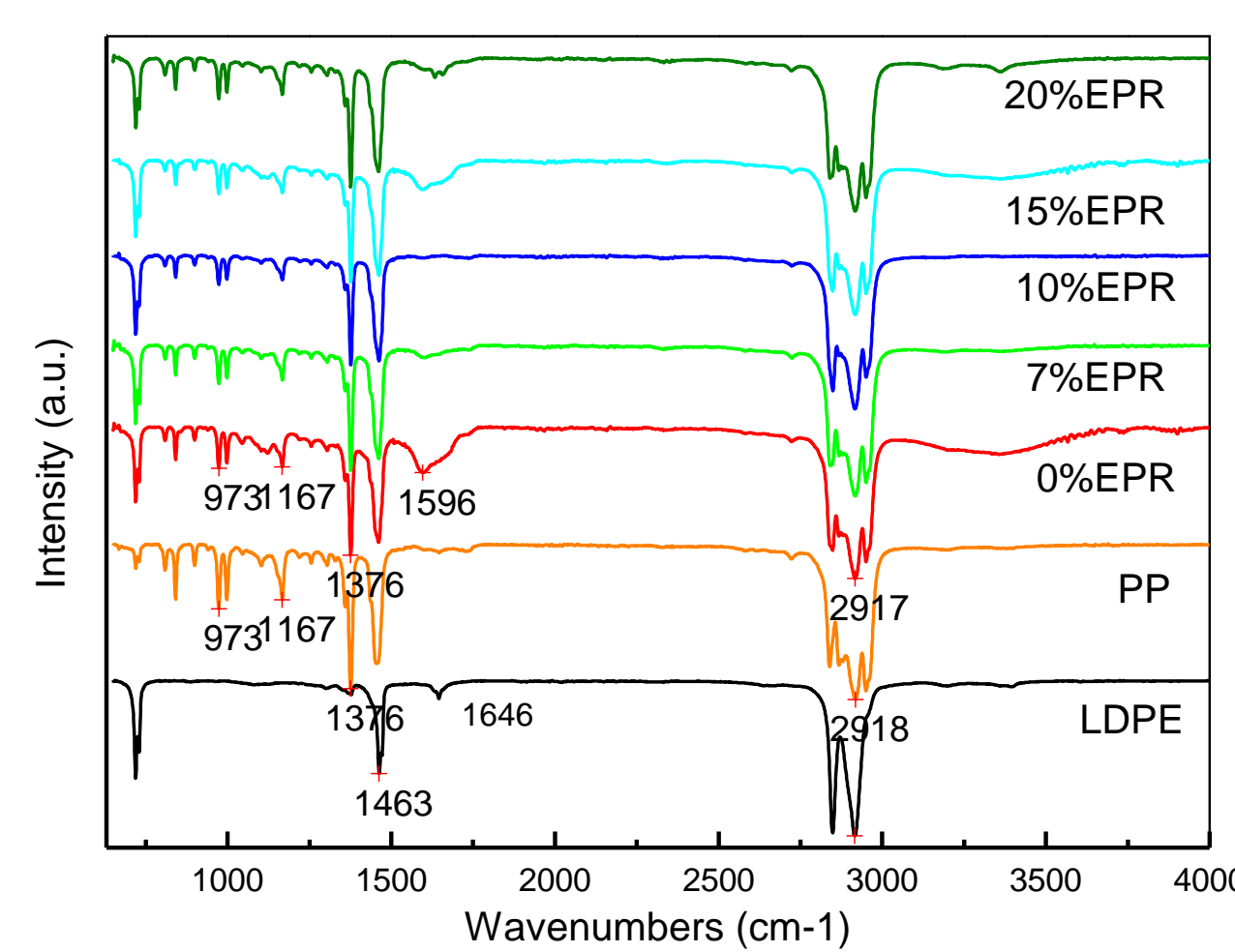


Figure 4: FTIR diffractograms of LDPE and PP and their blends

WAXD diffraction patterns of LDPE/PP/EPR technological waste blends (Figure 5) show that the incorporation of the rubber does not significantly change the crystal structure of the PP and LDPE mixture. It's seen appearance of two single small and sharp peaks at $2\theta = 10^\circ$ and $2\theta = 28,5^\circ$ which are not observed in the single polymers LDPE and PP. These peaks belongs to EPR.

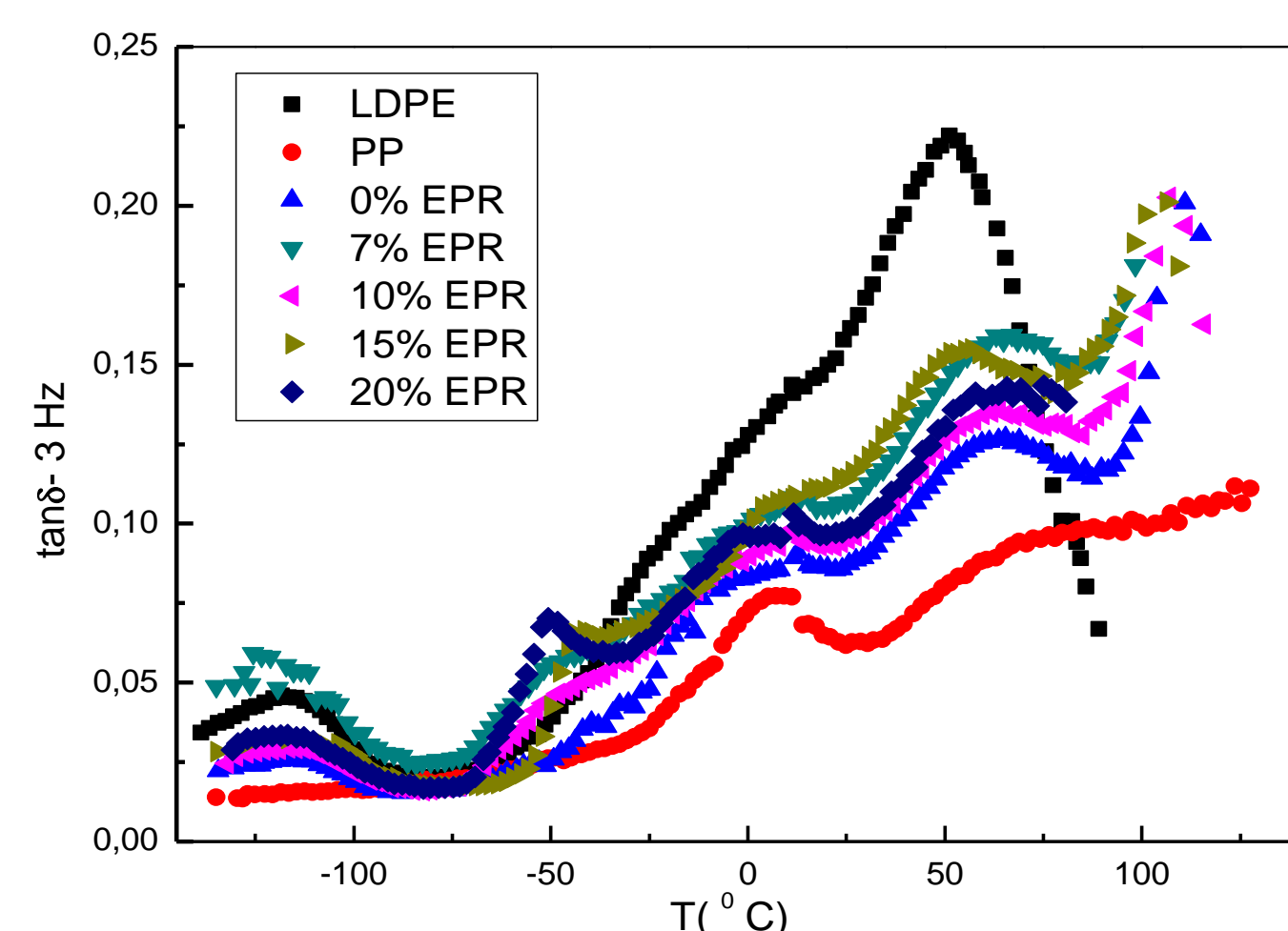


Figure 6 The $\tan \delta$ versus temperature curves for LDPE and PP and their blends .

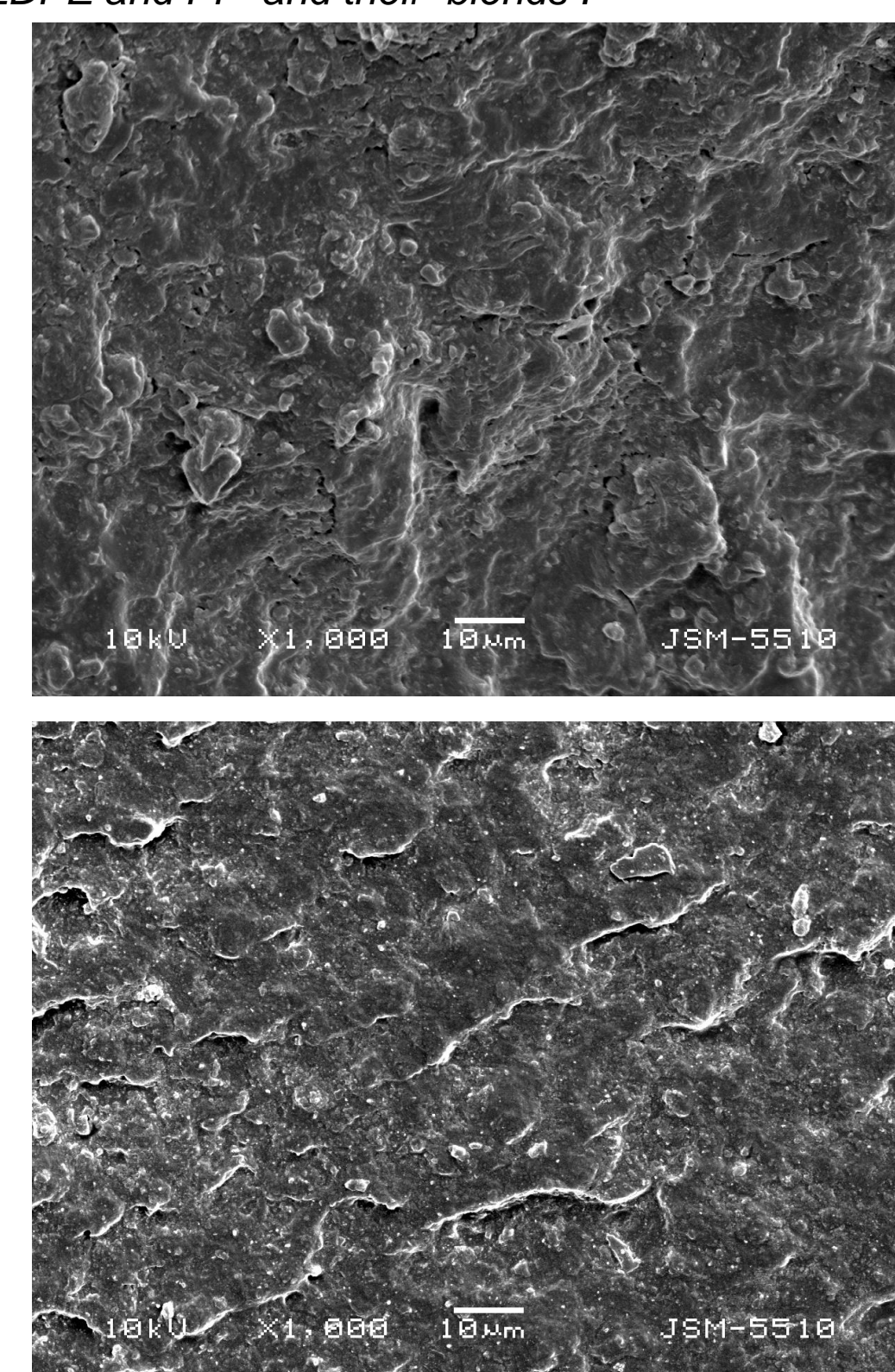


Figure 7: SEM morphologies of the blend LDPE:PP= 50:50(up) and of the blend LDPE:PP:EPR= 42,5:42,5:15(down)

The blends were foamed with 1wt.% azodicarbonamide. The foam recycled materials extent the spectrum of the possible applications. The sound absorption of foamed blends was higher than unfoamed ones(Fig.8)

IV. CONCLUSION

The effects of modification with rubber on the structure of industrial scrap LDPE/PP blends were studied. Differential scanning calorimetry shows a double peak when PP and LDPE are separately melted. For LDPE this suggests that it has endured some degree of degradation and some portion imperfected crystals which melt at lower temperatures. PP is not pure material and contents some quantity of LDPE, which deteriorate its properties. The addition of rubber move the melting temperatures of both polymers to the smaller values. The crystallinity of the blends decreased with increasing of quantity of modifier.

FTIR give us clear evidence about obtaining of some oxidational products and mechanical destruction. Modification with rubber minimize these unpleasant effects.

SEM images revealed better compatibility of the triple blends with EPR.

V. REFERENCE

- Galli P., Vecellio G., Polyolefins: The Most Promising Large-Volume Materials for the 21st Century, J. Appl. Polymer Sci.: Part A: Polymer Chemistry(2004) 42, 396-415
- Leszek A. U., Compatibilization of Polymer Blends, Can. J. Chem. Eng. (2002) 80, 1008-1016.
- Datta S., Lohse D., Polymeric Compatibilizers, Uses and Benefits in Polymer Blends, Carl Hanser Verlag, New York (1996) 3-9.
- Stangenberg F., Agren S., Karlsson S., Quality Assessments of Recycled Plastics by Spectroscopy and Chromatography, Chromatographia (2004) 59,101-106

ACKNOWLEDMENT: The authors wish to express their gratitude for the financial support of the Ministry of Education and Science through contract № BG051PO001/07/3.3-02/51.

Weak and broad absorption peak at 1646 cm⁻¹ in FTIR diffractograms LDPE (Fig.4) is connected with the stretching vibration of the carbonyl group (C=O) resulting from the oxidation process.

The absorption at the frequency 1167 cm⁻¹ in the spectrum of PP was attributed to anhydride groups (C-O-C) also formed after oxidation.

The broad peak at 1596 cm⁻¹ in the blends without EPR may be result from mechanical destruction, which is due to the bigger shear stresses and this is mechanism for formation of C=C bonds. When we added the EPR - modifier the polymer melt undergoes less shear stresses and smaller peak at 1596 cm⁻¹.

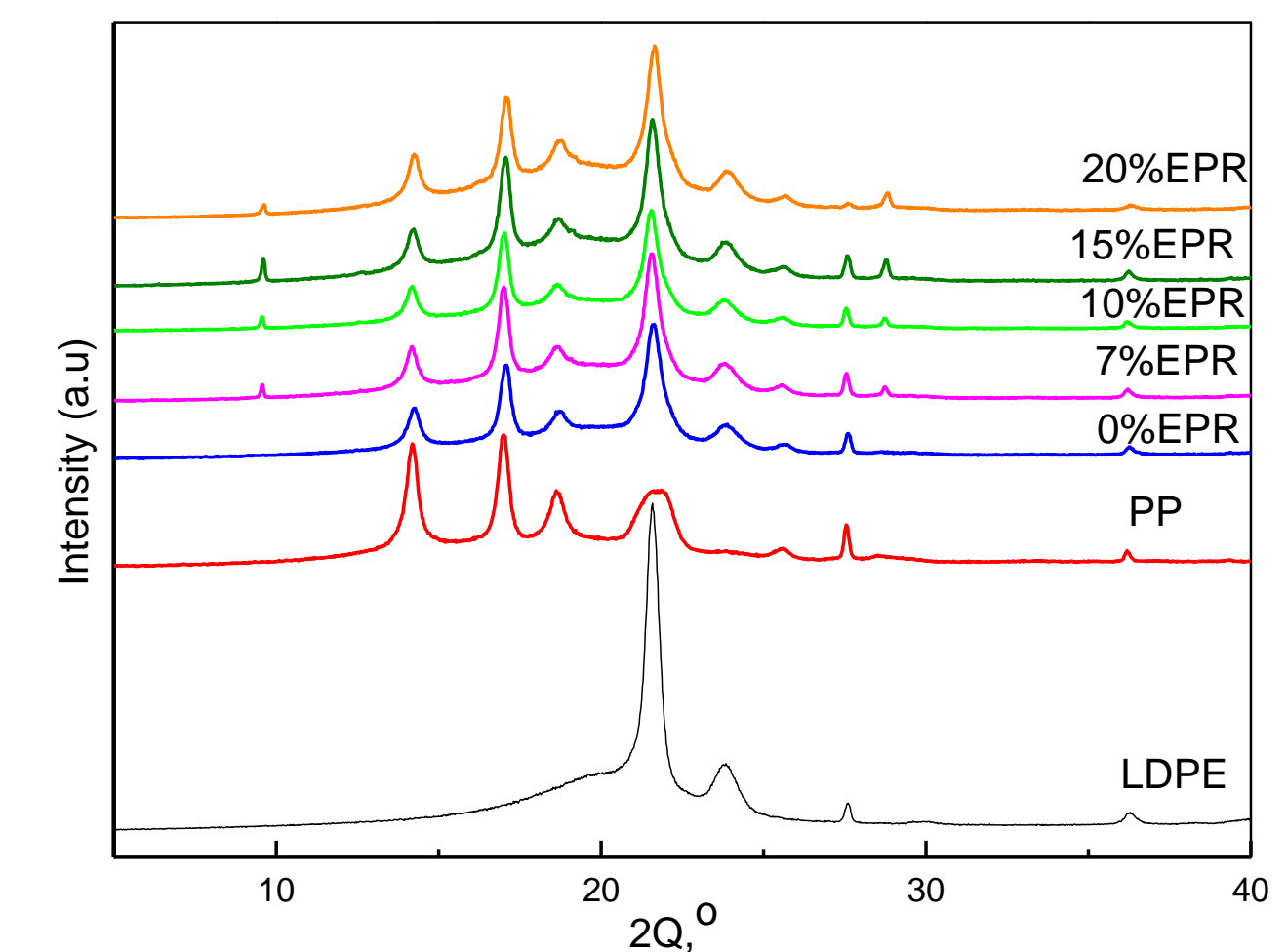


Figure 5: X-ray diffractograms of LDPE and PP and their blends .

Two distinct transition temperatures are recorded for PP for $\tan \delta$ (Fig. 6), one at about 7 °C that corresponds to the β -transition, and the other at about 69 °C representing the α -relaxation.

The T_g of LDPE is in the temperature region of approximately -25°C. The γ transitions of LDPE in Figure 6 is in the temperature regions of approximately -126°C

The new relaxation maximum at -51 °C was more expressed with higher EPR content and was noted as T_g of EPR phase.

SEM observations of the both double blends LDPE:PP= 50:50 (Fig.7) revealed comparative good compatibilisation between the both phases. We have amphitheatrically morphology. As a result from interfacial tension in the blend of technological waste have generated propagations and crazes and obviously can see the phase recession and shrinkage of the components.

The addition of elastomer EPR (down) increase interfacial adhesion between both polymers and prevent formation of cracks and phase separations.

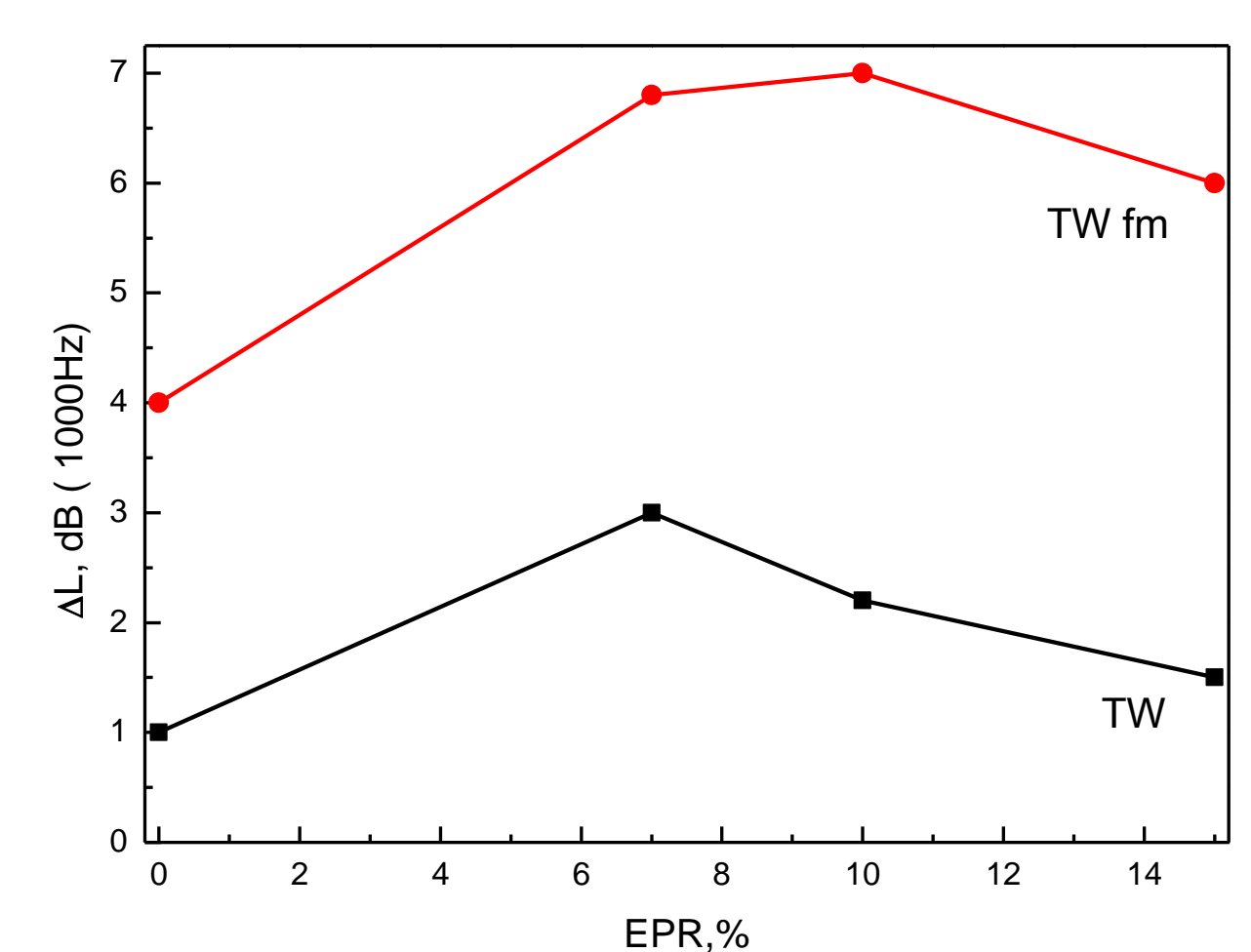


Figure 8: Sound absorption in dB of the blend LDPE:PP= 50:50, not foamed and foamed (TW fm), with different quantity of EPR.



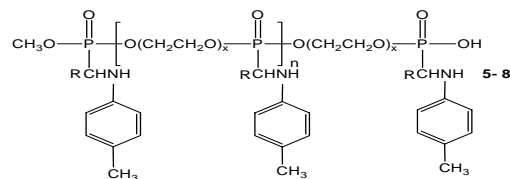
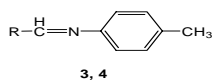
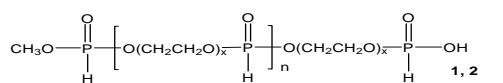
INTRODUCTION

The development of new effective polymeric systems for the treatment of different diseases, including cancer, diabetes, ischemia, severe combined immunodeficiency, neurodegenerative, offers enormous possibilities to the advanced pharmaceutical technology. The polymer-drug conjugates have much potential to improve the therapy of variety human pathologies, solving major problems in medicine, such as the toxic effects of the drugs and the duration of drug action.

A great deal of attention and research efforts are being concentrated on the synthesis of diverse biodegradable polymers and on the investigations of their viability as drug carriers in the design of these new types of therapeutics. Among the numerous macromolecular systems studied for drug delivery purposes, the polymers with phosphorus ester (C-O-P-O-C) repeating units in the backbone occupy a particularly important place, because they can degrade into biocompatible and non-toxic components under physiological conditions. These polymers possess reactive functional groups in their backbone, which allows for conjugation of bioactive molecules to the chains and gives much opportunities for the preparation of new drug delivery systems with improved therapeutic indexes. On the basis of poly(oxyethylene H-phosphonate)s we synthesized poly(oxyethylene aminophosphonate)s – alternating copolymers built only of aminophosphonate units with potential biological activity and non-toxic poly(ethylene glycol) links.

The immobilization of aminophosphonates to biodegradable polymer carriers like poly(oxyethylene H-phosphonate)s appears a promising approach in the design of new polymer drug carriers, as well of new polymers with own activity.

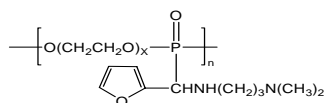
Chemistry



X = 4 (PEG 200) : 1, X = 13 (PEG 600) : 2

R = (CH₃)₂N-C₆H₄-CH₃ : 3, 5 (X = 4), 6 (X = 13)

R = furfurylidene-C₆H₄-CH₃ : 4, 7 (X = 4), 8 (X = 13)



X = 4 (PEG 200) : 9 : X = 13 (PEG 600) : 10

Pharmacology

The compounds were tested for cytotoxicity in a panel of human tumor cell lines, representative for some clinically important types of neoplastic diseases, namely HL-60 (acute promyelocyte leukemia), its multi-drug resistant sub-line HL-60/DOX (characterized by overexpression of MRP-1 efflux pump), LAMA-84 and K-562 (chronic myeloid leukemias). The cells were exposed to serial dilutions of the tested compounds for 72 h and thereafter their viability was assessed using the MTT-dye reduction assay. The clinically used antineoplastic drug cisplatin was used as reference cytotoxic agent.



Table 1. Cytotoxic effects of the aminophosphonates 5-10 vs. the clinically applied antineoplastic drug cisplatin, as assessed by the MTT-dye reduction assay after 72 h continuous exposure.

Compounds	IC ₅₀ (μmol/L)			
	HL-60	HL-60/DOX	LAMA-84	K-562
5	105.9	> 400.0	> 400.0	> 400.0
6	19.2	27.2	17.2	14.9
7	19.9	20.4	14.0	15.2
8	14.2	14.4	12.3	13.7
9	157.5	159.1	88.8	62.3
10	66.2	16.2	41.9	18.3
Cisplatin	7.8	14.5	18.2	25.7

CONCLUSION

Novel poly(oxyethylene aminophosphonate)s 5-8 were synthesized via addition of poly(oxyethylene H-phosphonate)s 1 and 2 to the Schiff bases N-(4-dimethylaminobenzylidene)-p-toluidine 3 and N-furfurylidene-p-toluidine 4.

The polymers 5-8 and poly(aminophosphonate)s 9 and 10 obtained on the basis of biodegradable polymer carriers 1 and 2 consist only of aminophosphonate (active substance) and non-toxic poly(ethylene glycol) units.

The polymers 5-10 have coordination centres in their repeating units and can be used as new biodegradable polymer carriers for physical immobilization of bioactive substances.

Compounds 6-8 and 10 caused prominent cytotoxic effects with low micromolar IC₅₀ values, whereas 9 was less active and 5 was only marginally cytotoxic.

The N-furfurylidene-p-toluidine-Schiff base with longer (14 units) PEO moiety abundant in 8 were identified as structural prerequisites affording superior activity, while the analogues bearing N-(4-dimethylaminobenzylidene)-p-toluidine or N,N-dimethyl-N'-furfurylidene-1,3-diaminopropane were generally less active than 8.

In spite of the Schiff base fragment however, in all sub series of compounds the reduction of the length of the PEO moiety from 13 to 4 units was consistent with significant reduction in relative potency and in case of 5 with dramatic loss of activity.

The established cytotoxicity of compounds 6-8 and 10, similar or comparable to that of the reference drug cisplatin findings give us reason to consider the presented compounds as a novel class of aminophosphonate-based cytotoxic agents.

References:

- [1] M. J. Vicent, The AAPS Journal 9 (2) Article 22 (2007) E200-E207 (<http://www.aapsj.org>).
- [2] J. Luten, C. F. van Nostrum, S. C. De Smedt, W. E. Hennik, J. Control. Release 126 (2008) 97-110.
- [3] J.-M. Park, B.-A. Shin, I.-J. Oh, Arch. Pharm. Res. 31 (2008) 96-102.
- [4] S.-W. Huang, R.-X. Zhuo, Phosphorus, Sulfur, and Silicon Relat. Elem. 183 (2008) 340-348.
- [5] I. Kraicheva, Iv. Tsacheva, K. Troev, Bulg. Chem. Commun. 40 (2008) 54-58.
- [6] I. Kraicheva, A. Bogomilova, I. Tsacheva, G. Momokov, K. Troev, European J. Of Med. Chem. 44 (2009) 3363-3367.

Acknowledgements: I. Tsacheva and A. Bogomilova thanks the European Social Fund, Structural Funds, Operational Programme "Human Resources Development" for financial support in the frame of Grant No. BG051PO001/07/3.3-02/51.



Polymer Networks Based on Gelatin and Chitosan as Matrices for Biomineralization

M. Golyakova¹, D. Rabadjieva², S. Tepavicharova², E. Vassileva¹

¹Laboratory on Structure and Properties of Polymers, Faculty of Chemistry, Sofia University

²Institute of General and Inorganic Chemistry, Bulgarian Academy of Sciences, Sofia

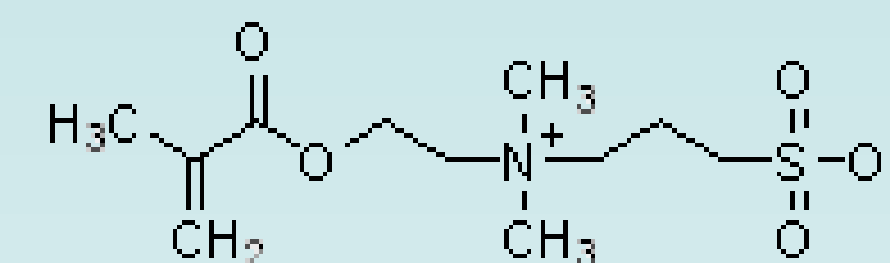
INTRODUCTION

Biopolymer scaffolds play an important role as a temporary support either for seeding cells or for calcium phosphate crystallization in order to repair or strengthen damaged tissues. Two main classes of biopolymers are mainly used as components of polymeric scaffolds – polysaccharides and proteins – as they are the main constituents of the extracellular matrix. The main disadvantages of biopolymers are their poor mechanical performance and their easy enzymatic degradation that could result into poor performance as a support.

AIM

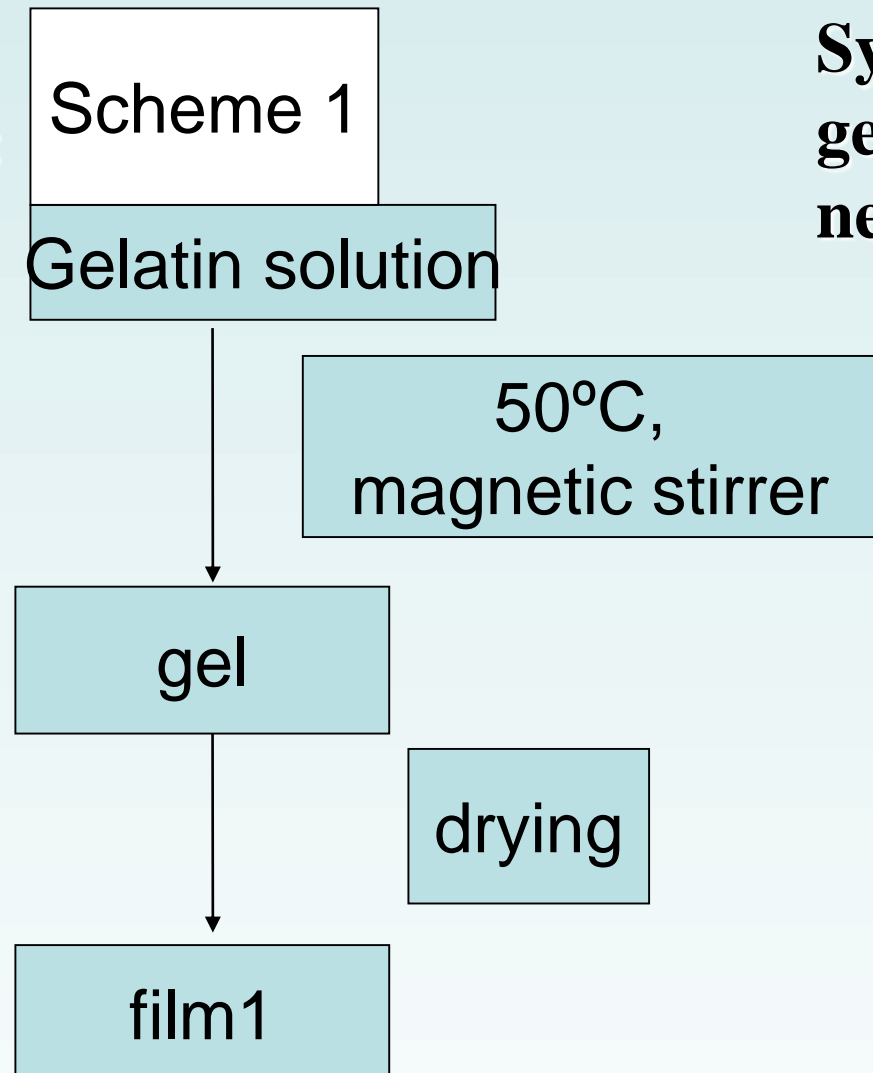
The aim of this study is to prepare polymer networks by combining biopolymers (gelatin and chitosan) with zwitterionic polymer (polySB) and to test their potential as matrices for biomineralization.

[2-(Methacryloyloxy)ethyl]dimethyl-(3-sulfopropyl)ammonium hydroxide (SB)

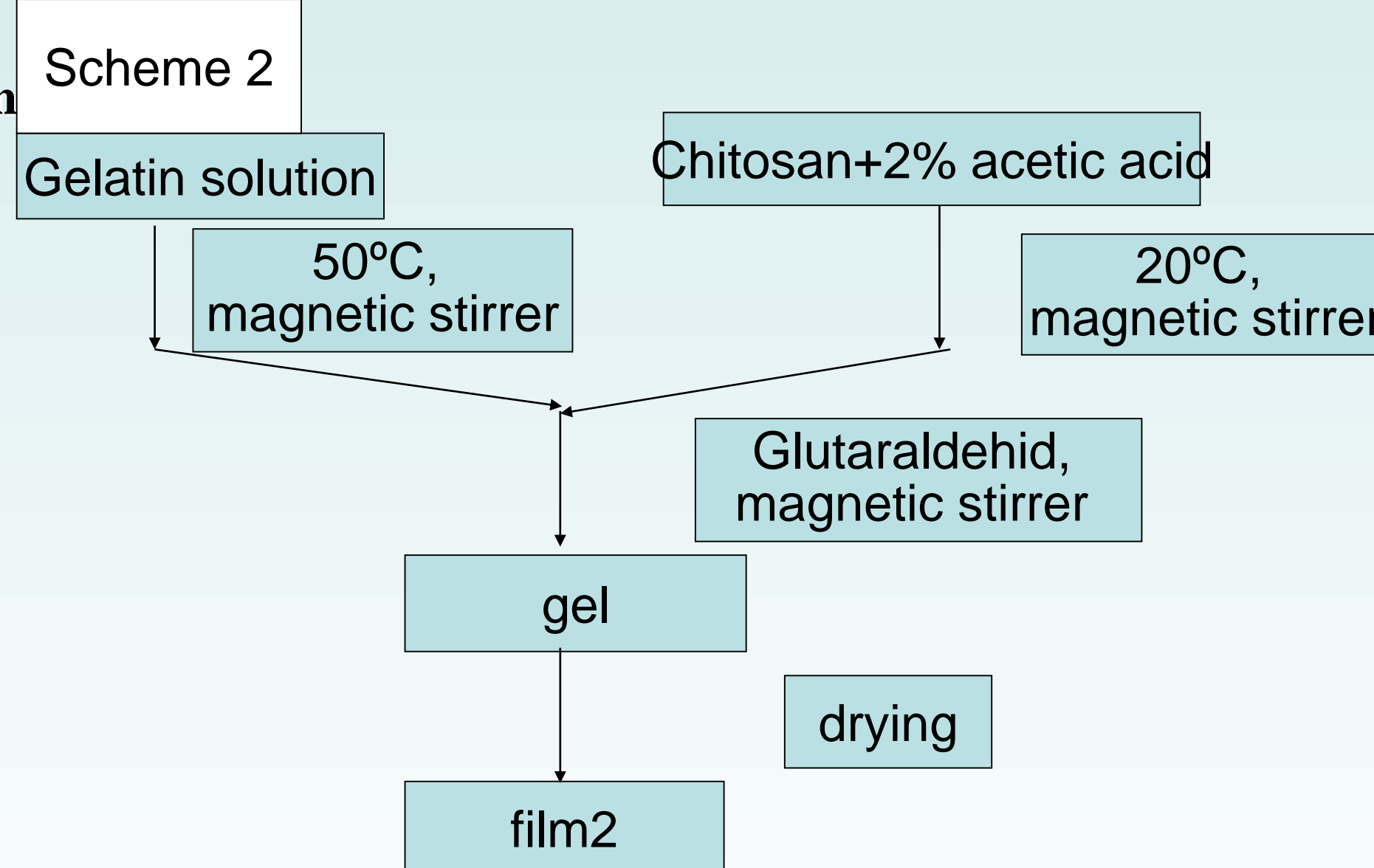


EXPERIMENTAL PART

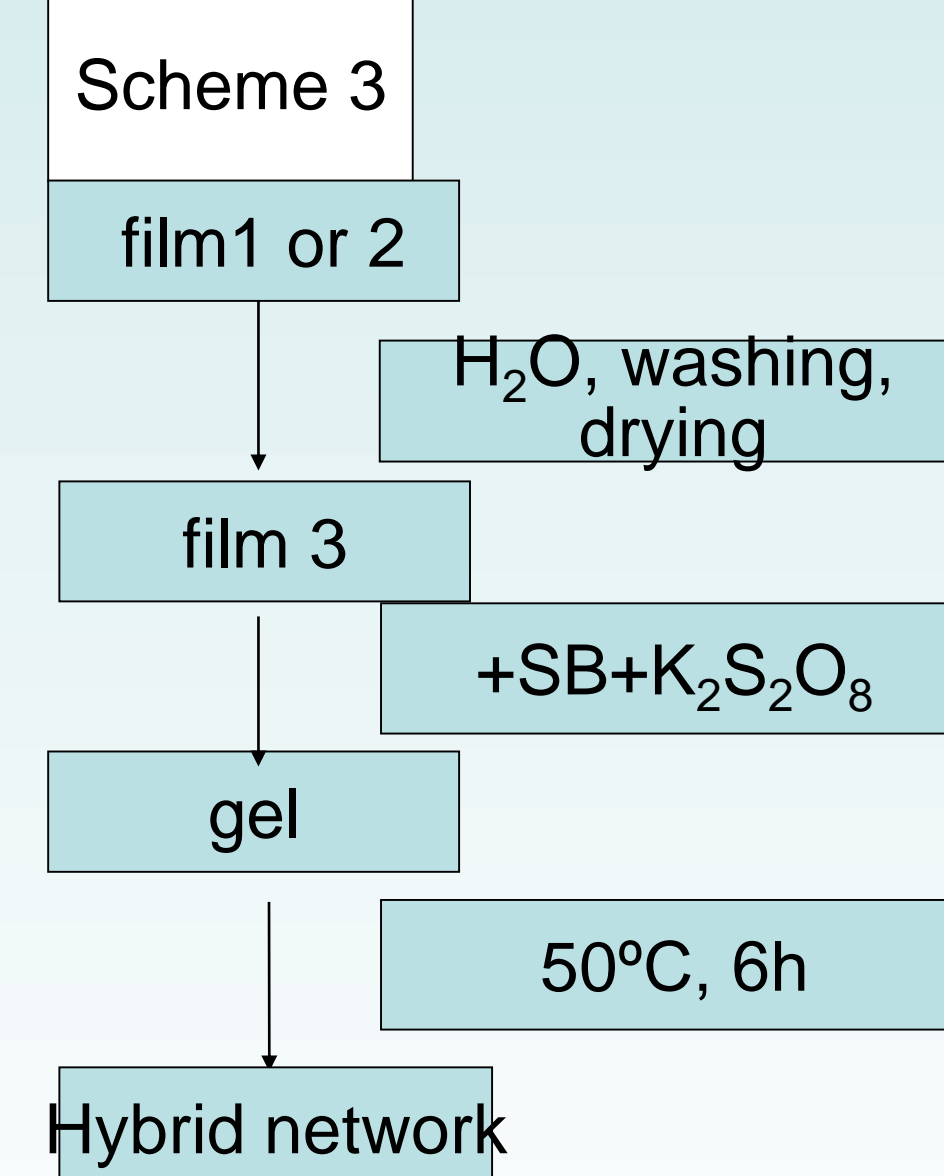
Synthesis of gelatin films:



Synthesis of gelatin-chitosan networks:



Synthesis of gelatin-SB networks:



Gels obtained at every stage as well the final gels were repeatedly washed from residual chemicals.

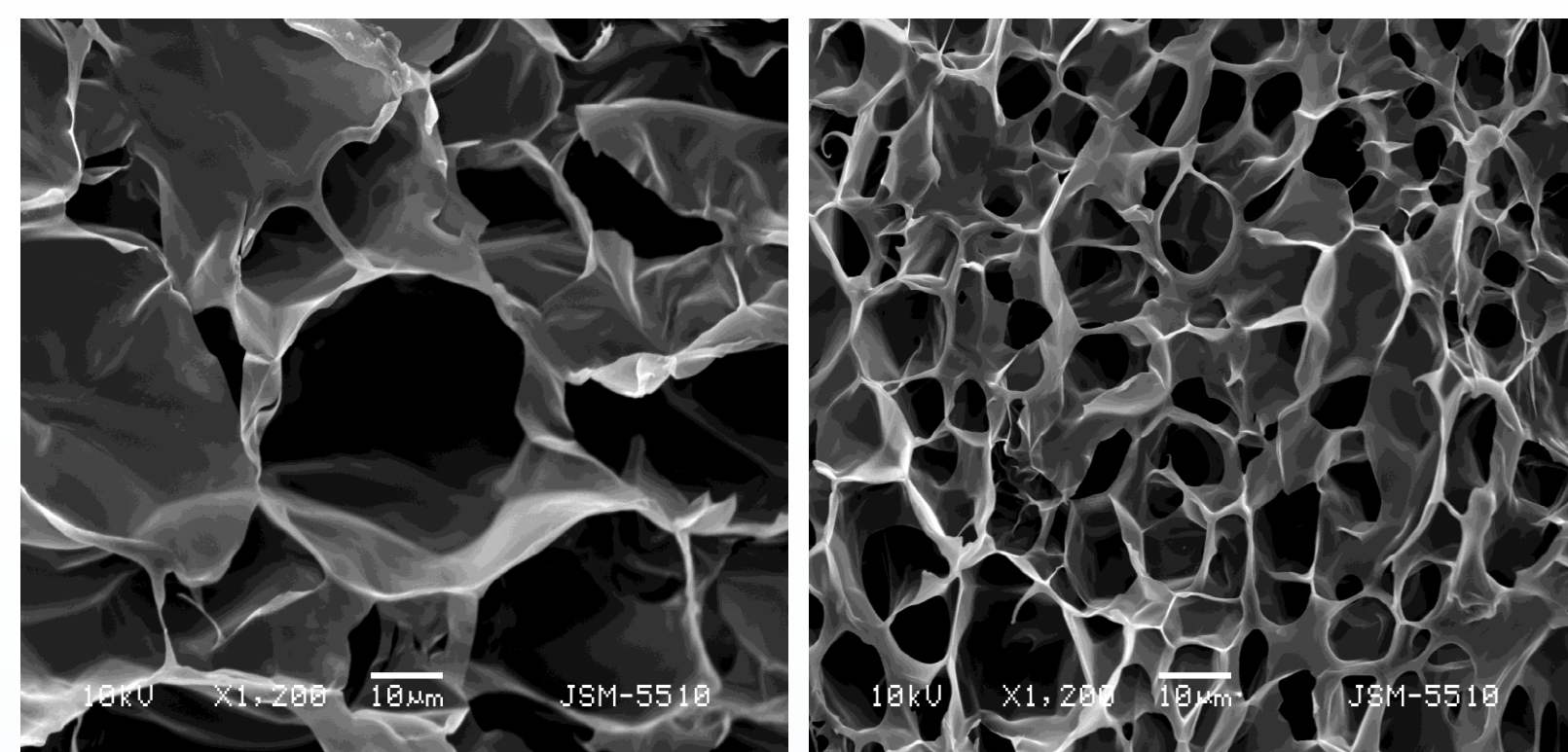
Freeze drying: After extensive washing of the films obtained through the three schemes, the gels were freeze dried in order to obtain porous structure.

The pore size of gelatin matrix could be varied by changing gelatin concentration (at equal water content). Above 3 wt% gelatin wide pore size distribution is obtained.

Scaffolds Characterization

Addition of chitosan to gelatin results into opening the pores of gelatin and obtaining of interconnected structure which allows easy passing of the cells, nutrients flow.

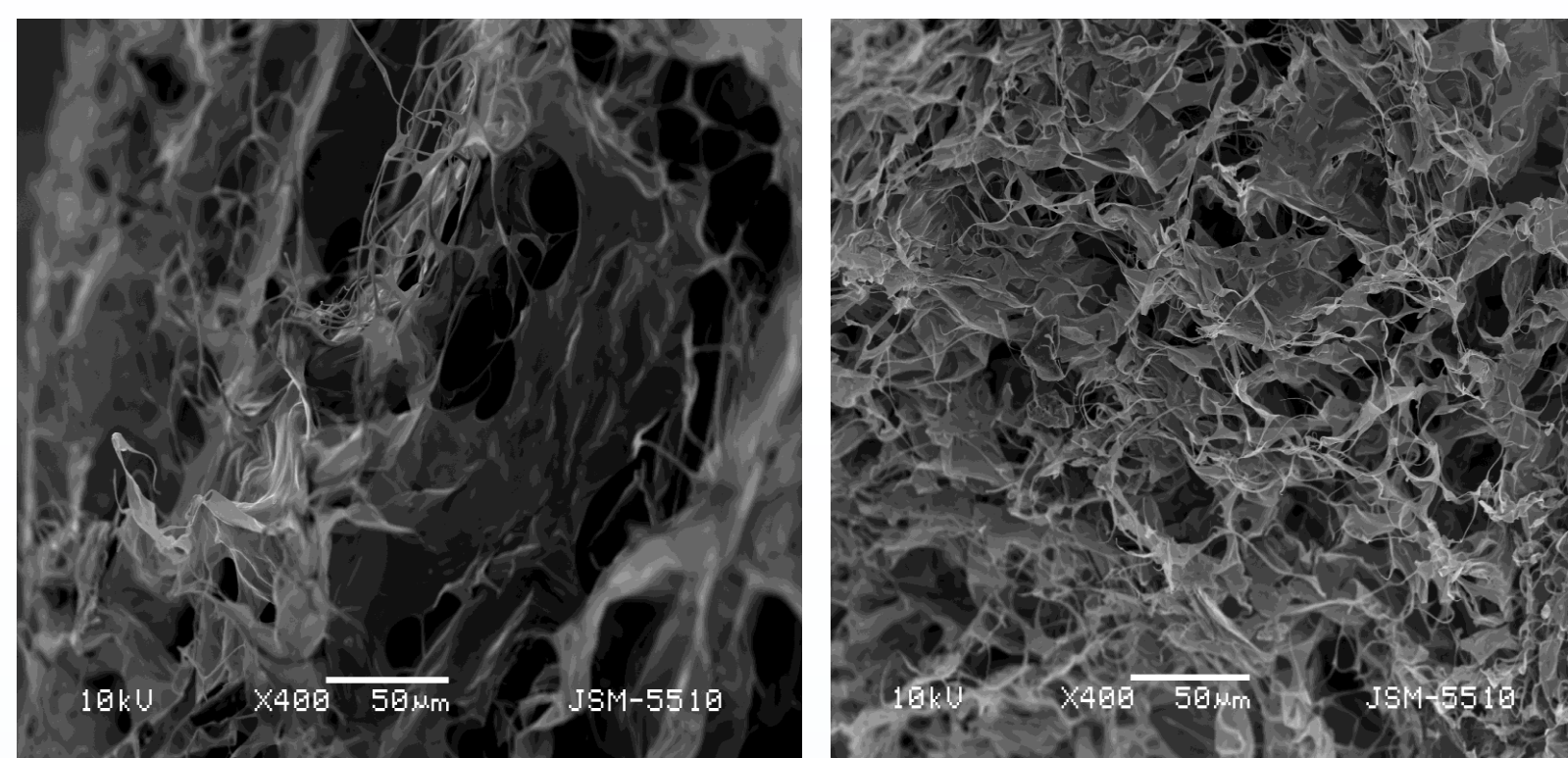
Hybrid networks were obtained from gelatin and polySB and their structure was proved to be the type small nano-sized inclusions of polySB (white grains in the Figure 3) evenly dispersed into gelatin matrix.



A

B

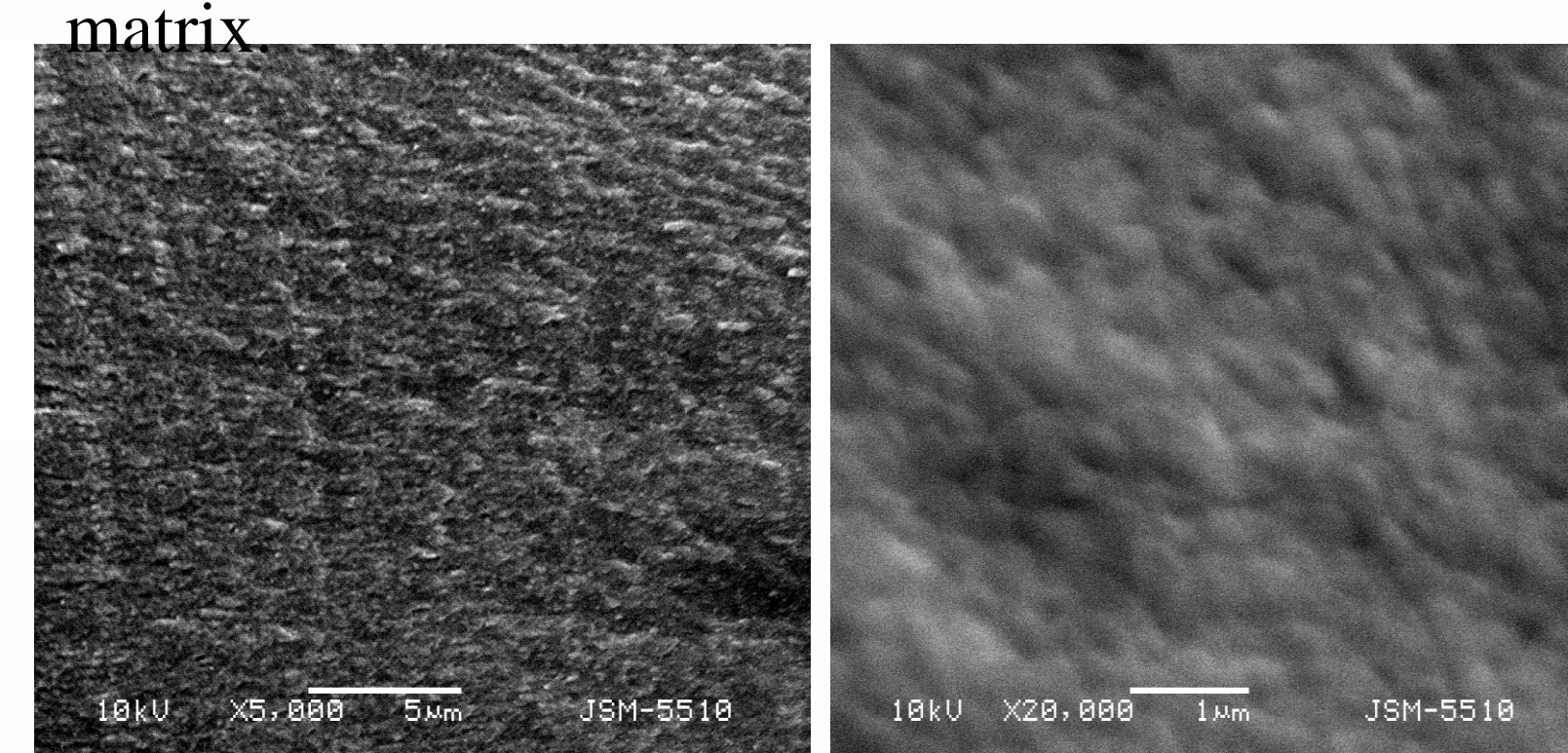
Figure 1. Gelatin porous samples obtained according Scheme 1 at (A) 1% and (B) 2% gelatin at equal water content.



A

B

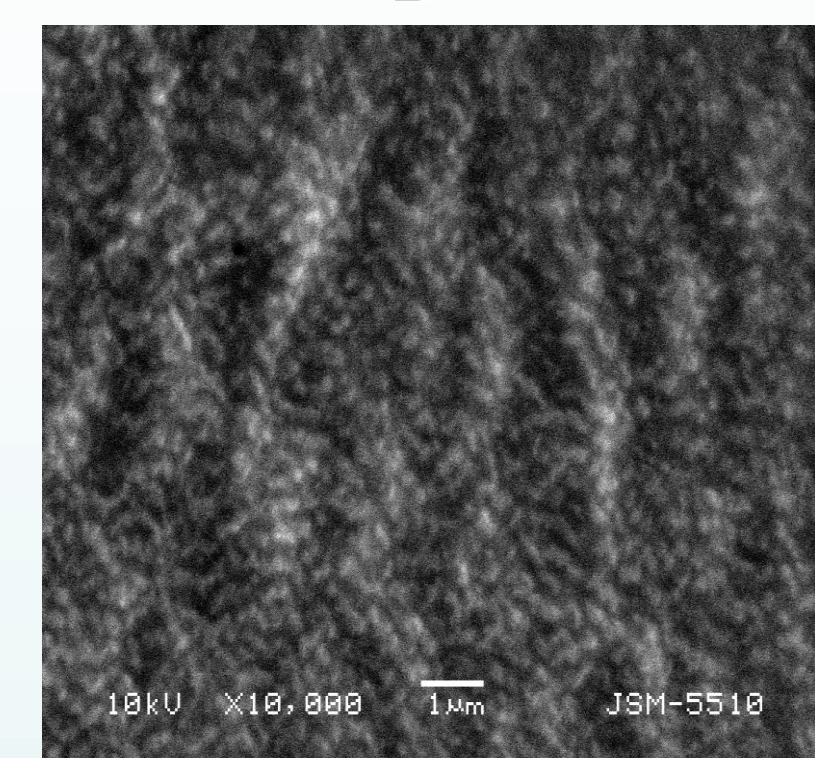
Figure 2. Gelatin:Chitosan porous samples, obtained, according to Scheme 2 with different ratio: (A) 1:1 and (B) 3:1.



A

B

Figure 3. Gelatin-SB hybrid networks, obtained according to Scheme 3 with different molar concentrations of SB: (A) 1.5, (B) 1 and (C) 0.5.



C

Test with blood plasma

Gelatin was immersed into blood plasma at 20°C for 1h and after that the number of **erythrocytes** was counted (Table 1). A control sample of plasma without any sample inside was also done. Each value in Table 1 is a result of three independent experiments

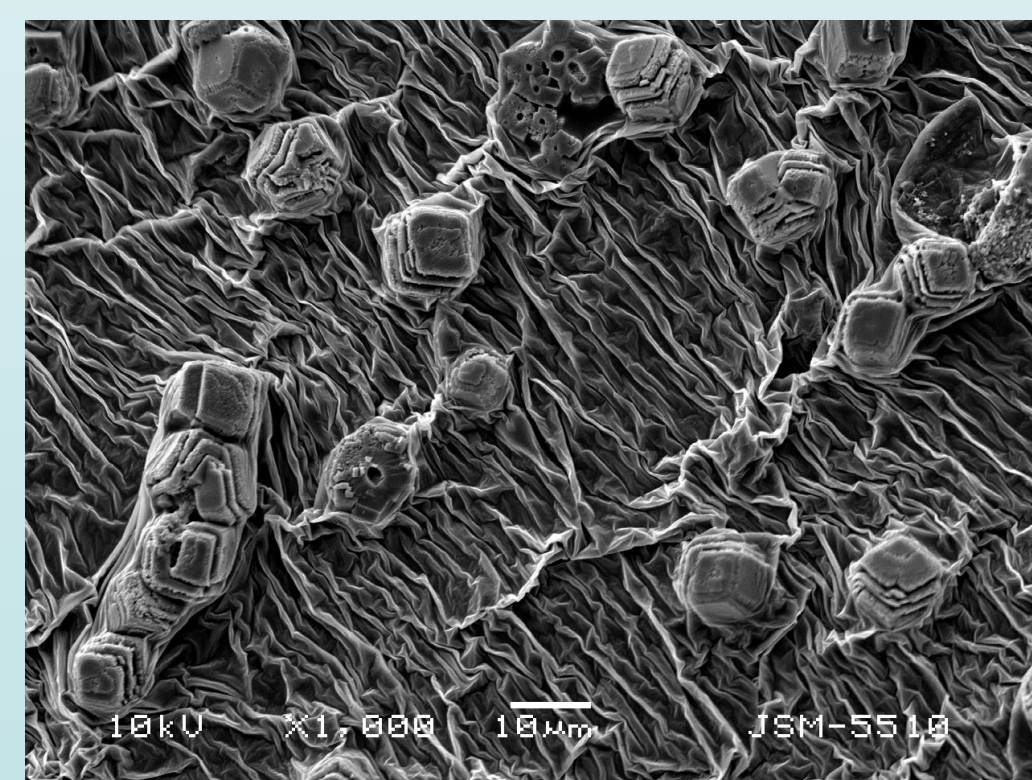
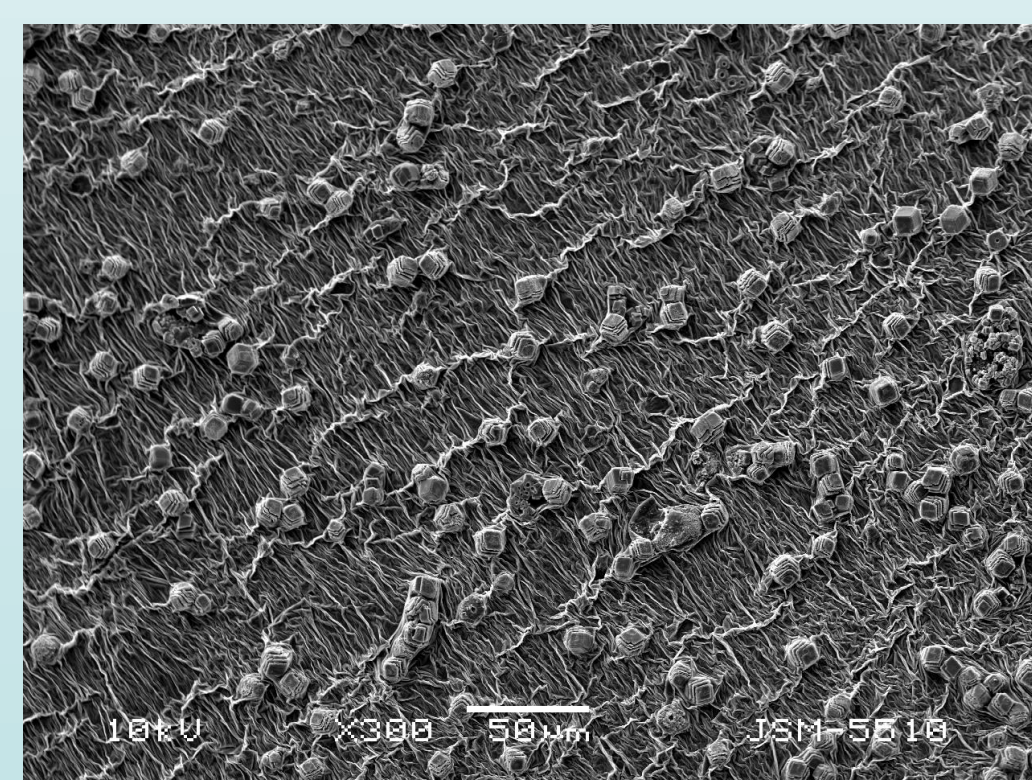
Visual test: After 1 h immersion in plasma, the samples had different appearance.

Table 1. Number of red blood cells per L*10¹² after incubation of different samples into blood plasma.

Blood plasma /control/	1% Gelatin	2% Gelatin	Gelatin: Chitosan 3:1	Gelatin: Chitosan 1:1
5.7	5.2	5.4	3.6	5.3



Figure 4. Photograph of samples 2% Gelatin (left) and Gelatin:Chitosan 3:1 (right).



Crystallization of calcium phosphates in polymer network gelatin-SB

Freeze dried film of gelatin-SB was left to swell in 0,003M K₂HPO₄ (pH=12, adjusted with KOH) for 3 days. The P content was determined to be 0,0007M and pH drop to 9. After washing the sample was immersed into CaCl₂ (0,005M, pH 9) for 7 days.

CONCLUSIONS

In this study, it was proved that the pore size and interconnectivity could be successfully modulated by choosing right components and preparation conditions. The grain structure of gelatin-SB hybrid networks is interesting and shows potential for directing cell behavior, however more biological tests are needed to prove the viability of this concept. Crystallization

ACKNOWLEDGEMENTS: This work is financially supported by the Bulgarian Ministry of Education Youth and Science under Projects DO-02-82/2008 and ДТК 02/70/17.12.2009. The financial support of Project BG051PO001/07/3.3.-02/51 Operational program Human Resources Development is also acknowledged.



Effect of irradiation dose on the degree of crystallinity.

DSC and WAXS analysis of Ultra-High Molecular Weight Polyethylene

M. Staneva, E. Nedkov
Institute of Polymers - BAS, 1113 Sofia, Bulgaria

Materials and methods

Materials investigated:

Ultra-High Molecular Weight PolyEthylene (PE-UHMW):
 ↳ 9 γ -irradiated (in air) samples
 (D = 1, 5, 10, 50, 100, 200, 500, 1000, 1500 kGy);
 ↳ 1 un-irradiated sample (D = 0.1 kGy).

Methods used:

↳ Wide Angle X-ray Scattering (WAXS) – reflection mode
 ↳ WAXS – transmission mode
 ↳ Differential Scanning Calorimetry (DSC) - melting

Aim of the research:

to estimate the effect of the irradiation dose on the degree of crystallinity of PE-UHMW.

Results and Discussion

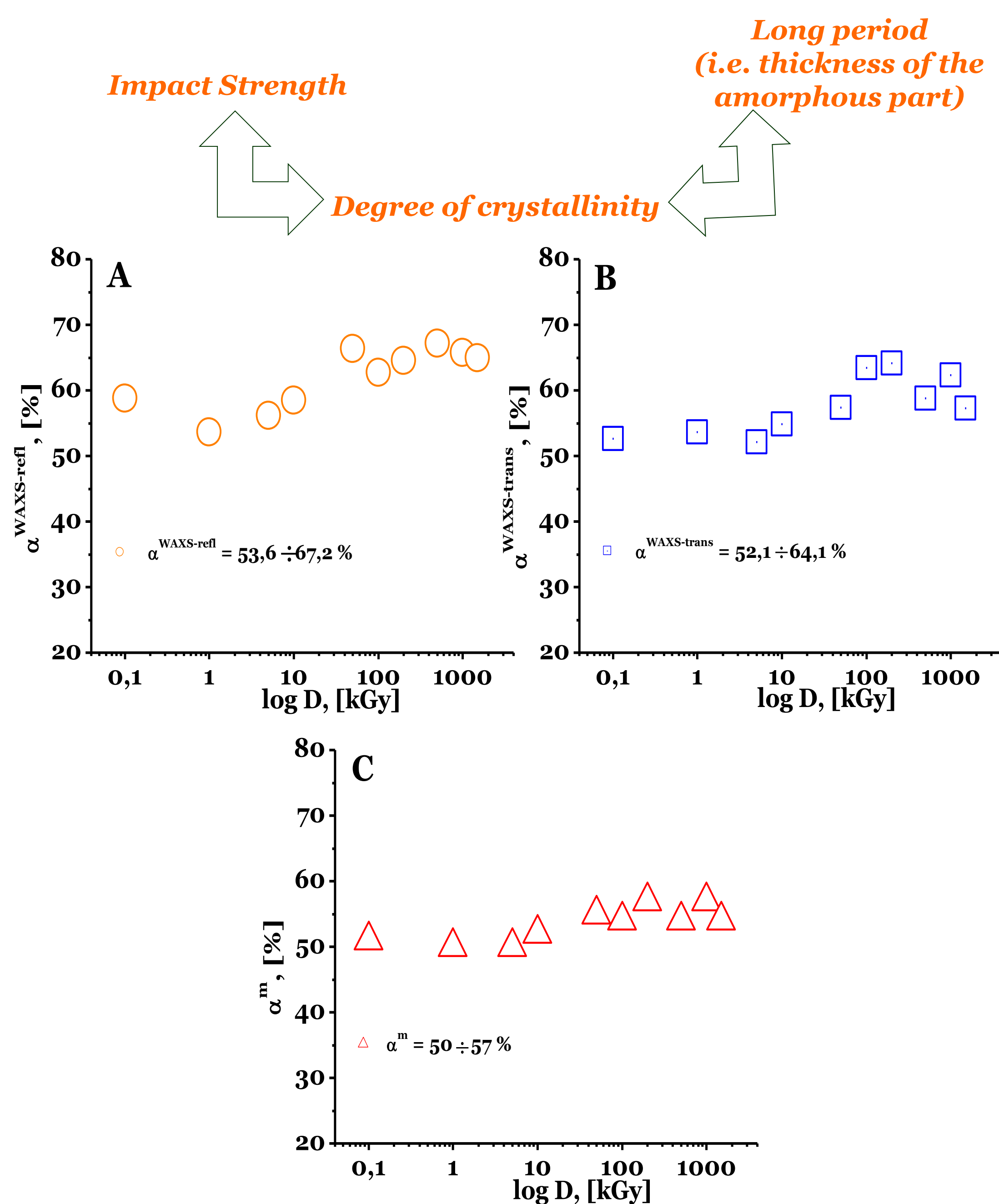


Figure 1. Effect of irradiation dose on the degree of crystallinity of PE-UHMW: A – calculated by WAXS-reflection mode ($\alpha^{WAXS-refl}$); B - calculated by WAXS-transmission mode ($\alpha^{WAXS-trans}$); C – calorimetric investigated (α^m)

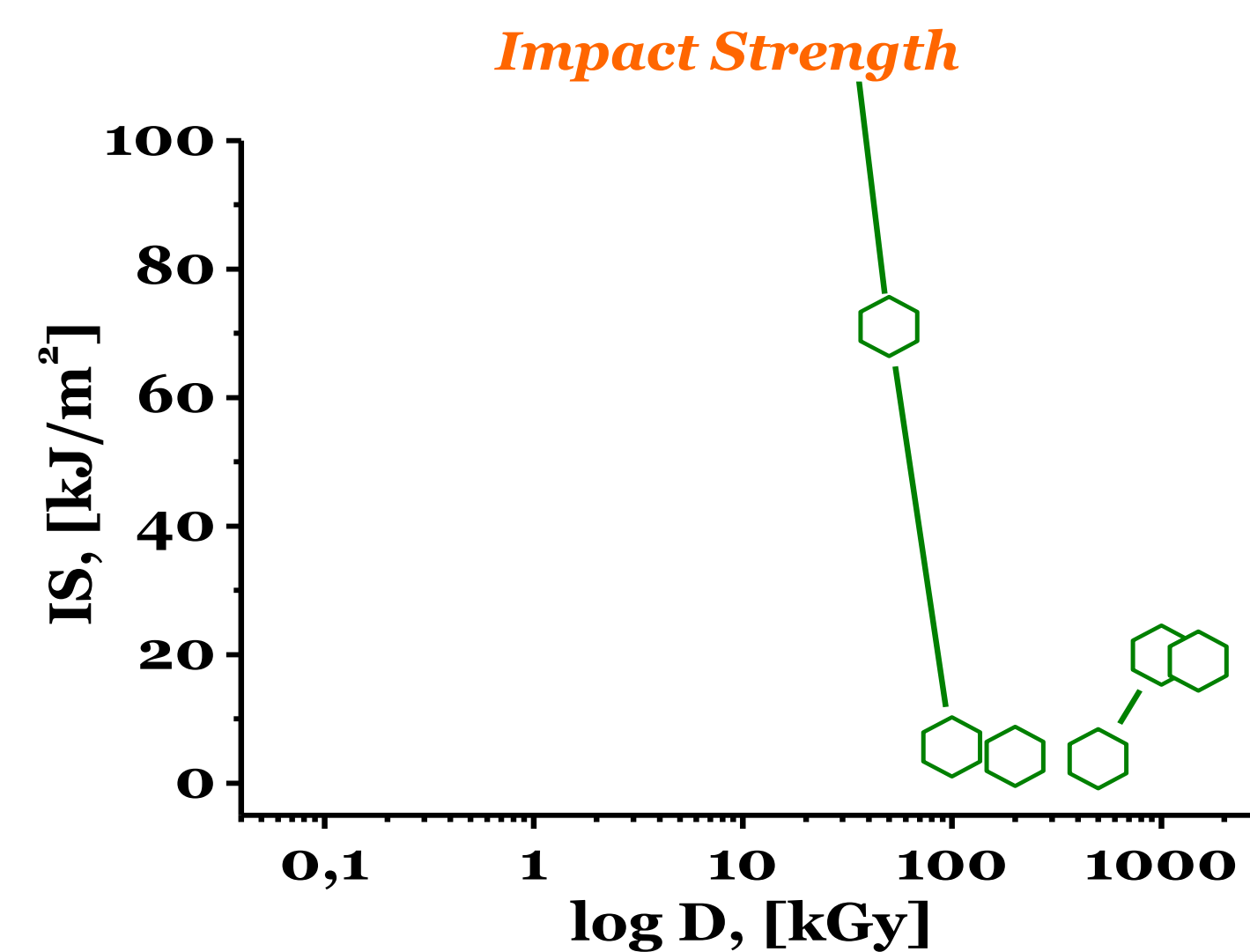


Figure 2. Effect of irradiation dose on the impact strength (IS) of PE-UHMW

Long period, Thickness of lamella and Thickness of amorphous part

$$L = L_{am} + L \cdot \alpha, \text{ where } L - \text{long period};$$

$$L_{am} - \text{thickness of lamella}; L \cdot \alpha = L_{cr} - \text{thickness of lamella}$$

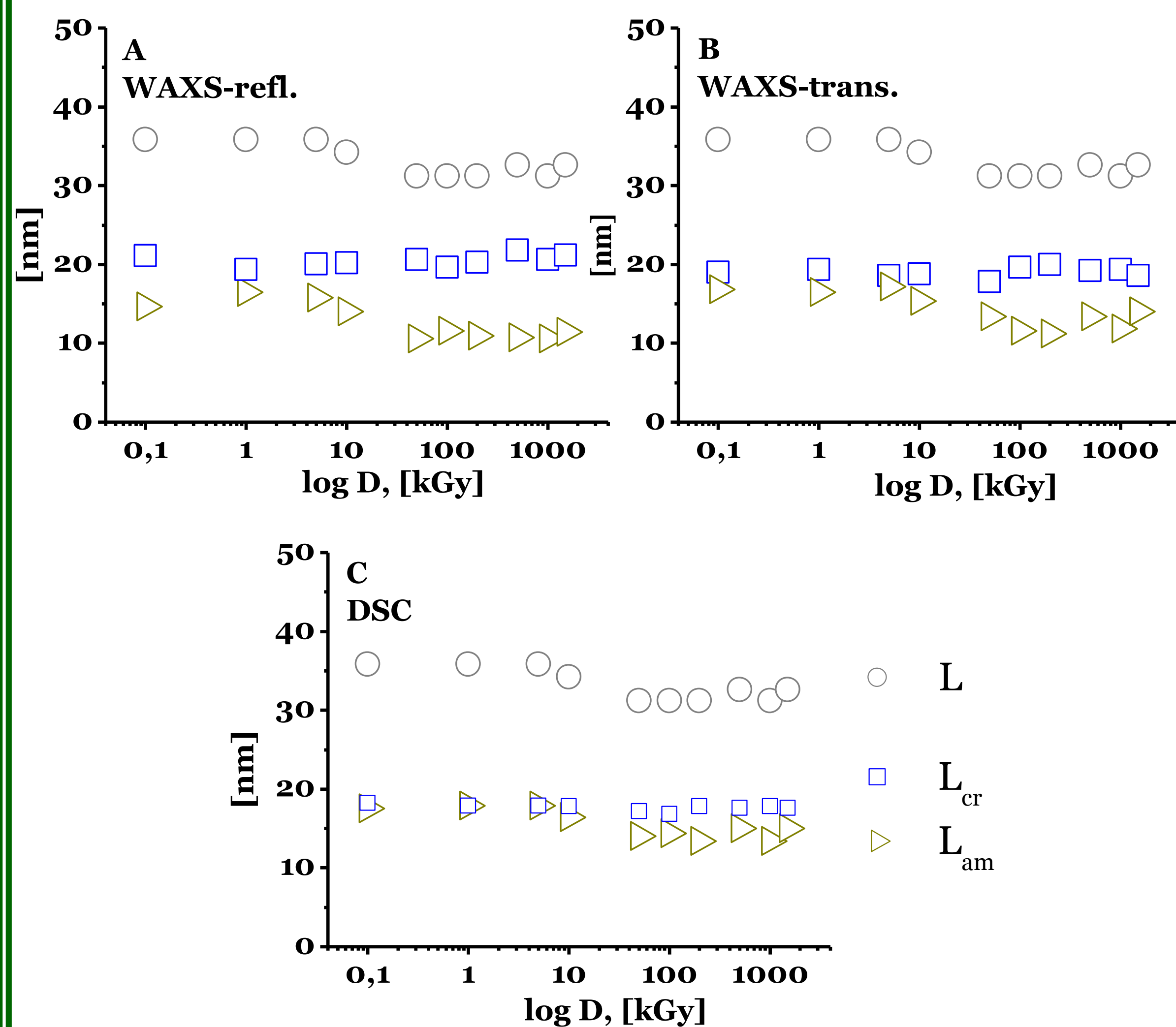


Figure 3. Effect of irradiation dose on the long period (L), thickness of lamellae (L_{cr}) and thickness of amorphous part (L_{am}) of PE-UHMW. The thickness of lamella (respectively the thickness of the amorphous part) was calculated using the degree of crystallinity, obtained by: A – WAXS-reflection mode; B - WAXS-transmission mode; C – calorimetric investigated

Conclusions

- ↳ WAXS and DSC analysis show similar results for degree of crystallinity.
- ↳ Our values for degree of crystallinity are in good agreement with the literature data.
- ↳ The dose 50 kGy is denoted as a critical dose (fig. 1):
 - ⇒ up to 5kGy the degree of crystallinity is almost constant;
 - ⇒ above 50 kGy degree of crystallinity slightly increases.
- ↳ The increase of degree of crystallinity makes PE-UHMW more brittle, which is in agreement with the data for impact strength (fig. 2)
- ↳ The increase of degree of crystallinity is due to the decreasing of the thickness of the amorphous part of the polymer (fig. 3)
- ↳ Our results for degree of crystallinity suppose destruction in the case of PE-UHMW, γ -irradiated in air.

Acknowledgement

Maya Staneva would like to thank the Structural Funds and Educational Programs Directorate for financial support in the frame of the Project "Support for the development and realization of PhD-students, post-docs and young researchers in the field of polymer chemistry, physics and engineering", Grant № BG051PO001/07/3.3-02/51 51.



Silica Obtained Via Pyrolysis of Waste "Green" Tyres – Reinforcing Filler for Rubber Industry

M. Mihaylov, M. Ivanov, L. Ljutzkanov



Abstract

A solid product (named SiO₂D) is obtained as a result of subjecting the tread of "green" tyres to pyrolysis in the presence of water vapour. It has been found by FT-IR and EDX-RF spectroscopy that the product contains 30 % of carbon, 65% of SiO₂, 3 % of ZnO and 2 % of other components. The physicochemical and dynamic properties of the vulcanizates based on SBR filled with 75 phr SiO₂D have been studied and compared to those of vulcanizates filled with conventional SiO₂ as well as with such filled with a mixture of SiO₂ and carbon black N 330 at a 2:1 ratio. Compositions with and without bis(3-triethoxysilylpropyl)disulfide have been also investigated. It has been established that there are no differences in the mechanical properties (modulus 300, tensile strength, abrasion, etc.) as well as the dynamic properties (heat build-up, tan δ , etc.) of the vulcanizates filled with SiO₂D and of those filled with conventional SiO₂ and carbon black at a 2:1 ratio.

Introduction

Waste tyres trigger a serious environmental problem. They are crucial environmental pollutants being highly stable to natural factors (sun radiation, moisture, oxygen, ozone and microbiological action). More than 5x10⁶ t/year of waste tyres result in the world, 2x10⁶ of which in Europe, 2.5x10⁶ in North America and 0.5x10⁶ in Japan [1]. There are several ways to dispose and re-use that waste such as tyre retreading, mechanical grinding, rubber reclaim, combustion, pyrolysis etc. Even if it is not a new method, the waste tyres pyrolysis generates oil, char, gas and steel products, all of which have the potential to be re-used. The oil obtained from pyrolysis can be combusted as a substitute fuel or, in case it does not contain larger amounts of polycyclic hydrocarbons, it can be used as plastiziser [2-4]. The gas can be used to provide the energy for the pyrolysis process [5-7] and char can be used as activated carbon or filler in the rubber industry [8-10]. The chemical recycling of the waste tyres by pyrolysis involves the decomposition of the waste tyres at high temperatures (300 – 1000 °C) under different conditions. It is known that precipitated silica having silanol groups on its surface is used as a filler in the tread for "green" tyres. Organosilanes like bis(3-triethoxysilylpropyl) disulfide (TESPD) and bis(3-triethoxysilylpropyl) tetradisulfide (TESPT) are implemented for improving the dynamic properties of those vulcanizates. During the mixing the silanes are coupled to the filler surface. That leads to a better dispersion of the precipitated silica in the rubber matrix. However, the technological mixing regime has a great importance for running the above mentioned reactions. Reactions between the second functional group of silane and the rubber molecules occur during vulcanization provoking chemical "polymer-filler" bonds. The interactions described reduce the rolling and abrasion resistance of the tyres and enhance their adhesion on wet roads [11, 12].

This paper aims at studying the solid product, named SiO₂D in the following, obtained from the pyrolyzed tread of waste "green" tyres carried out according to the above mentioned method and its behaviour as filler in rubber blends and vulcanizates of SBR.

Experimental

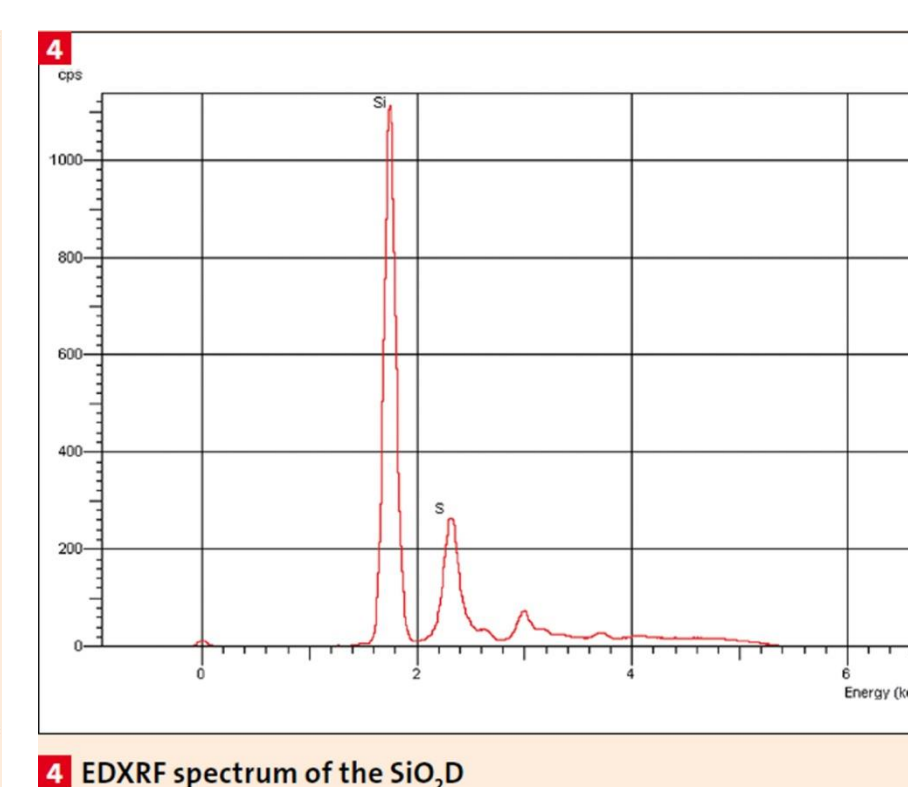
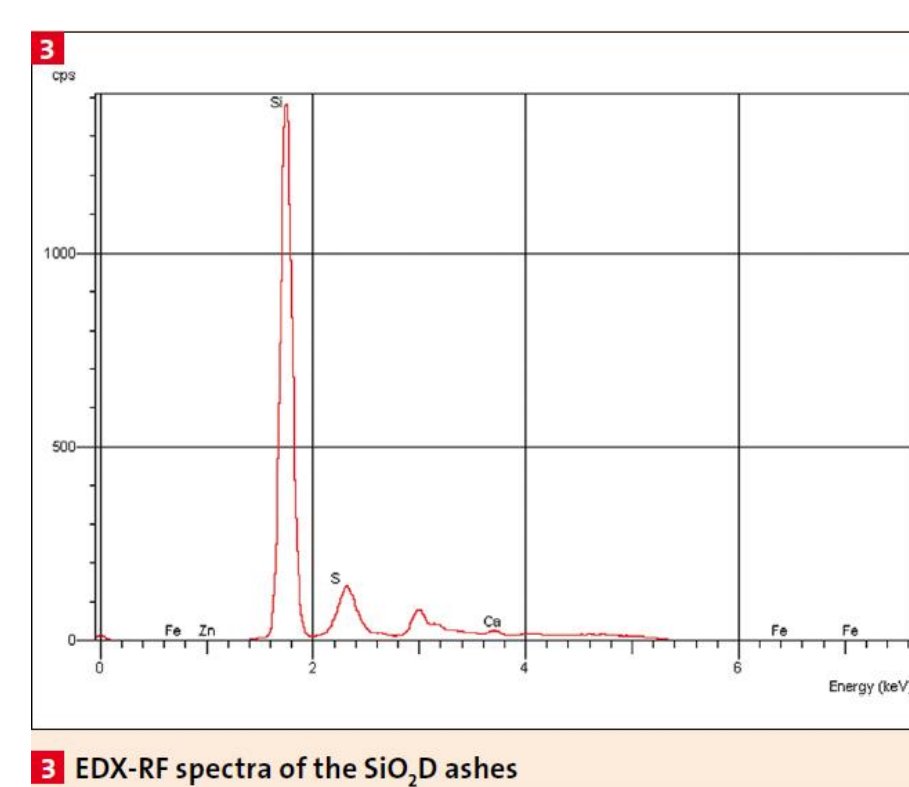
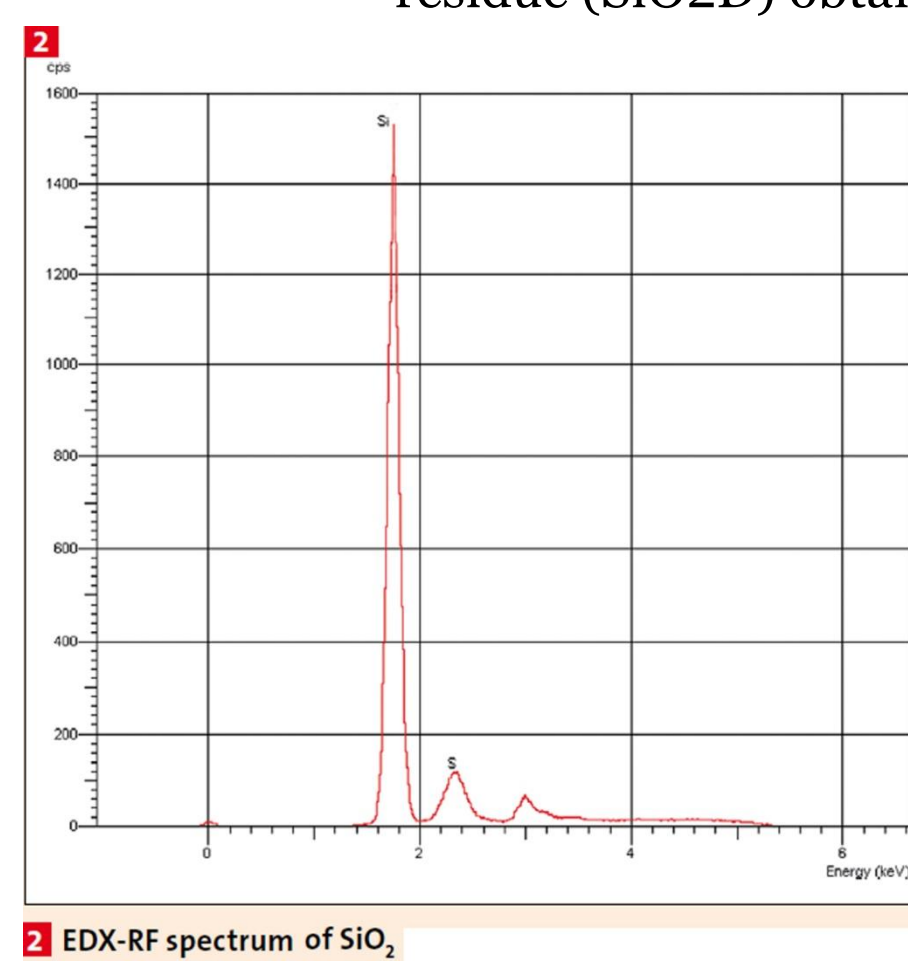
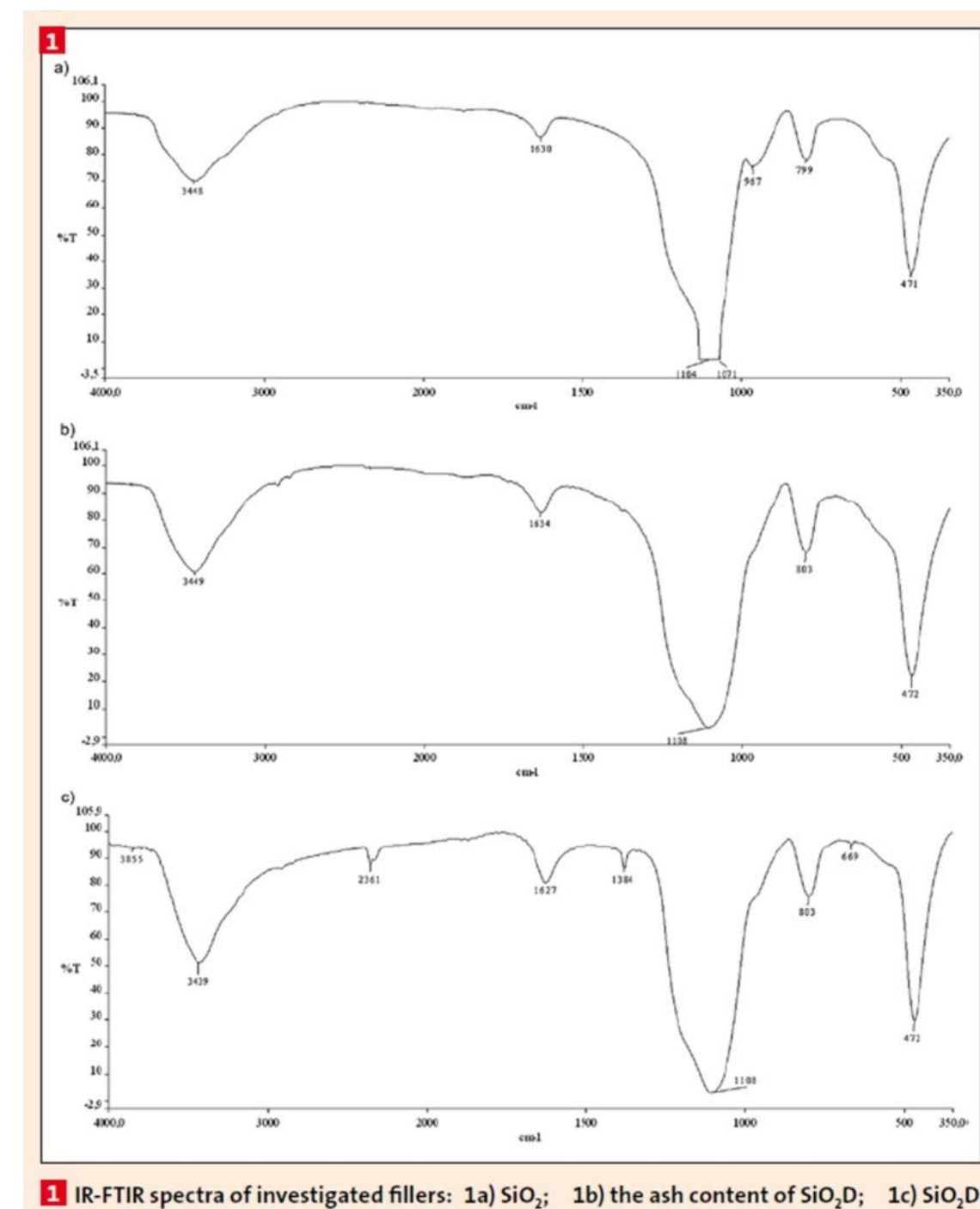
The solid residue (SiO₂D) obtained by the "Method of processing carbon-containing materials" [14] via pyrolysis of waste "green" tyres tread (Michelin energy 195/65 R 15) has been studied by FT-IR and ED-XRF (Energy Dispersion X-Ray Fluorescent) spectroscopy. The investigated rubber compounds have the following composition in phr (Table 1). The following raw materials were used without any subsequent purification: E-SBR (SynthosKralax 1500) produced by cold emulsion polymerization; precipitated silica (Silica WL 180 Gr), solid residue (SiO₂D) obtained via pyrolysis of waste "green" tyres; TESPD (Si 266, Bis(3-triethoxysilylpropyl)disulfide, Evonik/Degussa; TBBS (N-ter-butyl-2-benzothiazol sulfenamid). The rubber compounds were produced on laboratory mixing rolls. The curing properties of the investigated rubber compounds were determined by "Monsanto" rheometer at 160°C according to ISO 3417(2002). The mechanical properties were determined according to ISO 37(2002). Tan δ of the investigated vulcanizates was determined by using the Dynamic Mechanical Thermal Analyser Mk III system (Rheometric Scientific).

Results and discussion

The pyrolysis of a Michelin energy 195/65 R 15 tyre tread has been run under the conditions described in the experimental part. The sample size was approximately 5x30x50 mm. The pyrolysis yielded 47 % of a liquid product, 48 % of a solid residue (SiO₂D) and about 5 % of gaseous products. 68 % of ash content was established after heating the solid residue at 7000C in oxygen atmosphere for 1 h. The solid residue, the ash from the solid residue and precipitated silica (Silica WL 180 Gr) have been studied by FT-IR spectroscopy as well as EDXRF (Energy Dispersion X-Ray Fluorescent) spectroscopy. Figure 1a shows the IR spectrum of SiO₂. As it can be seen, the absorption bands registered for the ashes of SiO₂D (Fig. 1b) correspond utterly to those of SiO₂. Besides the characteristic absorption bands for SiO₂ there are also corresponding bands for NO₃- (at 1384 cm⁻¹) and for sulphur compounds (at 670 cm⁻¹) in the IR - spectrum of SiO₂D (Fig. 1c). The EDXRF analysis with regard to light elements has revealed the amount of SiO₂ in the ash of SiO₂D (Fig. 3) that corresponds to 96 % of silicon in SiO₂ (Fig. 2). The amount of silicon in SiO₂D (Fig. 4) is 70 % with regard to the amount of silicon in SiO₂ which is in agreement with the amount of the obtained SiO₂D ash. The EDXRF analysis of SiO₂D and SiO₂D ash for heavy metals (Fe, Zn) has demonstrated that they contain about 3-5 % of ZnO (the spectra are not presented here). The analyses allow the conclusion that the solid residue (SiO₂D) obtained from the pyrolysis of tyre tread of "green" tyres contains about 30 % of carbon, 65 % of SiO₂, 3 % of ZnO and 2 % other components.

1 Composition of the investigated rubber compounds (phr).

Compound	E-1	E-2	E-3	E-4	E-5	E-6
ESBR	100	100	100	100	100	100
ZnO	3	3	3	3	3	3
Stearic acid	2	2	2	2	2	2
SiO ₂	50	50	50	-	-	-
SiO ₂ D	-	-	-	50	75	75
Carbon black N 330	-	-	25	-	-	-
TESPD	-	5	5	3.5	-	5
TBBS	1.75	1.75	1.75	1.75	1.75	1.75
Sulfur	2	2	2	2	2	2



2 Properties of the investigated rubber composites.

Compound	Curing properties					
	E-1	E-2	E-3	E-4	E-5	E-6
ML (dNm)	44	22	34	26	60	37
MH (dNm)	85	75	90	84	112	98
ΔM (dNm)	41	53	56	58	53	61
T ₁₀ (min:s)	5:45	6:45	4:00	3:15	3:00	3:00
T ₉₀ (min:s)	22:30	17:45	13:00	10:30	15:15	10:30
M _c	4600	2750	2300	2050	3200	1750
Mechanical properties						
M ₁₀₀ (MPa)	1.2	1.6	3.2	2.5	3.0	5.1
M ₃₀₀ (MPa)	3.1	8.3	16.3	13.8	12.1	21.9
Tensile strength (MPa)	18.4	24.1	24.0	21.4	20.6	22.0
Elongation at break (%)	780	590	410	410	470	300
Residual elongation (%)	30	20	20	15	20	10
Shore A hardness	70	62	73	60	79	72
Abrasion (mm3)	180	96	109	100	141	116

The blends filled with precipitated silica that do not contain silanes or other dispersants demonstrate a high melt viscosity. The mixture E-1 has a minimum torque of 74 dNm. The presence of TESPD in mixture E-2 leads to a lower minimum torque (22 dNm). The minimum torque of E-4 mixture is somewhat higher (26 dNm), which is probably due to the presence of carbon black in SiO₂D. Similar results have been obtained when filling the rubber mixtures with a combination of SiO₂ and carbon black (mixture E-3) and with SiO₂D in the absence of silane (mixture E-5) and finally with SiO₂D in the presence of TESPD (mixture E-6). Mixture E-5 demonstrates a minimum torque value of 60 dNm which is considerably higher than the one of mixture E-6 (ML=37 dNm). The decrease in melt viscosity might result from the dispersing effect of silane and the reduced "filler-filler" interaction. This requires the presence of silanol (Si-OH) groups on the surface of SiO₂D. The difference between the maximum and minimum torque (ΔM) of the compositions comprising SiO₂D are negligibly higher than those of the corresponding compositions filled with SiO₂ and with combinations of SiO₂ and carbon black. The compositions filled with SiO₂D form a denser curing network and demonstrate shorter optimum curing time (M_c=1750, t₉₀=10:30 min) for mixture E-6, if compared to the corresponding compositions filled with SiO₂ and carbon black (M_c=2300, t₉₀=13 min) for mixture E-3. That might be due to the fact that the compositions filled with SiO₂D comprise a certain amount of ZnO (SiO₂D contains 3 % of ZnO). The presence of nitrogen and sulphur containing compounds could also act as vulcanization accelerators. The modulus 300 of the vulcanizates comprising SiO₂ and silane is about 8 MPa (mixture E-2) which is about 170 % higher than that of the vulcanizates without silane (M₃₀₀=3.1 Mpa) for mixture E-1. The modulus 300 in the case is on account of the chemical bonds formed between the SiO₂ surface and the rubber via the bifunctional silane. The formation of such bonds is facilitated by the availability of -OH groups on the filler surface as well as by the certain amount of adsorbed water which favours the hydrolysis of the silane ethoxy groups. The vulcanizates containing SiO₂D and silane also have a very high modulus 300 (M₃₀₀=21.9 Mpa) as shown for mixture E-6 in comparison to those without silane (M₃₀₀=12.1 Mpa) for mixture E-5. The high modulus 300 of the vulcanizates containing SiO₂D can be explained only by the availability of -OH groups on the surface of SiO₂ particles in SiO₂D. The increase in modulus 300 of the vulcanizates containing SiO₂D is not as pronounced as that of the vulcanizates comprising SiO₂ and silane. But one should keep in mind that about 30 % carbon black are present in SiO₂D which predicts the chemical bond between the former and the elastomer matrix. The tensile strength of vulcanizates containing SiO₂D and silane does not differ significantly (σ =22 Mpa) for mixture E-6 from that of vulcanizates containing SiO₂, silane and carbon black (σ=24 MPa) for mixture E-3. The same observation could be drawn as far as abrasion resistance is concerned. The abrasion value of the vulcanizates containing SiO₂D and silane (116 mm³) for mixture E-6 is close to that of vulcanizates containing SiO₂, carbon black and silane (109 mm³) as shown for mixture E-3 (Table 2). The high values for modulus 300 and outcome strength as well as the low values of abrasion and elongation at break of the vulcanizates containing SiO₂D could be achieved only, if SiO₂ particles preserve their initial size and surface activity under the pyrolysis conditions used.

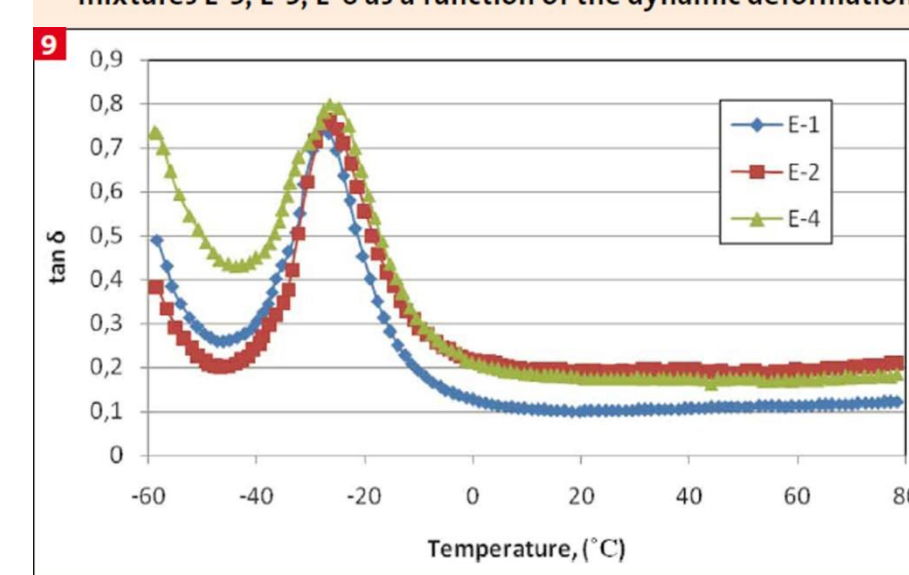
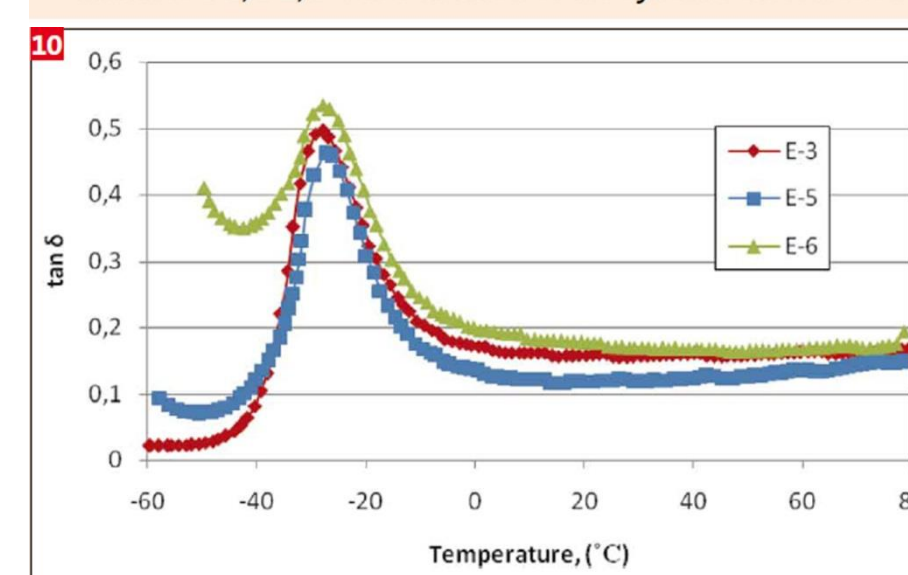
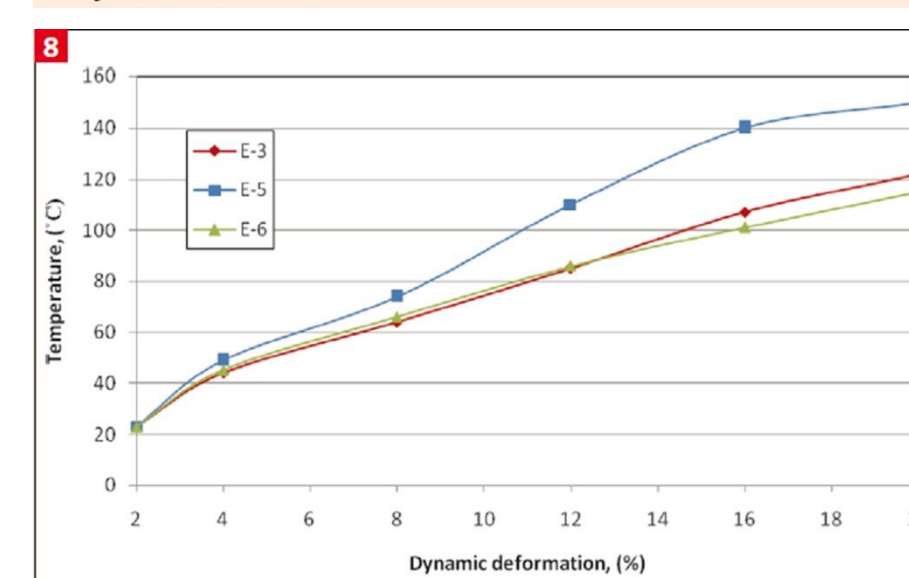
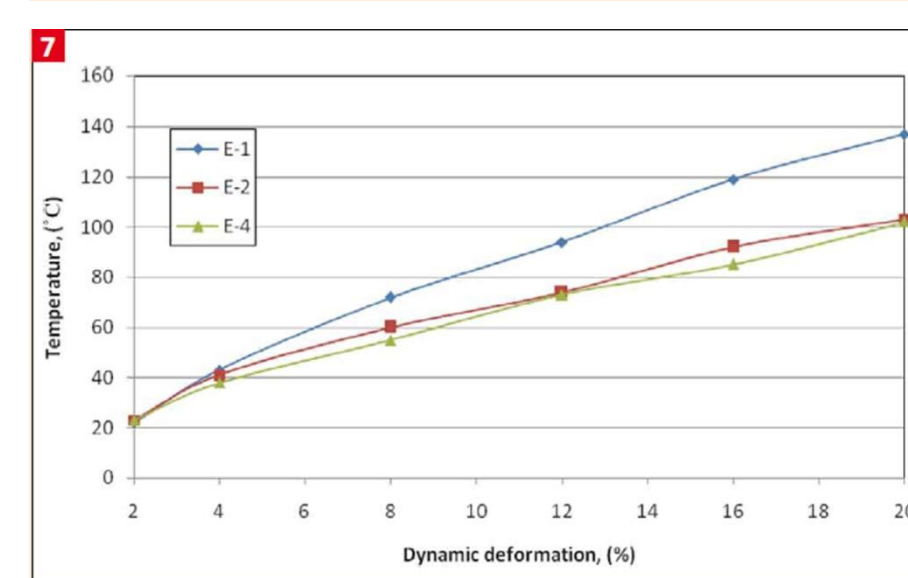
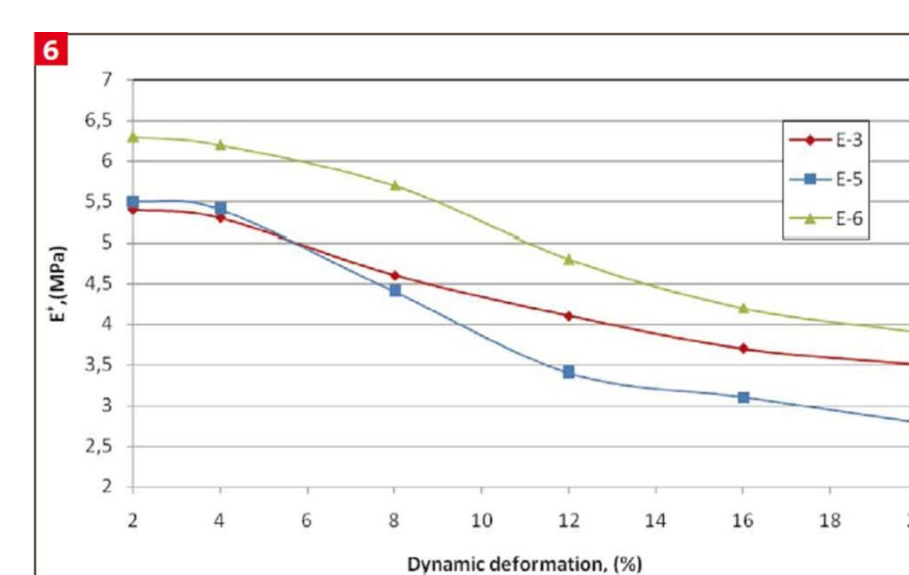
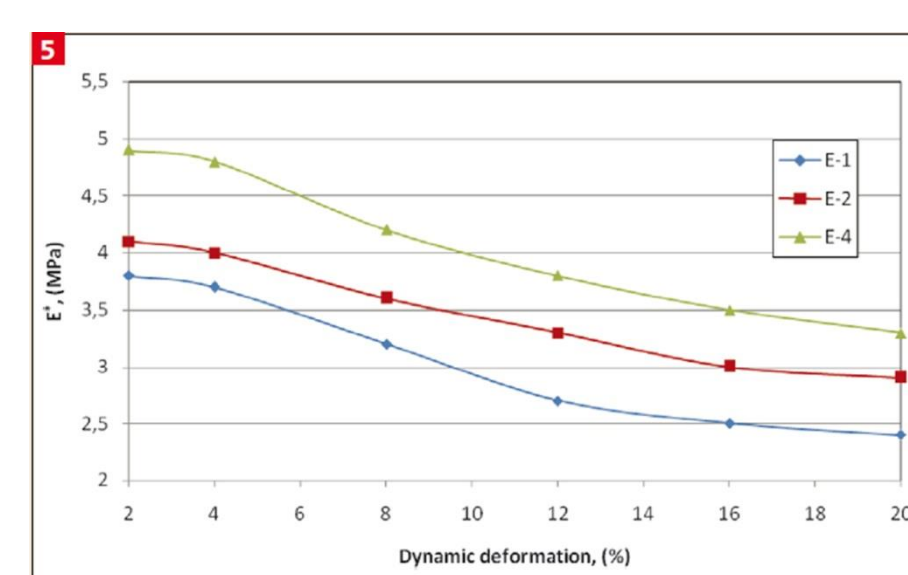
The filler dispersion in the rubber mixtures has an important effect upon the dynamic properties of the vulcanizates and particularly on the heat build-up which corresponds to the rolling resistance of tyres. The dependences of the complex dynamic modulus (E*) and the heat build-up on the dynamic deformation have been determined by using a Goodrich flexometer. Figure 5 presents the dependence for vulcanizates containing SiO₂, SiO₂ and silane, and in addition SiO₂D and silane. As it can be seen the greatest decrease of the dynamic modulus (Payne effect) takes place in vulcanizates filled with SiO₂ that do not contain silane (mixture E-1), which is due to the poor dispersion of the filler particles and the formation of a "filler-filler" structure which is not destructed at small dynamic deformations. The presence of silane favours the dispersion of the filler particles (mixture E-2). That reduces quite the decrease of the dynamic modulus at larger dynamic deformations. The higher dynamic modulus values of E-2, if compared to those of E-1, are probably due to the denser vulcanizate structure of the former. The dynamic modulus values of vulcanizates containing SiO₂D (Fig. 5, mixture E-4) at small dynamic deformations are the highest and their decrease with the increasing dynamic deformation is more pronounced than that of the vulcanizates containing SiO₂ and silane. That might be owing to the presence of some amounts of carbon black in SiO₂D and of an amount of SiO₂ which is smaller than that in the vulcanizates of mixture E-2. The vulcanizates containing SiO₂D without silane have the most pronounced decrease of E* with the increasing dynamic deformation (Fig. 6, mixture E-5). The curves for the vulcanizates containing SiO₂D and silane (Fig. 6, mixture E-6) have a pattern similar to that for the vulcanizates containing SiO₂, carbon black and silane (Fig. 6, mixture E-3) but have higher dynamic modulus values for all deformations studied. That probably results from the denser curing network of those vulcanizates. The heat build-up is the highest for the compositions without silane (Fig. 7, mixture E-1 and Figure 8, mixture E-5). The vulcanizates containing SiO₂ and silane (Fig. 7, mixture E-2) and SiO₂D and silane (Fig. 8, mixture E-6) have the same heat build-up. The vulcanizates containing SiO₂, carbon black and silane (Fig. 8, mixture E-3) and those containing SiO₂D and silane (Fig. 8, mixture E-6) also have the same heat build-up. The temperature dependence of tan δ (tan δ =E"/E') deserves interest since it is considered that tan δ at 60 °C corresponds to the rolling resistance of the tyres, while tan δ at 0 °C it corresponds to the traction on wet road. Figures 9 and 10 show how tan δ of the vulcanizates studied depends on temperature. As seen there is not a significant difference in the patterns of the curves for the vulcanizates containing SiO₂ and silane (Fig. 9, mixture E-2) and SiO₂D and silane (Fig. 9, mixture E-4) as well as those containing SiO₂, carbon black and silane (Fig. 10, mixture E-3) and those for vulcanizates containing SiO₂D and silane (Fig. 10, mixture E-6). However, it is inexplicable why the vulcanizates without silane have lower tan δ values at 60 °C, what is in disagreement with the heat build-up, which is higher (Fig. 7 and 8), and the fact is in contradiction with the conventional statements.

Conclusion

The results achieved demonstrate no differences in the mechanical properties (modulus 300 %, tensile strength, abrasion resistance, etc.) of the vulcanizates filled with SiO₂D and of those filled with conventional SiO₂ and carbon black at a 2:1 ratio. There are no differences in the dependences of the complex dynamic modulus and of the heat build-up on the degree of dynamic deformation as well as in the thermal dependences of tan δ of the vulcanizates studied – those filled with SiO₂D and those filled with conventional SiO₂ and carbon black in the presence of bis(3-triethoxysilylpropyl)disulfide. The results obtained could be explained only, if the initial size of SiO₂ particles and their surface physical and chemical activity is recovered under the pyrolysis conditions mentioned. Having in mind the tendency that SiO₂ is going to replace carbon black both in light and heavy tyres, the pyrolysis of waste tyres in the presence of vapour seems to be a perspective method for SiO₂ recovery.

Acknowledgement:

This research work was supported by Bulgarian Ministry of Education and Science, Structural Funds and Educational Programs Directorate, Project "Support for the development and realization of PhD-students, post-docs and young researchers in the field of polymer chemistry, physics and engineering", Grant № BG051PO001/07/3.3-02/51 51.



Десислава Петрова-Плачкова¹, Росица Горанова¹, Мария Стайкова¹, Стоян Милошев¹, Христо Новаков², Илияна Берлинова²

¹ Химикотехнологичен и Металургичен Университет, катедра „Полимерно инженерство“, бул. „Кл.Охридски“ 8, 1756 София, email: stuci@uctm.edu

² Институт по полимери, Българска Академия на науките, ул. „Акад. Г.Бончев, бл. 103 А., 1113 София

Цел: Изследване възможността за провеждане на контролирана радикалова полимеризация на N-изопропилакриламид по RAFT методиката, за създаване на звездовидни полимерни архитектури на базата на функционализиран p-изопропенилкаликс[n]арен.

Въведение.

Един от начините за провеждане на контролирана полимеризация за получаване на полимери с определена архитектура е с използване възможностите на RAFT полимеризацията.

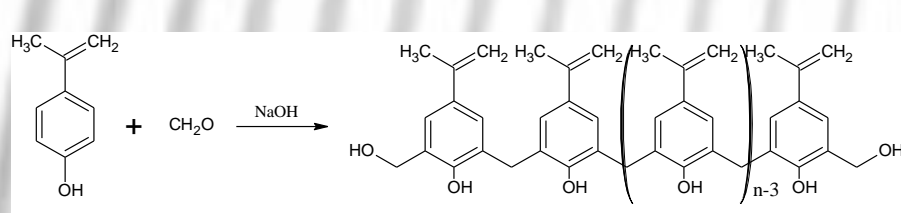
Известно е, че мономери съдържащи двойна връзка - стирен, метилметакрилат и други винилови производни могат да бъдат полимеризирани по радикалов механизъм при различни условия, но получените хомо- и съполимери се характеризират със значителна полидисперсност. Чрез методите на контролираната радикалова полимеризация (RAFT, ATRP) могат да се получат полимери с определена архитектура и ниска полидисперсност.

Ние се насочихме към синтеза на p-изопропенилкаликс[n]арен и дитиобензоена киселина, като макроагент за RAFT полимеризация на N-изопропилакриламид.

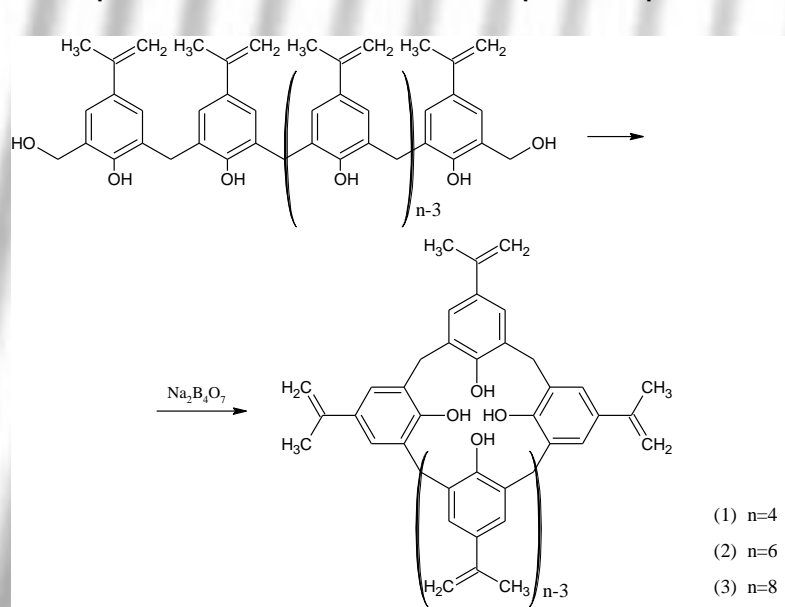
1. Синтез на p-изопропенилкаликс[n]арен

Синтезът на p-изопропенилкаликс[n]арени е проведен по известна методика с установени молни съотношения и реакционни условия в два етапа:

✓ Първи етап - синтез на линейни олигомери с определена дължина на макроверигата от p-изопропенил-фенол и алдехид:



✓ Втори етап - циклизация на получените линейни олигомери в среда на високо кипящ разтворител:



Получените p-изопропенилкаликс[4]-, p-изопропенил каликс[6]- и p-изопропенилкаликс[8]арени са охарактеризирани чрез ГПХ, ИЧ- и УВ-спектроскопия и ¹H ЯМР. Отместването на характерните ивици за ОН-групата в ИЧ-спектъра при 3400 cm⁻¹, както и химичното отместване на синглета, характерен за протоните от ОН-групите в ¹H ЯМР спектъра (таблица 1) при 9 ppm показват напрегане на олигомерните вериги, което е характерно за циклична структура.

Таблица 1
¹H ЯМР и ИЧ спектрални характеристики на p-изопропенил-каликс[4]-арен, p-изопропенилкаликс[6]арен и p-изопропенил-каликс[8]арен

Съединение	¹ H ЯМР, ppm					ИЧ, cm ⁻¹	
	ArH	ArCH ₂ Ar	OH	C=CH ₂	CH ₃	U _{OH}	U _{C-S}
p-изопропенил-каликс[4]арен	δ 6.67	δ 4.38-4.41H _{ar}	δ 9.25	δ 4.47-4.64	δ 2.29	3368	1656
p-изопропенил-каликс[6]арен	δ 6.65	δ 3.41-3.51H _{ar}	δ 9.23	δ 4.44-4.67	δ 2.25	3368	1654
p-изопропенил-каликс[8]арен	δ 6.67	δ 4.37 H _{ar} δ 3.51 H _{ar}	δ 9.23	δ 4.55-4.67	δ 2.26	3369	1654

2. Синтез на RAFT агент (дитиобензоена киселина)

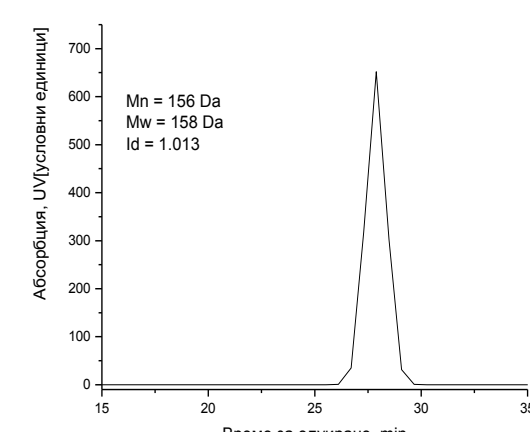
Ефективен агент за създаване на макроинициатори за RAFT полимеризация на p-заместени феноли е дитиобензоената киселина (DTBA) и нейни производни. За нейното получаване бе избран един от най-често цитираните като добър от технологична гледна точка методи - чрез използване на Гриняров реактив.

Заключение

Синтезиран е макроагент за RAFT полимеризация на базата на функционализиран p-изопропенилкаликс[8]арен с дитиобензоена киселина. Установено е, че той може успешно да се прилага за създаването на звездовидни архитектури при полимеризация на N-изопропилакриламид.

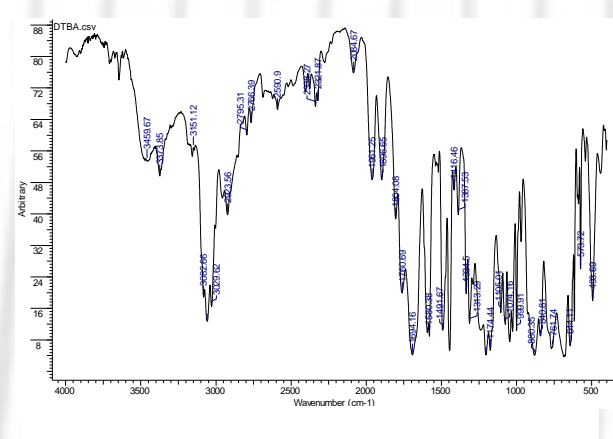
Благодарности

Авторите изказват своята благодарност на НФ „Научни изследвания“ към Министерството на образованието, младежта и науката за финансовата подкрепа по проект ВУ Х-304/2007, фонда за изследвания и развитие на Химикотехнологичния и Металургичен Университет -София, проект № 10793, както и на проект № 51, BG051PO001/07/3.3-02, Европейски социален фонд, Оперативна програма Развитие на човешките ресурси за предоставените възможности.

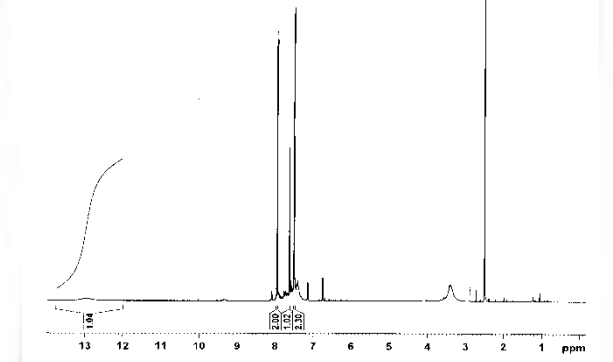


Фиг. 1. ГПХ хроматограма на дитиобензоена киселина

ГПХ хроматограмата на фиг.1 показва наличие на продукт с мономодално разпределение по MM. Изчислената средно масова MM от 158 Da съответства на теоретично изчислената за това съединение от 154Da. Тясното масово молекулно разпределение (D = 1.013) доказва синтеза на дефиниран продукт с висока чистота. В ИЧ спектъра (фиг.2) се наблюдават характерните трептения при 1430 cm⁻¹ за C=S връзка (от ароматно ядро); 1380 cm⁻¹ за C=S връзка и 630 cm⁻¹ за (C-S) връзка.



Фиг. 2. ИЧ спектър на дитиобензоена киселина

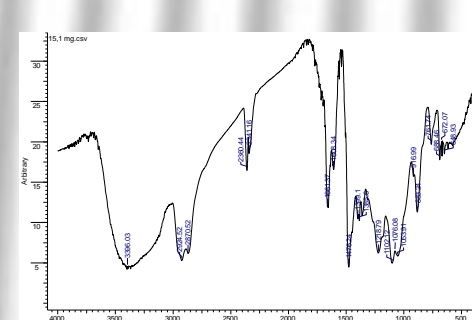


Фиг.3. ¹H ЯМР спектър на дитиобензоена киселина

В ¹H ЯМР спектъра се наблюдават отмествания при 7.95 ppm (2H, o-ArH) 7.61ppm (2H, m-ArH), 7.63 ppm (1H, p-ArH) и 6.75 ppm (1H, C-SH).

3. Синтез на макро-RAFT агент за свободно – радикалова контролирана полимеризация

За синтез на макро-RAFT агент се спряхме на получения p-изопропенилкаликс[8]арен, чиято конформационна структура дава възможност за разполагане на изопропениловите фрагменти в различни равнини, което би позволило максимално функционализиране на каликсареновия пръстен. Реакцията е извършена при условия известни в литературата, а полученият продукт е охарактеризиран чрез ГПХ, ИЧ и ¹H ЯМР спектроскопия. Получената от ГПХ молекулна маса на получения продукт от 2400 Da отговаря на теоретично изчислената от 2403.5 Da за напълно функционализиран p-изопропенилкаликс[8]арен.

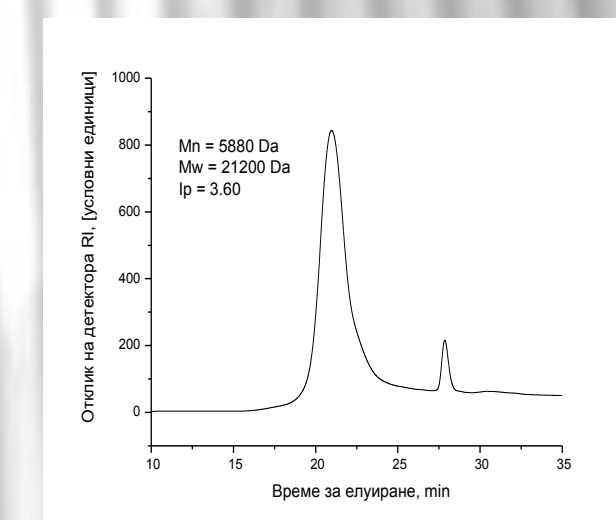


Фиг.4. ИЧ спектър на макроагент, получен при функционализиране на p-изопропенилкаликс[8]арен с дитиобензоена киселина

В ИЧ спектъра се наблюдават наред с характерните за изопропенил-каликс[8]арени и дитиобензоената киселина ивици и такива при 1476 cm⁻¹ (C-(CH₃)₂) и мултиплет с максимален интензитет при 1360 cm⁻¹ (C-S-C). Наличието на мултиплет при 688-648cm⁻¹ (характерен за C-S връзка) вероятно се дължи на различните конформационни състояния на отделните различни функционализиранни елементарни звена. Освен това в ¹H ЯМР спектъра на получения продукт не се наблюдават химични отмествания при около 4.6 ppm, характерни за C=CH₂ връзка. Всичко това ни дава основание да твърдим че е получен напълно функционализиран „макроагент“.

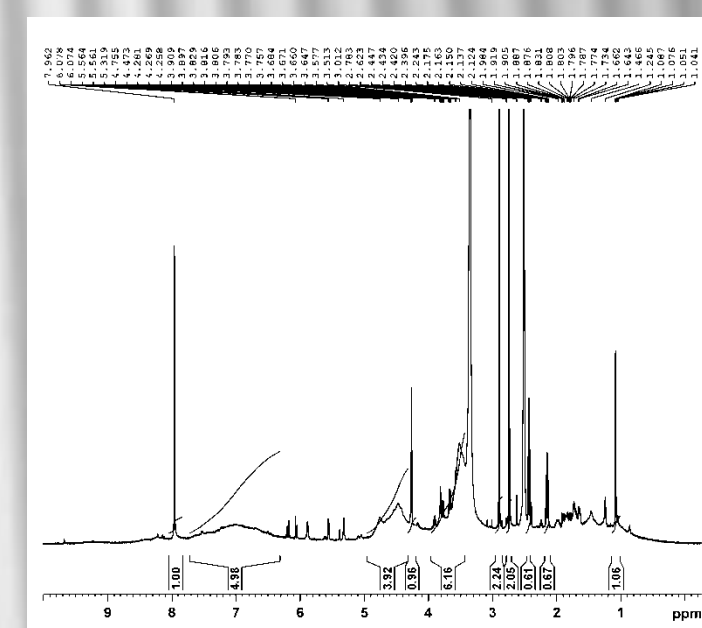
4. Синтез на звездовиден полимер чрез RAFT полимеризация на N-изопропилакриламид

RAFT полимеризацията на N-изопропилакриламид (NIPAM) е осъществена в присъствието на линейни RAFT агенти и инициатор AIBN, в среда на ТХФ или ДМФ при температура 70 °С, а получените продукти са утаявани в диетилов етер и сушени под вакуум.



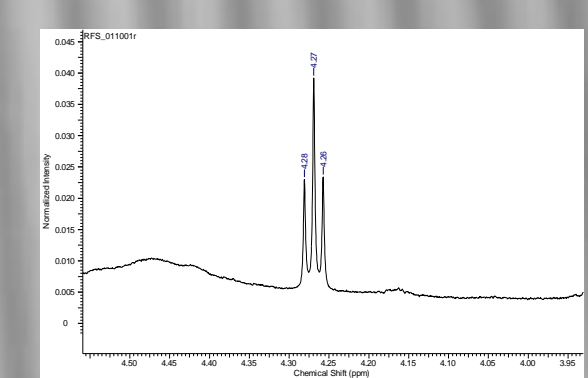
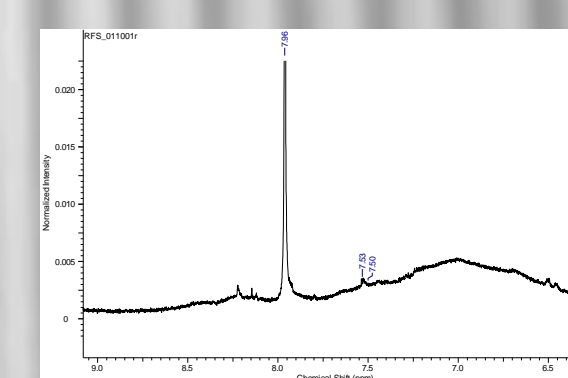
Фиг. 5. ГПХ хроматограма на продукт от RAFT полимеризация на NIPAM и макроагент на основата на функционализиран p-изопропенилкаликс[8]арен

От показаната ГПХ хроматограма (фиг. 5) е определена средномасова MM на продукта около очакваната при едновременно нарастване на всички звездовидни краища с около 2000 Da (2400 + 2260 x 8 = 20 480 Da).



Фиг. 6. ¹H ЯМР спектър на продукт от RAFT полимеризация на NIPAM и макроагент на основата на функционализиран p-изопропенилкаликс[8]арен

В ¹H ЯМР спектъра на получения продукт се наблюдават всички характерни отмествания за макроагента, както и специфичните за нарастващата верига на PNIPAM. От отношението на интензитета на сигнала отговарящ за протон от метиновата група на нарастващото звено от NIPAM (a) при 7.53 ppm и това на протон на p-място в бензеновото ядро от дитиобензоеновия фрагмент (б) при 4.27 ppm се определя дължината на полимерната верига.



Фиг. 7. Фрагменти от ¹H ЯМР спектъра (фиг. 6) на продукта от RAFT полимеризация на N-изопропилакриламид

От сравняването на фрагментите в ¹H ЯМР спектъра (фиг. 7) е изчислено съотношение около 10 т.е. е постигнато нарастване на молекулната маса във всеки край на звездовидната структура с 10 елементарни NIPAM звена, което отговаря на предварително заложеното съотношение, както и на наблюдаваното увеличение на средно масовата молекулна маса на продукта.

Следователно избраният макроагент - функционализиран p-изопропенилкаликс[8]арен с дитиобензоена киселина - е подходящ за RAFT полимеризация на N-изопропилакриламид.

Thermoresponsive Poly(ethoxytriethyleneglycol acrylate)s: From Different Synthesis Approaches to Preparation of Colloidal Nanoparticles in Water

N. Toncheva¹, E. Petrova¹, B. Trzebicka², A. Dworak², Ch. Tsvetanov¹

¹Institute of Polymers, BAS, Sofia 1113 Bulgaria, ²Center of Polymer and Carbon Materials, PAS, Zabrze 41-819 Poland

Poly(ethoxytriethyleneglycol acrylate) (PETEGA) as a Template for Core-Shell Polymeric Nanoparticles. Why?

1 PETEGAs' Properties:

- Temperature-responsive polymer - LCST is 34 °C;*
- LCST does not change with MW (unlike poly(2-isopropyl-2-oxazoline) (PIPOX) and poly(oxyethylene methacrylate) (POEGMAs), reversible phase transition;
- Flexible polymer chain Tg ~ -60°C;
- Under heating can form sub 100 nm colloid particles with or without a surfactant;*
- Colloidal nanoparticles are suitable as nano-templates for preparation of hollow nanocapsules.

2 Benefits of Nanocapsules:

- in contrast to polymeric micelles nano-capsules can carry larger quantities of guest molecules;
- mechanically more stable than polymer vesicles;
- open possibilities for outer shell modification;

2 Motivation:

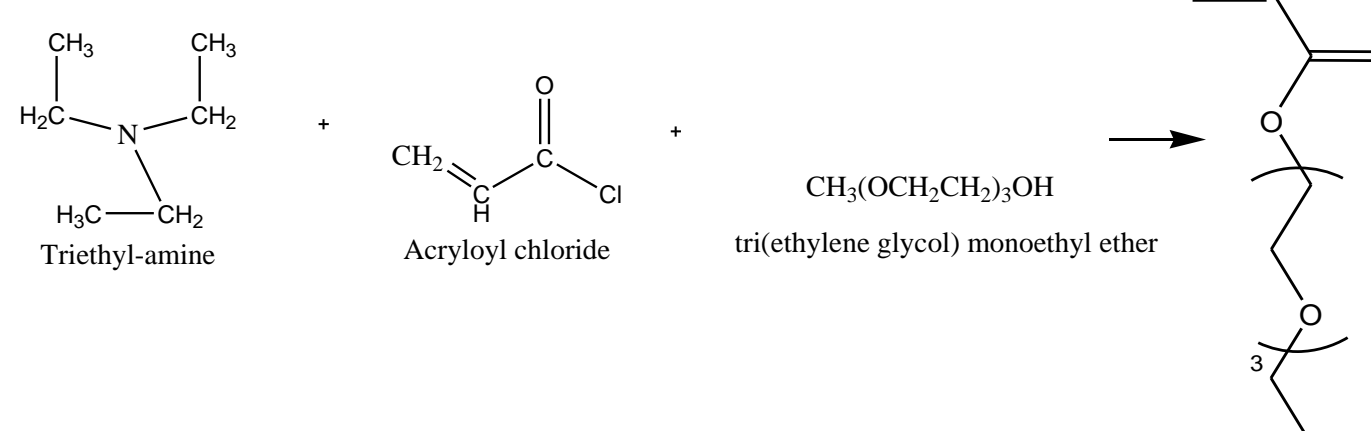
- PETEGA forms nano-templates that is suitable for preparation of hollow nanospheres. Thus, very important to know is how easily to receive polyacrylates with desired Mn and PD. For this purpose three controlled polymerization techniques were used and the characteristics of the obtained polymers have been compared.

3 Objective:

- To synthesize series of well defined temperature responsive poly(ethoxytriethyleneglycol acrylate)s; (PETEGAs) by ATRP, RAFT or anionic polymerization (AP);
- To synthesize sub 100 nm polymeric nano-capsules by mild and non-destructive means;

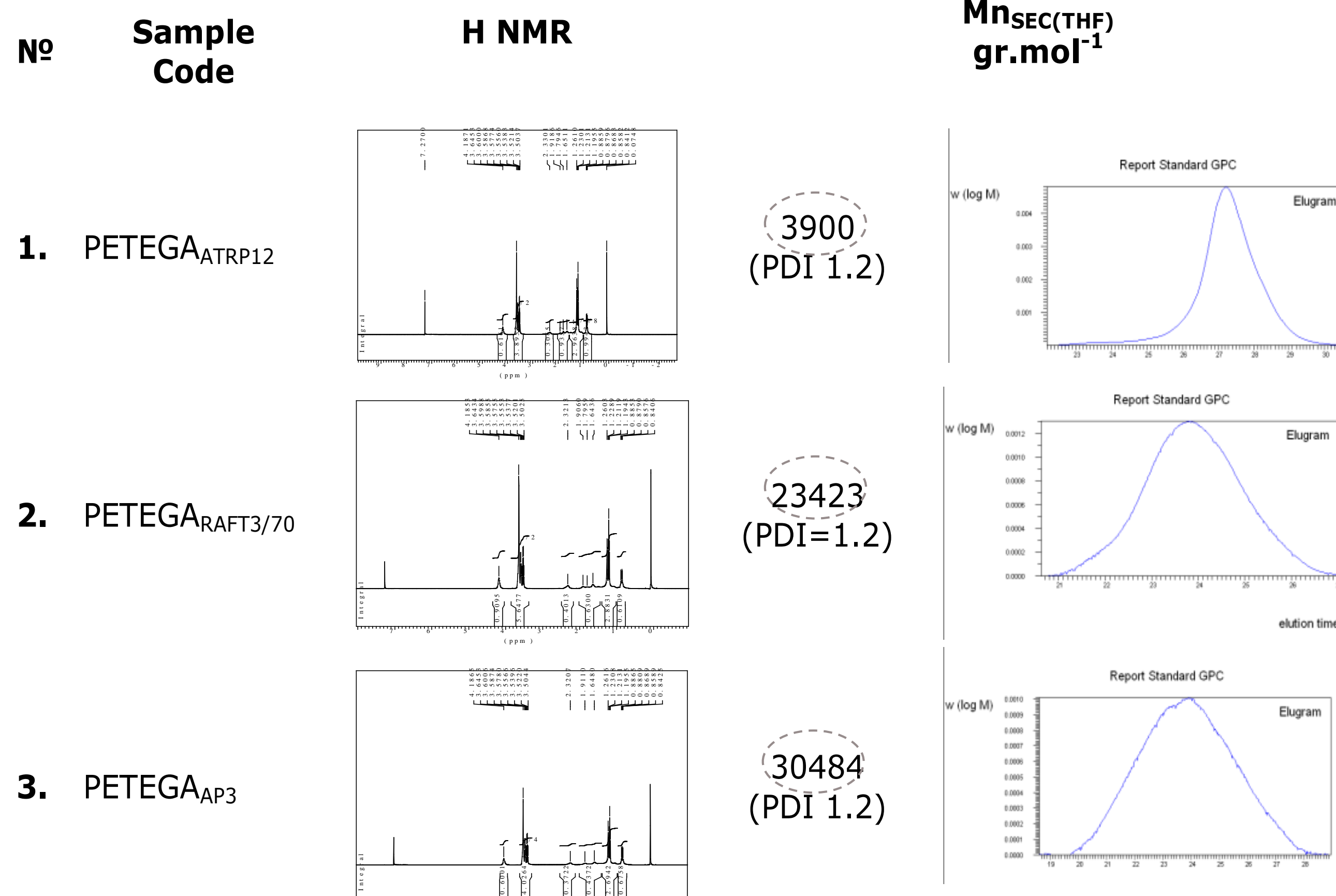
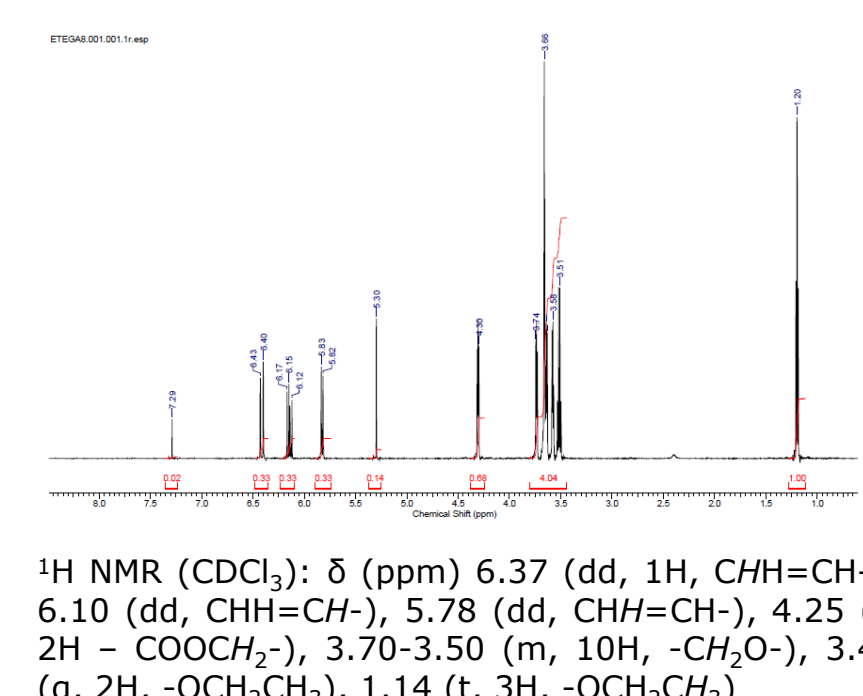
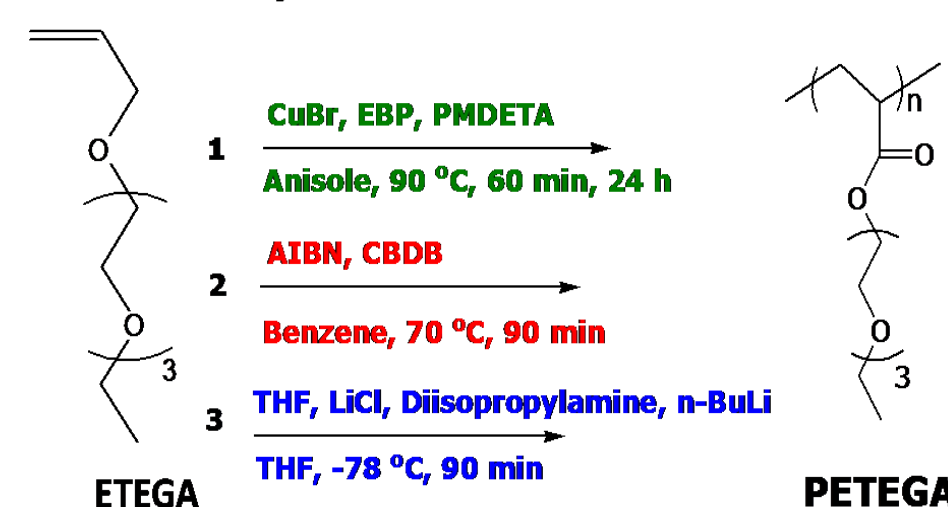
Benefits of Nanocapsules:

Monomer Synthesis:



Polymer Synthesis:

Synthesis of PETEGA

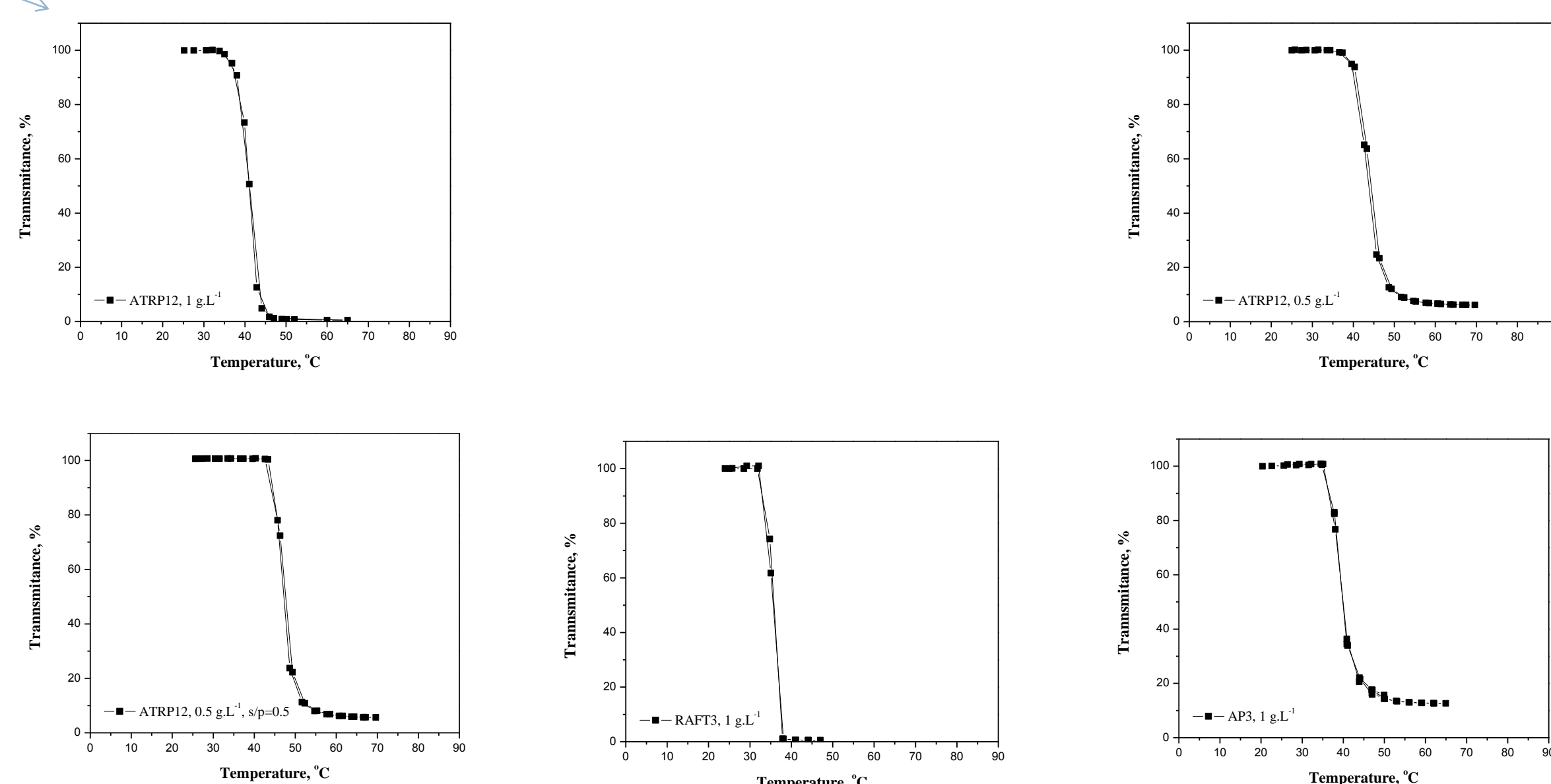


Dynamic Light Scattering measurements:

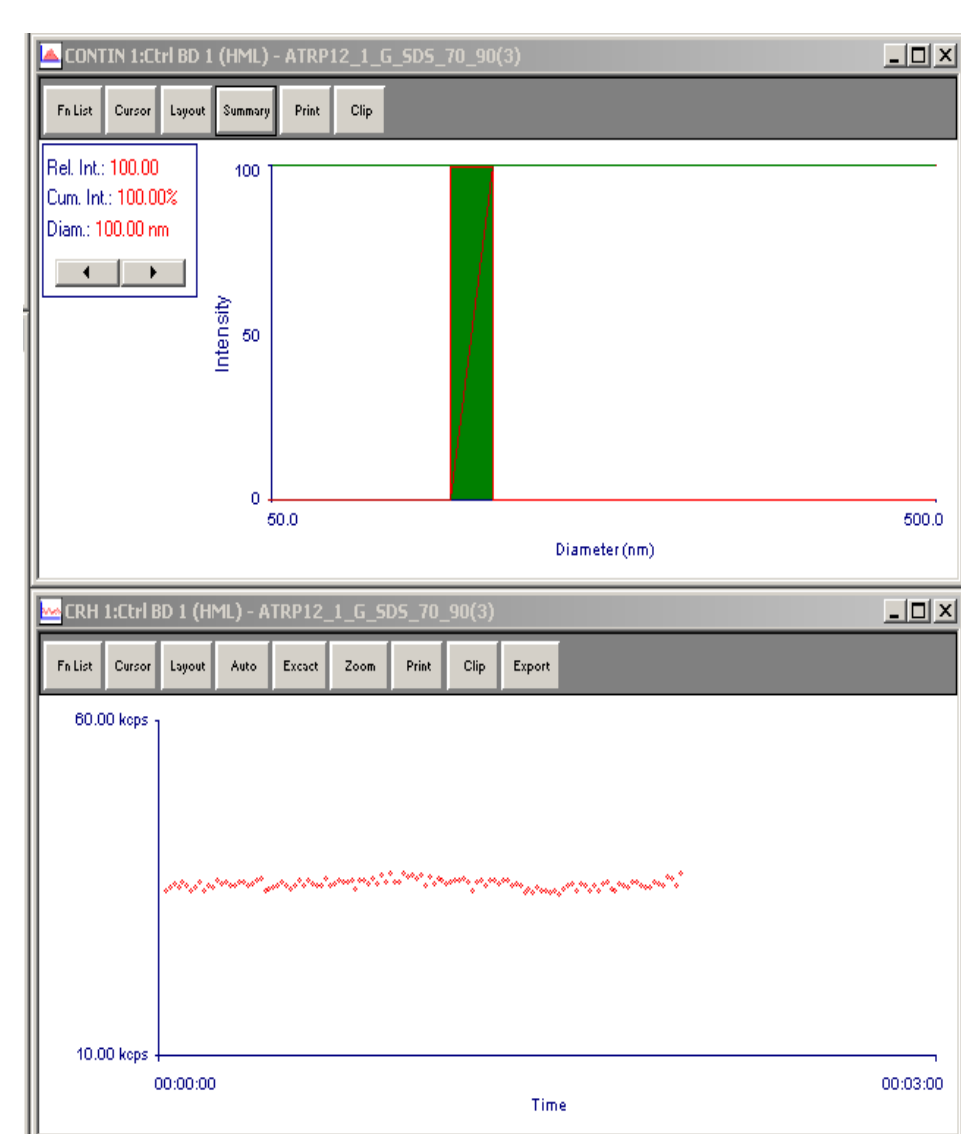
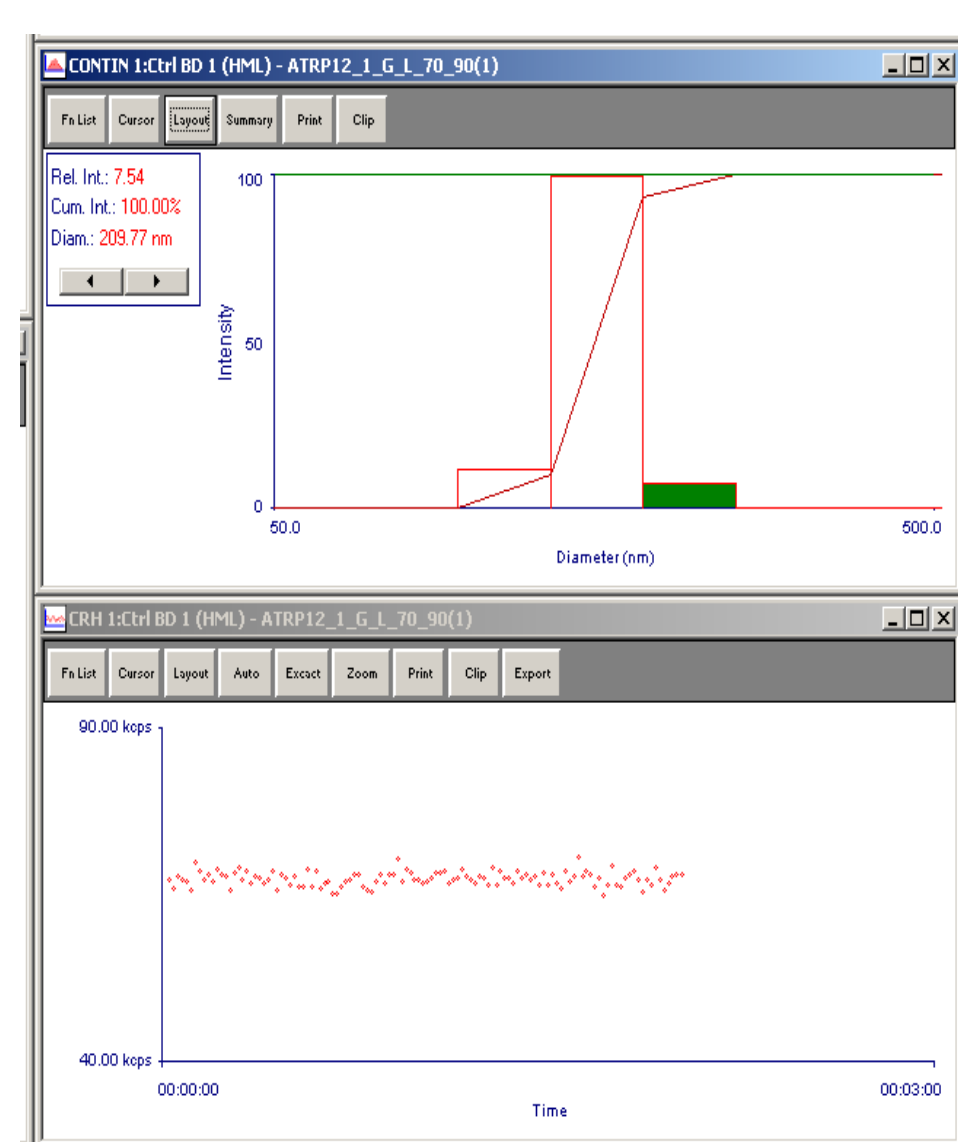
Nº	Sample Code	Conc. g.L ⁻¹	Surfactant/ Polymer g/g	Mean Diameter nm	PDI Factor	kcps
1.	PETEGA _{ATRP12}	1	-	151 (T=70 °C)	0.093	67
2.	PETEGA _{ATRP12}	1	0.5	100 (T=70 °C)	0.056	143

Turbidity measurements:

Nº	Sample Code	Conc. g.L ⁻¹	Surfactant/ Polymer g/g	Cloud Point °C
1.	PETEGA _{ATRP12}	1	-	34
		1	0.5	40
		0.5	0.5	43
2.	PETEGA _{RAFT3/70}	1	-	33
3.	PETEGA _{AP3}	1	-	35



1. X. Jiang, C.A. Lavender, J. W. Woodcock, B. Zhao *Macromolecules* **2008**, *41*, 2632.
2. Patent WO98/01478
3. (a) Antoun, S.; Teyssie, P.; Jerome, R. *Macromolecules* 1997, *30*, 1556-1561.
(b) Antoun, S.; Teyssie, P.; Jerome, R. *J. Polym. Sci., Part A*, 1997, *35*, 3637-3644.



Summary:

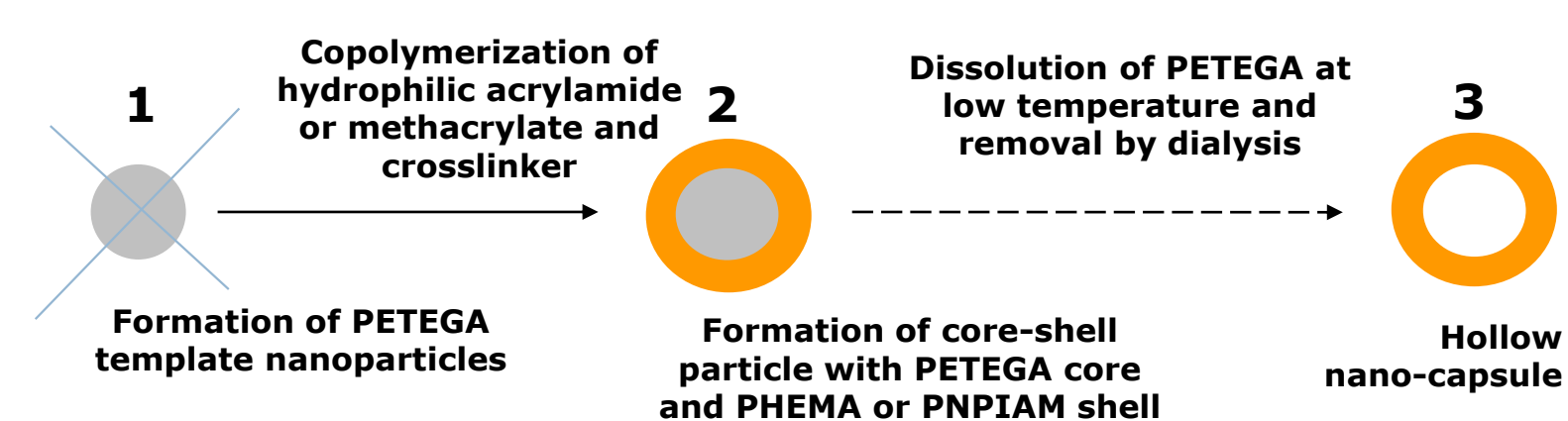
- Using ATRP, RAFT and AP techniques was successfully prepared three different PETEGAs with controlled molar mass and polydispersity. The easiest way for obtaining low molecular PETEGAs is ATRP. Obtaining of high molecular polyacrylates with low polydispersity is possible using both AP or RAFT. However, taking into account the simplicity of the both technics the AP is preferable.
- PETEGA phase transition in aqueous medium is fully reversible.
- From the DLS data could be stated that PETEGA forms uniform nano-templates and it is suitable for preparation of hollow nanospheres.

Funding:

- Under project - BG051P0001/07/3.3-02/51 "Support for the development and realization of Ph.D-students, post-docs and young researchers in the field of polymer chemistry, physics and engineering".
- Bulgarian NSF project DO 02-47/18.12.2008 (ID01/034)



Future Outlook:



Crystallization of Calcium Phosphates in Polysaccharide Matrices



D. Rabadjieva¹, S. Tepavicharova¹, S. Shopova², E. Vassileva², R. Titorenkova³

¹Bulgarian Academy of Sciences, Institute of General and Inorganic Chemistry, "Acad. G. Bonchev" Str., bl. 11, 1113, Sofia, Bulgaria

²University of Sofia "St. Kliment Ohridski", Faculty of Chemistry, Laboratory on Structure and Properties of Polymers, 1, James Bourchier Blvd., 1164, Sofia, Bulgaria

³Central Laboratory of Mineralogy and Crystallography, Bulgarian Academy of Sciences, Acad. G. Bonchev Str., Bl.107, 1113 Sofia, Bulgaria

INTRODUCTION

In nature, living organisms produce mineralized tissues such as bone, teeth and shells by a sophisticated process called biomineralization. Recently, the preparation of organic-inorganic hybrid materials with controlled mineralization analogous to those produced by nature has received much attention because it can:

- aid in understanding the mechanisms of the biomineralization process and
- result in development of new biomimetic materials.

AIM

To study crystallization of calcium phosphates in biopolymeric matrices by adsorption and diffusion of CaCl₂ and K₂HPO₄ solutions.

I Experiment:

- K₂HPO₄ is preadsorbed in biopolymers;
- Ca²⁺ diffusion in hydrogels
- pH 3-9
- Crystallization time – 2 – 120 h
- Drying – room temperature

X-Ray characterization

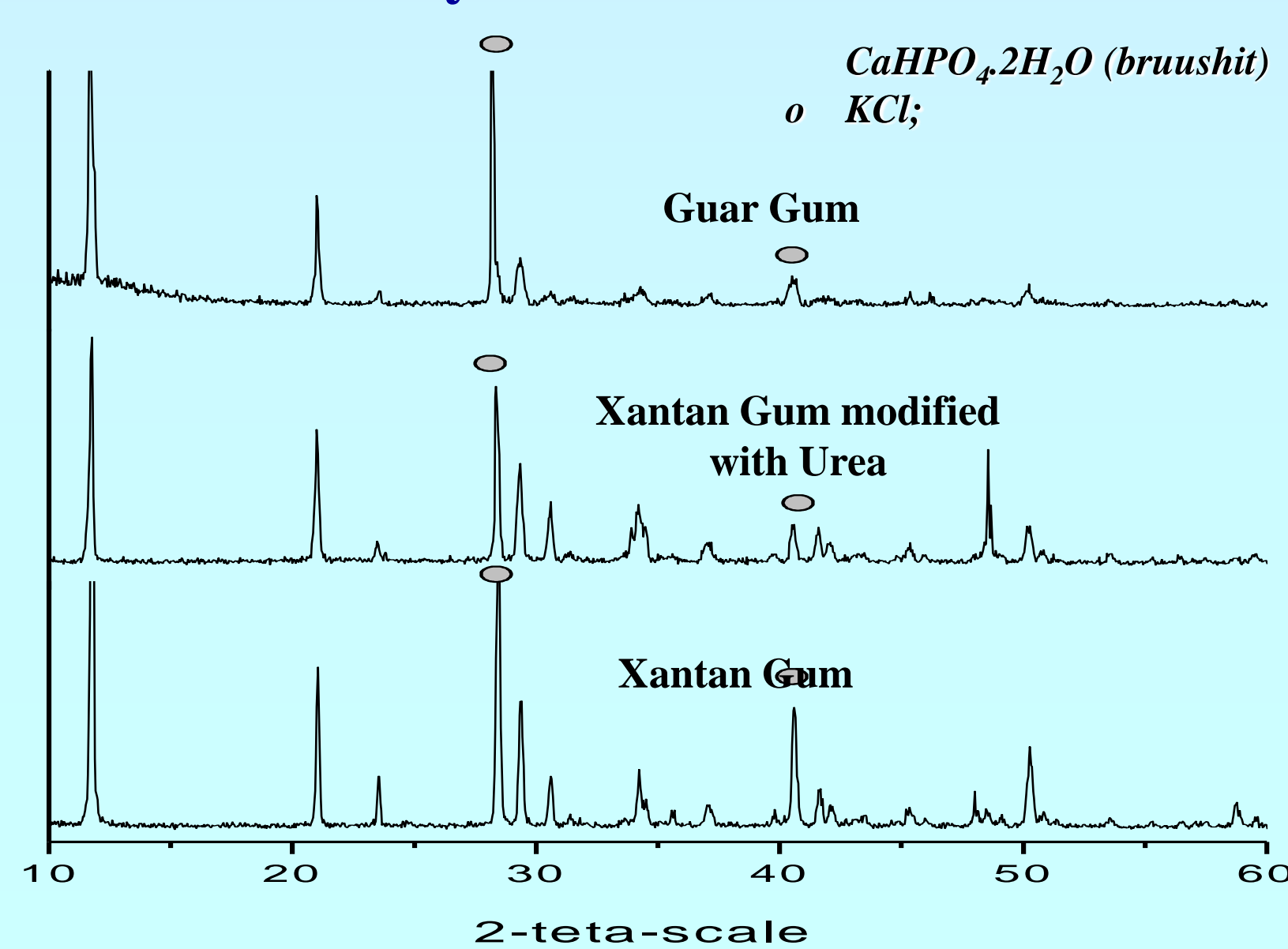


Table. Size of the brushite crystallites

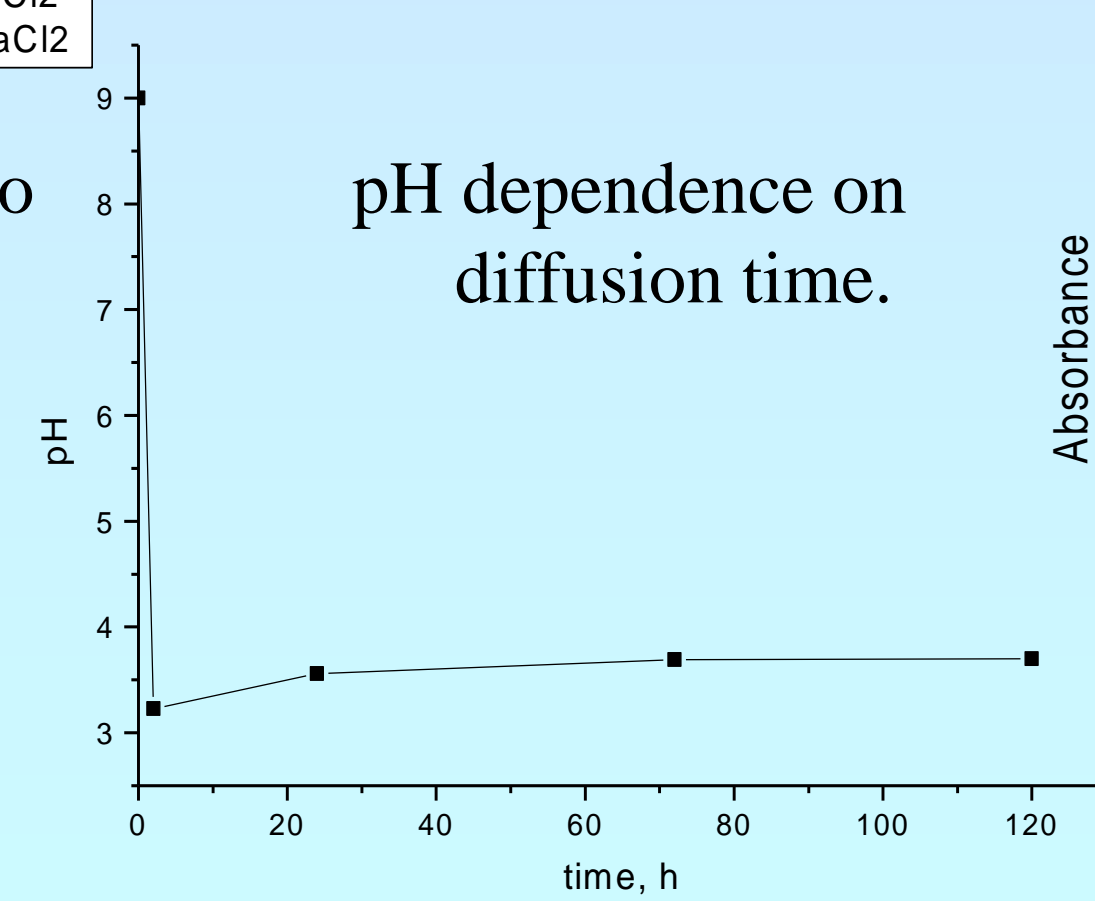
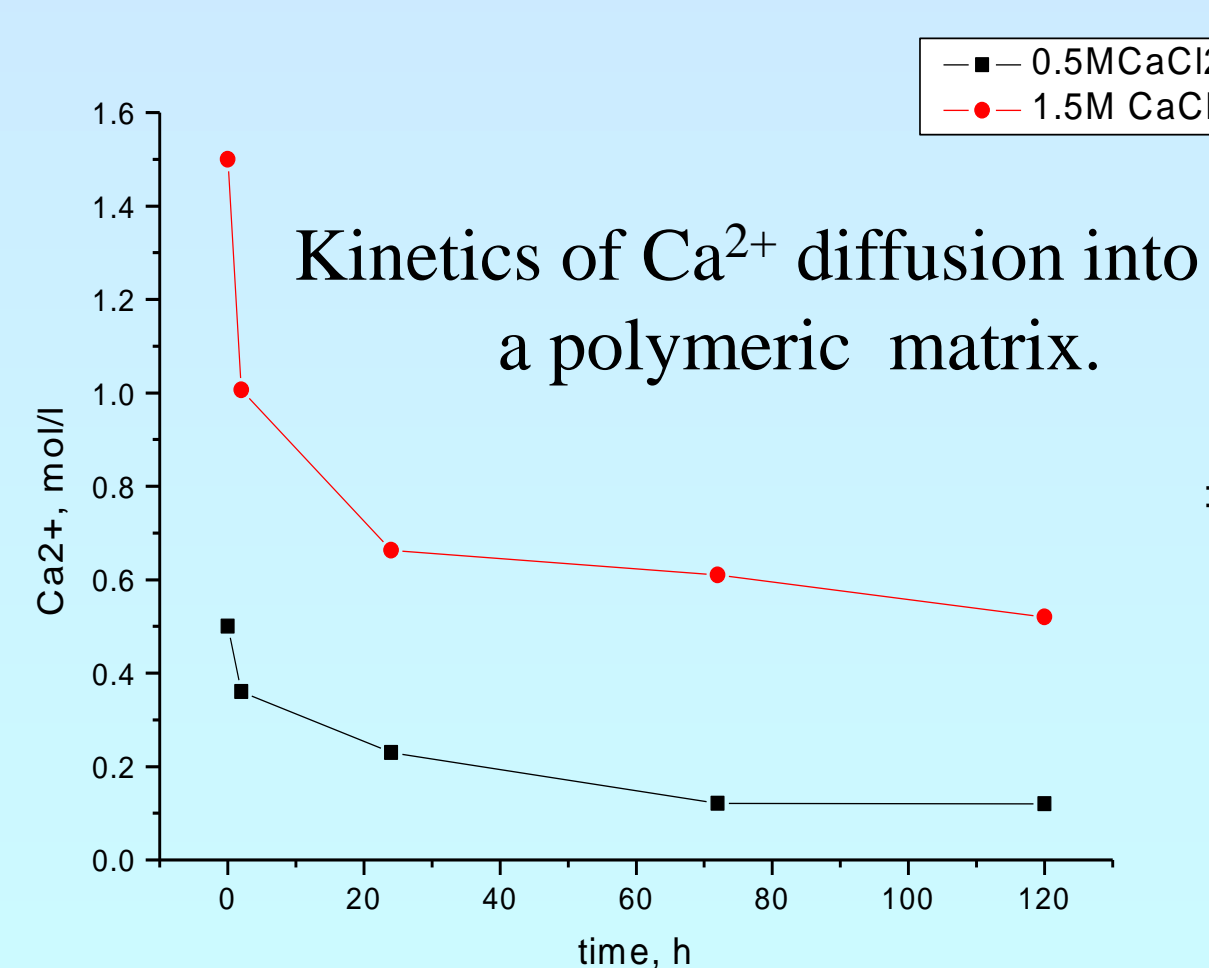
Polymer	Size, nm
Xantane Gum	80.3
Xantane Gum + Urea	51.2
Guar Gum	40.3

EXPERIMENT

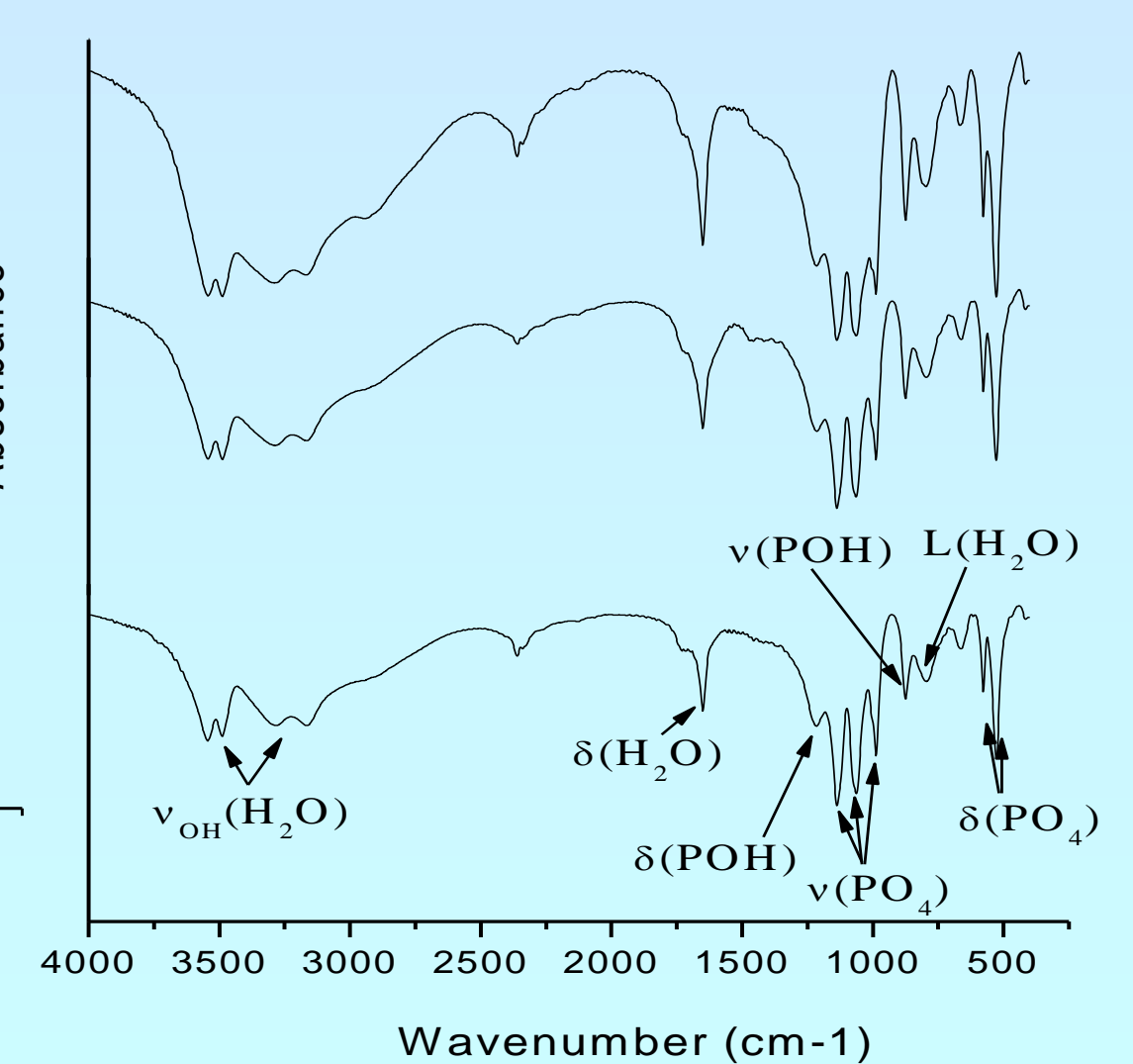
Reagents:

- Polysaccharides- Xantane Gum, Guar Gum, Alginate;
- Inorganic salts, aqueous solutions - 0.3 M K₂HPO₄; 0.5 M /1.5M CaCl₂
- Media modifying agents - Urea; Simulated body fluid (SBF)

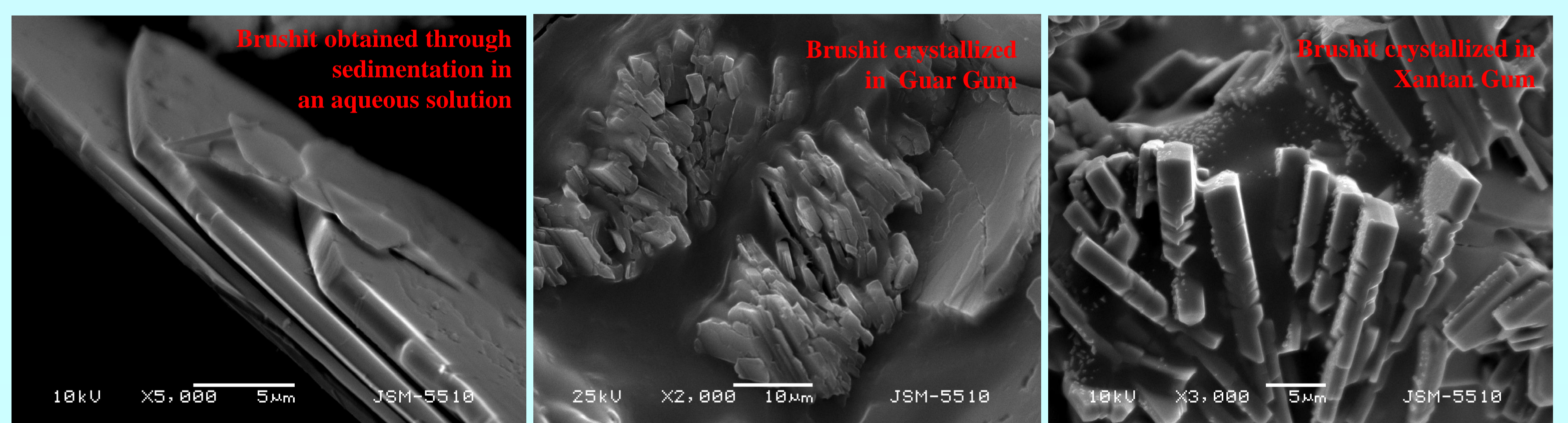
RESULTS



IR characterization



SEM characterization

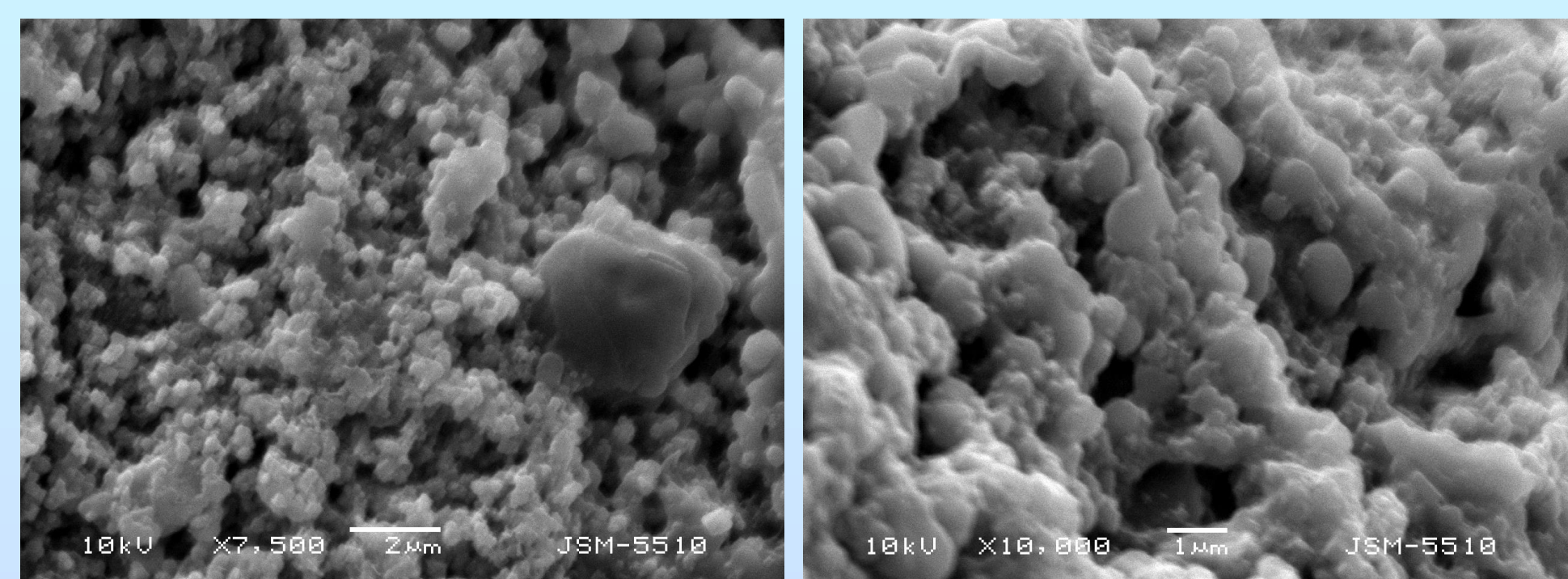


Incorporation of brushite into the organic matrix (biopolymer)

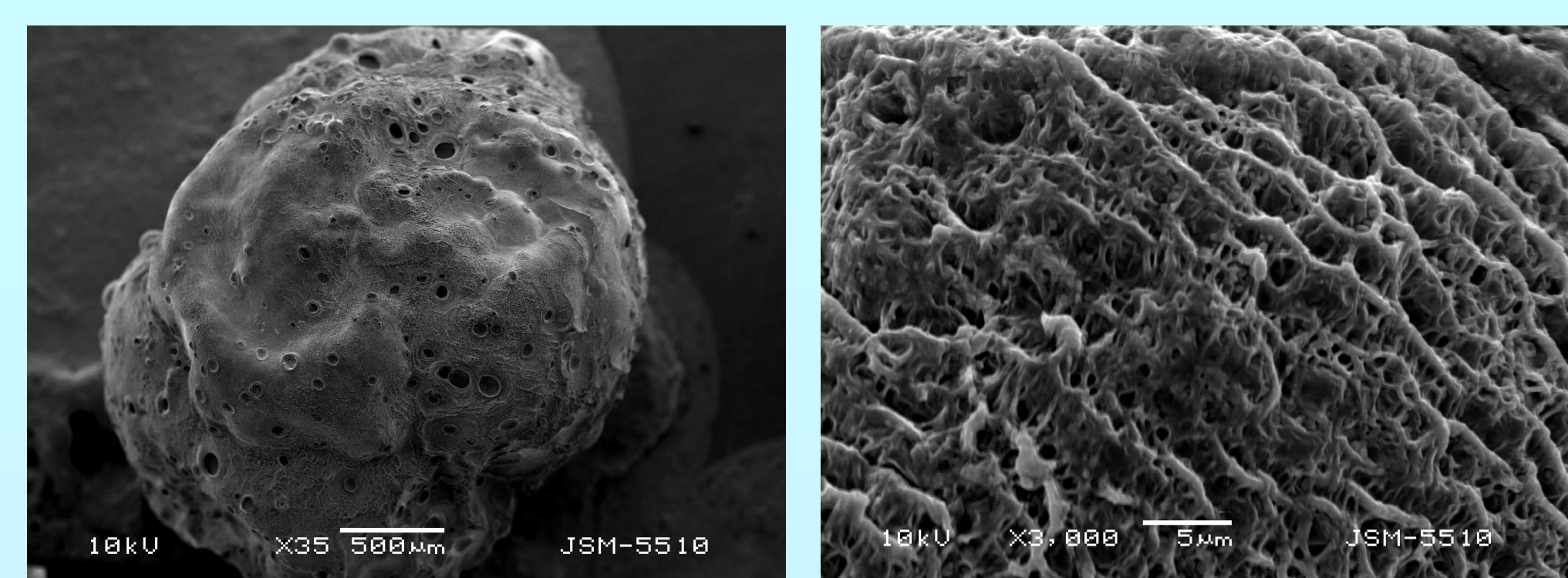
II Experiment:

- Ca²⁺ crosslinked alginate beads;
- K₂HPO₄ diffusion in the beads;
- pH 8-10;
- Crystallization time – 9 or 28 days;
- Drying – room temperature.

Alginate beads after 28 days in **0.003 M K₂HPO₄** (pH=7.97)

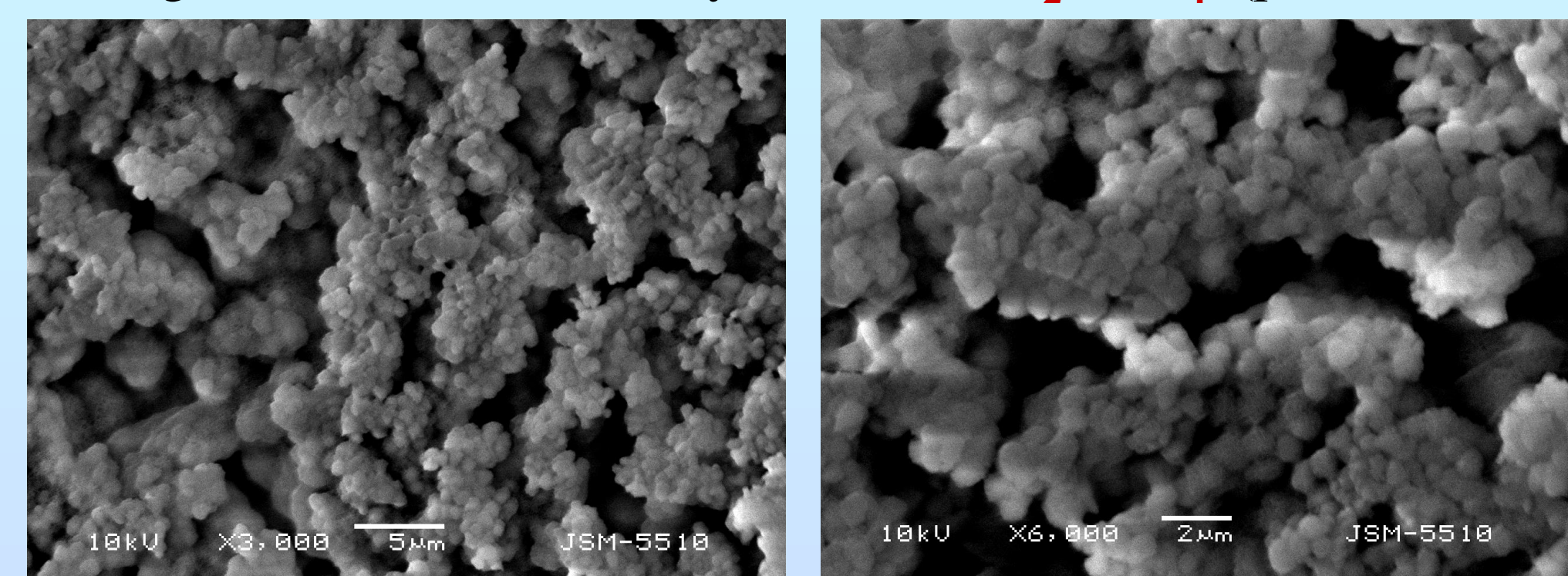


days	pH
1	7.97
6	6.56
28	6.08



Alginate beads after 28 days in **0.3 M K₂HPO₄** (pH=8.71)

Ca²⁺ crosslinked alginate beads.



Alginate beads after 9 days in **simulated body fluids** (SBF) (pH=7.3).

days	pH
1	8.71
28	8.4

CONCLUSIONS

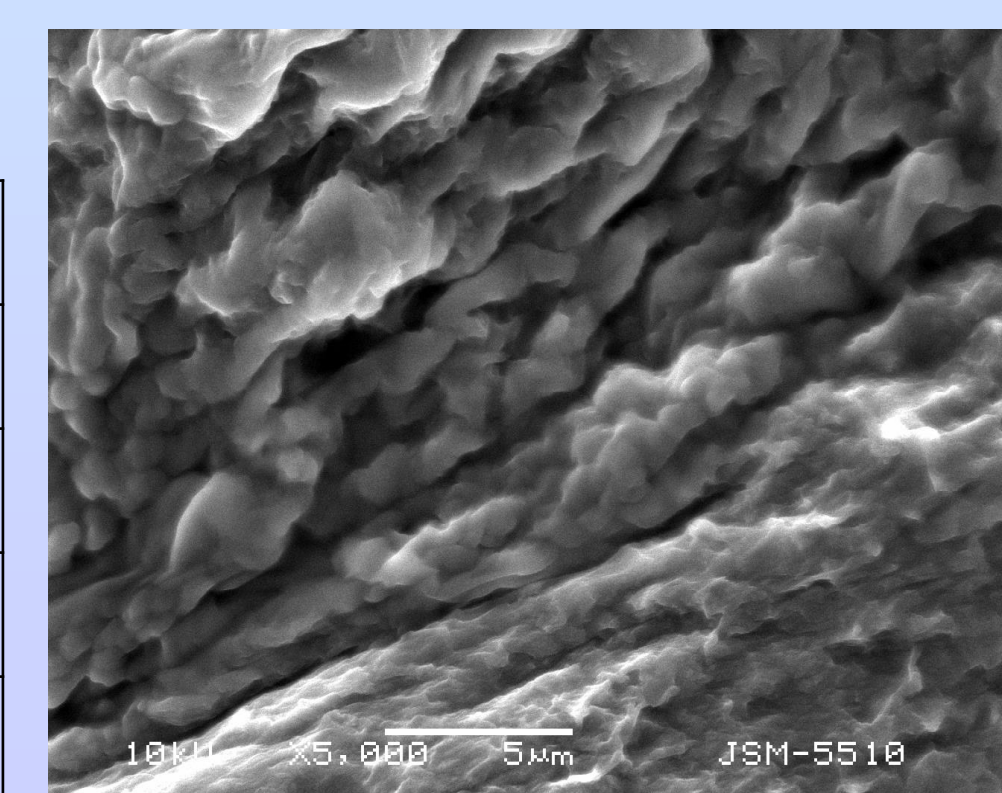
This study is an attempt to mimic the natural occurring process biomineralization.

- Two different polymeric matrices were used as a media for calcium phosphates crystallization. In all cases brushite (CaHPO₄·2H₂O) was obtained due to the drastic drop in pH after the very beginning of Ca²⁺ diffusion into the polymer.
- Depending on the polymer ability to swell into K₂HPO₄ aqueous solution the size of the crystallites varied being smaller in case of Guar and larger in Xantane Gum.
- By using modifying agents for K₂HPO₄ solution we were able to influence the size of crystallites, Urea being the modifying agent with the most pronounced effect – in its presence the size significantly decreases.

- The crystallization of calcium phosphates when alginate beads are immersed in K₂HPO₄ solution takes place through Ca²⁺ in the alginate. Thus pH of the solution decreases and most probably brushite is formed. In a simulated body fluid the crystallization of calcium phosphates takes place through Ca²⁺ from the SBF. pH of the solution increases and the obtained calcium phosphate is most probably hydroxyapatite. X-ray and IR characterization of the samples are under way.

Composition of SBF

	mmol/l		mmol/l
Na	144.0	Cl	147.9
K	4.0	SO4	0.5
Mg	1.5	PO4	1.0
Ca	2.6	CO3	4.2



days	pH
1	7.3
3	8.28
6	8.49
9	8.54

Acknowledgements: This research is financed through the National Fund for Scientific Investigations, Project № DO-02-82/2008.

The presentation of this investigation is with the financial support of Project No BG051PO001/07/3.3.-02/51.



Нов подход за имобилизиране на уреаза в температурно-чувствителен криогел на поли(N-изопропилакриламид)

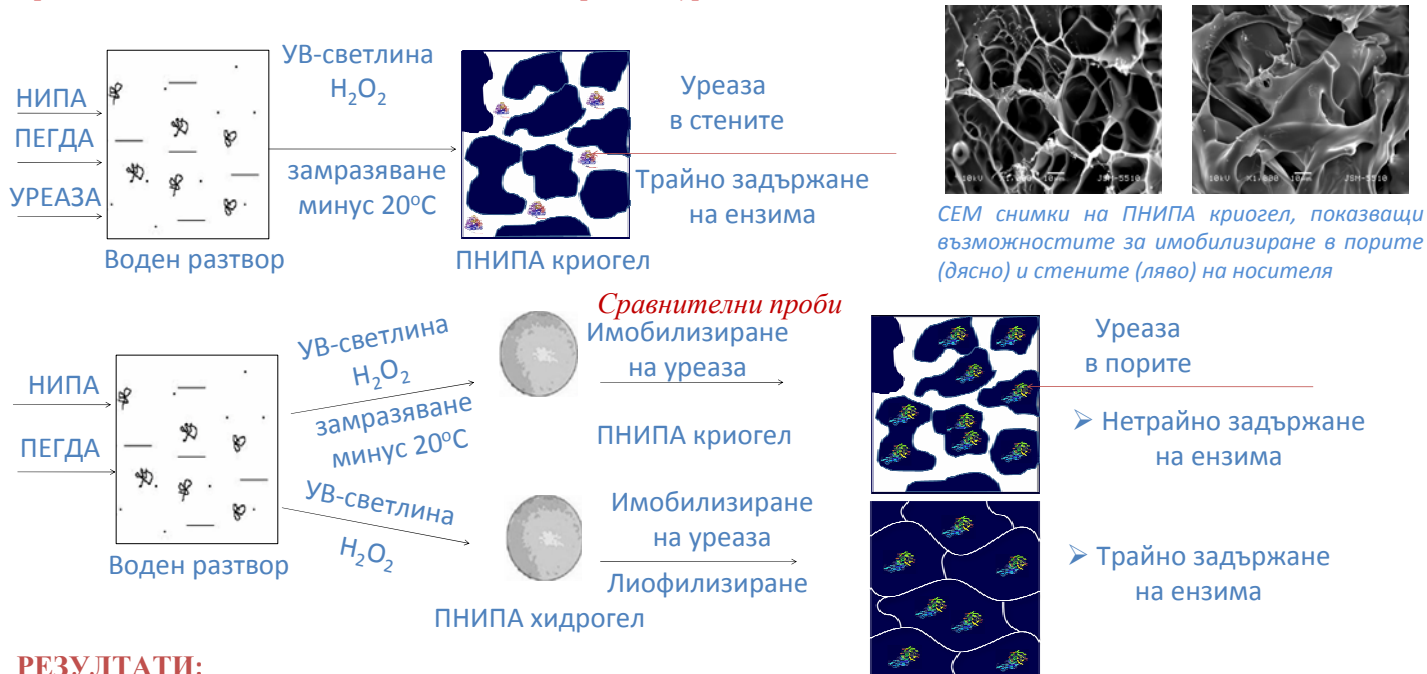
Северина Павлова,¹ Петър Петров,¹ Христо Цветанов,¹ Райчо Димков,² Яна Топалова²

¹Лаборатория Полимеризационни процеси, Институт по полимери, Българска Академия на Науките; ²КОПХ, Биологически факултет, СУ "Св.Климент Охридски"

ВЪВЕДЕНИЕ:

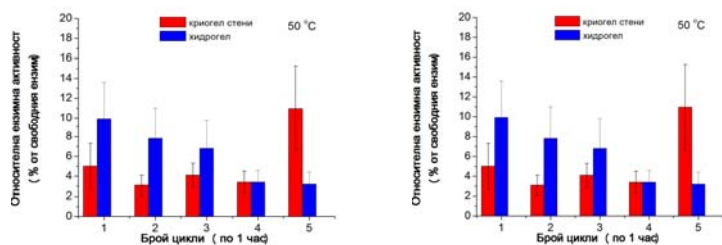
В последно време особен интерес представляват полимерните хидрогелове, способни да реагират на промяна на околната среда. Системи, проявяващи подобни „интелигентни“ свойства по възпроизводим начин, са в основата на една нова генерация материали с голям потенциал в биомедицината и биотехнологията. Целта на изследването е да се разработи нов метод за нековалентно имобилизиране на уреаза в стените на температурно-чувствителен криогел на основата на поли(N-изопропилакриламид).

Принципна схема на нековалентно имобилизиране на уреаза



РЕЗУЛТАТИ:

ЕНЗИМНА АКТИВНОСТ



Сравнение на ензимната активност на уреаза, имобилизирана в стените на ПНИПА криогел и в ПНИПА хидрогел за различни периоди от време

➤ Бе установено, че при включването на уреазата в стените на ПНИПА криогел и ПНИПА хидрогел, ензимът не изтича.

➤ Криогеловите с уреаза, имобилизирана в стените, показват постоянна каталитична активност при многократни тестове.

ИЗВОД: Беше разработен успешно нов метод за трайно нековалентно имобилизиране на уреаза в стените на температурно-чувствителен криогел на поли(N-изопропилакриламид) като бе запазена ензимната активност. Така имобилизираната уреаза може да намери приложение като биосензор за откриване на урея.

БЛАГОДАРНОСТИ  BG051P0001/07/3.3.-02/51, "Подкрепа за развитие и реализация на докторанти, пост-докторанти и млади учени в областта на полимерната химия, физика и инженерство" и Фонд Научни Изследвания: договор ВУ-Х-302

Biodegradable Scaffolds from PLA/EVOH Drawn Blends

S. Simeonova, M. Evstatiev

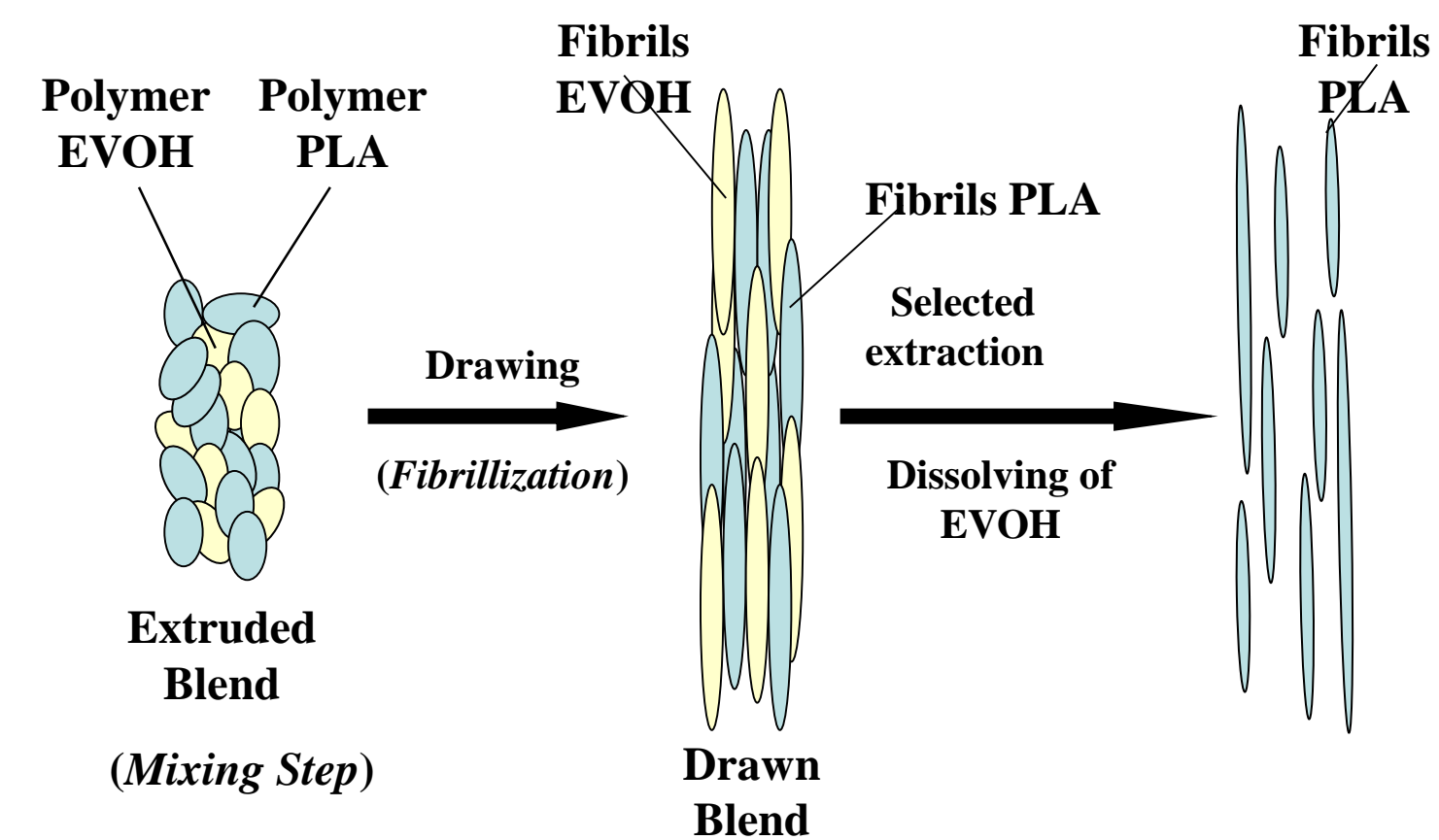
Sofia University, Faculty of Chemistry
Laboratory on Polymers
1164 Sofia, Bulgaria



Goal and MFC Concept

The main goal of this investigation is to offer a new technology for manufacturing of bio-degradable 3-dimensional (3D) scaffolds free from contacts with toxic solvents. For this purpose the concept for microfibrillar-reinforced composites (MFC) is utilized [1]. The biodegradable polymer is melt blended with another one and extruded, followed by cold drawing, where both polymers are converted into a fibrillar state. After dissolving of the second blend component with not-toxic solvent, the fibrils from the biodegradable polymer can be isolated and a scaffold to be formed.

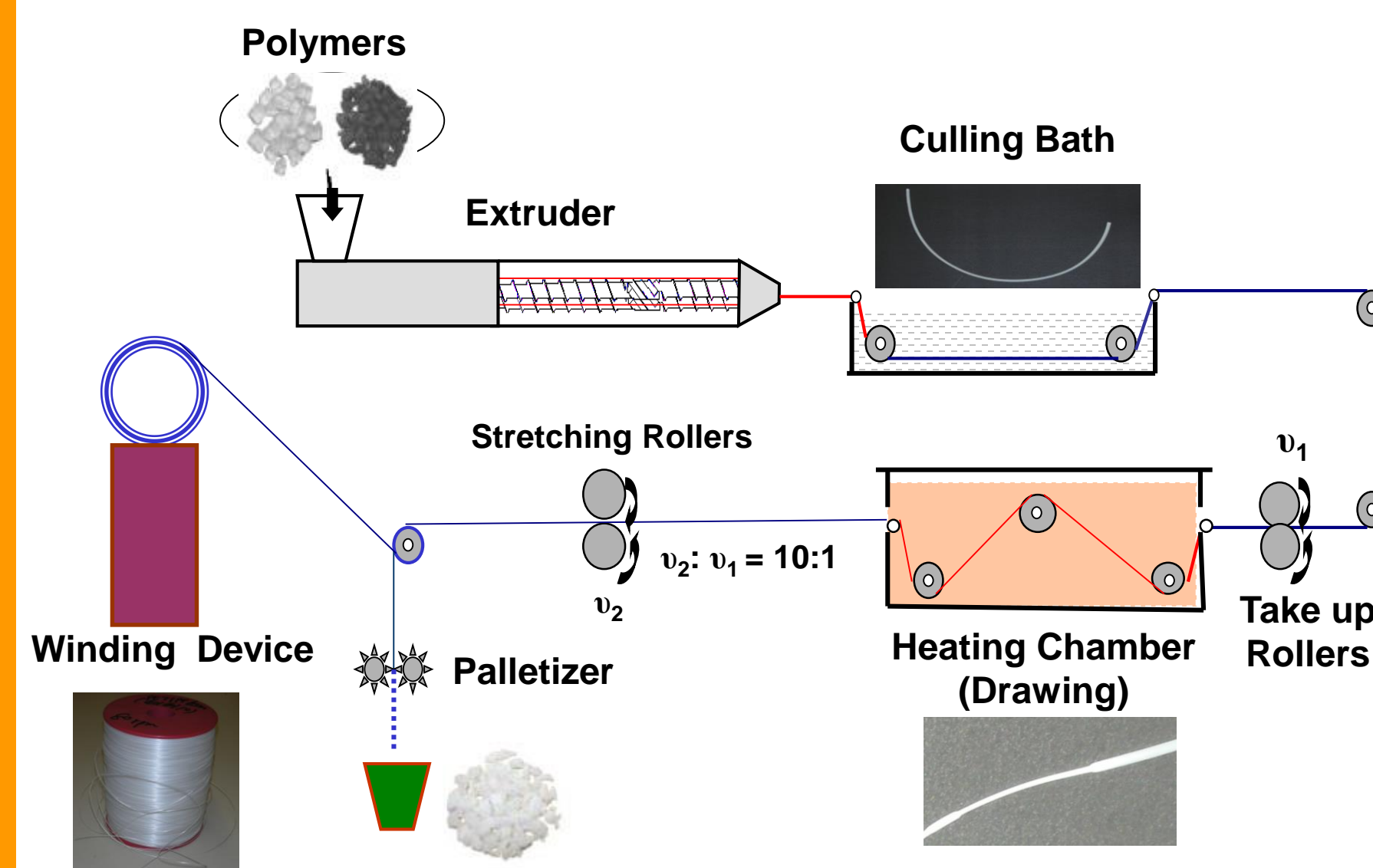
Sketch of the Mode for Obtaining of Isolated Polymer Fibrils from Drawn Polymer Blends



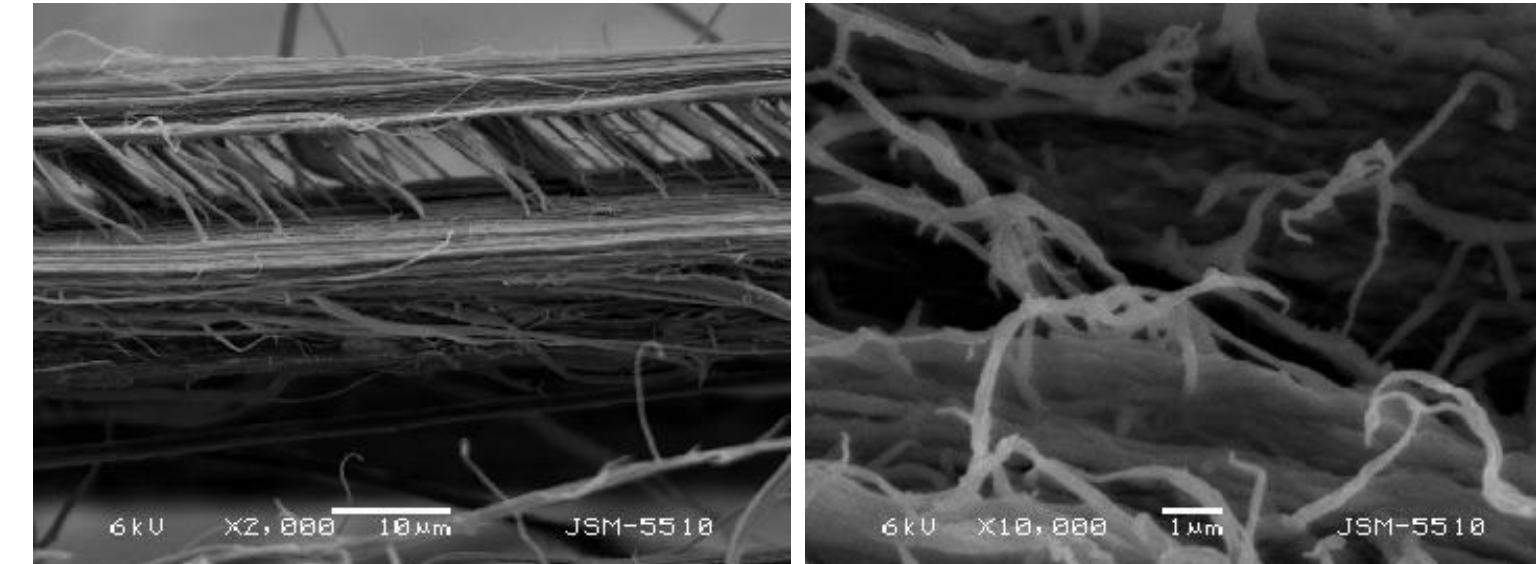
Materials and Methods

- Polylactic acid (PLA) - biodegradable
- Ethylene-co-vinyl alcohol EVOH – water soluble
- PLA/EVOH (30/70 and 40/60 by wt.) blends
- SEM observation and Mechanical test

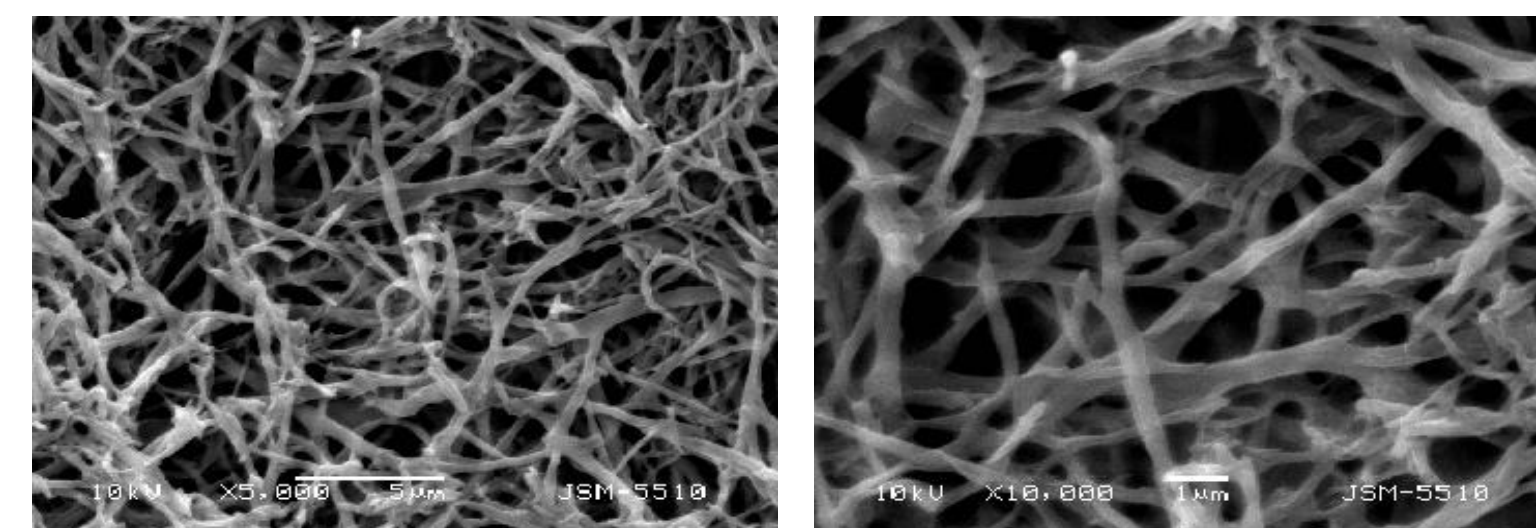
Schematic of Extrusion and Drawing Line (MFC Concep)



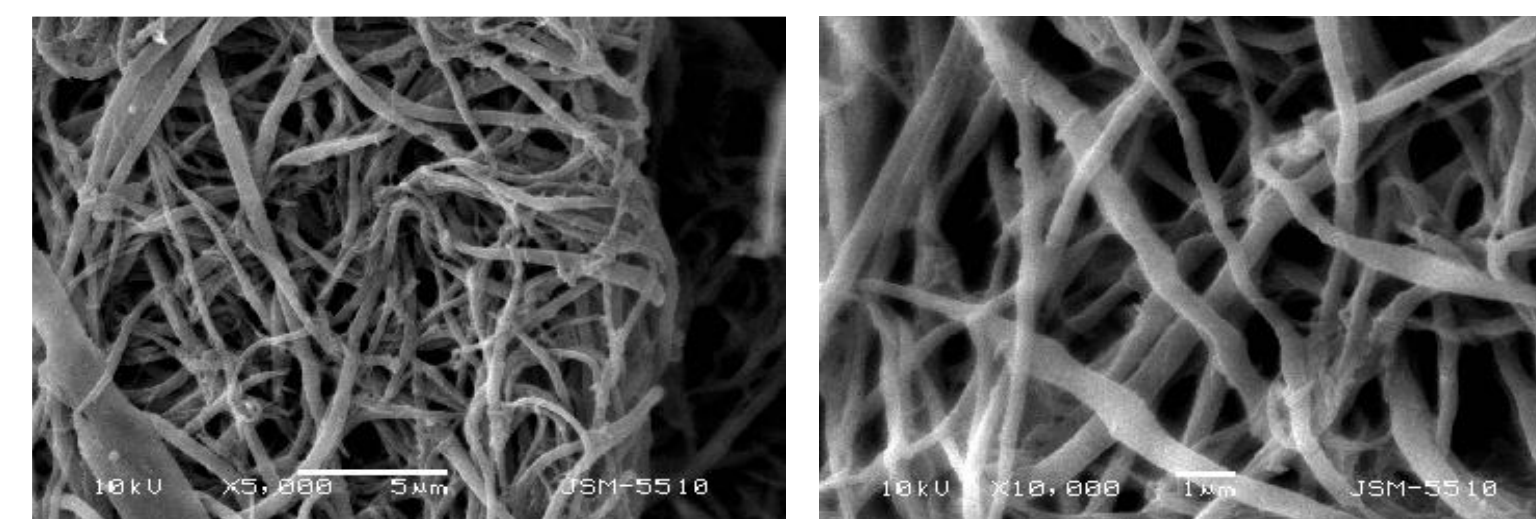
SEM Observation



Splited Drawn Blend



Scaffold Surface



Transverse Wiew

Results and Discussion

After drawing, both PLA and EVOH are transformed from isotropic into a highly oriented (fibrillated) state. The SEM observations of the slited fracture surfaces show a very well orientated PLA and EVOH fibrils with a high aspect ratio. The tensile modul and strength of the drawn blends were found to be about 300-500% higher than those measured for the neat PLA, EVOH and the extruded blends.

By means of selective dissolving of EVOH from the drawn blends with propanol/water mixture, bundles formed of individual PLA fibrils were isolated. The SEM observations shows that the length and the aspect ratio of the fibrils isolated from 40/60 wt.% blend is much higher than these of 30/70 wt.% one.

High porous 3-dimensional scaffolds from isolated PLA fibrils were manufactured by freeze-drying method. The morphological peculiarity of the scaffolds was observed by SEM. The diameter of the PLA fibrils are in the range of 150 nm to 1,5 µm, and the diameter of the scaffold pores vary between nano- and micro-scale.

Conclusions

In this study, high porous 3D scaffolds from PLA microfibrils, using PLA/EVOH orientated blends, were successfully produced. In the best of our knowledge this is the first successful attempt for manufacturing scaffolds applying a modified MFC concept.

Acknowledgement

The authors gratefully acknowledge the financial support of the MON, Fund Scientific Investigation (Project DTK 02-70/09) and Project BG051PO001/07/3.3.-02/51.

References

1. M. Evstatiev, S. Fakirov and K. Friedrich, *Polymer Composites: from Nano- to Macro scale*, Chap. 3. Kluwer Academic Publishers, Nowell, MA, USA, 2005.



S. Petrova^{a,c}, R. Riva^b, Ch. Jérôme^b, Ph. Lecomte^b and R. Mateva^c

^aInstitute of Polymers, Bulgarian Academy of Sciences, Acad. G. Bonchev str., bl. 103-A, 1113 Sofia, Bulgaria; ^bCenter for Education and Research on Macromolecules (CERM), University of Liège, Sart-Tilman, B6, B-4000 Liège, Belgium; ^cUniversity of Chemical Technology and Metallurgy, Department: "Polymer Engineering" 8 Kl. Ohridski, 1756 Sofia, Bulgaria

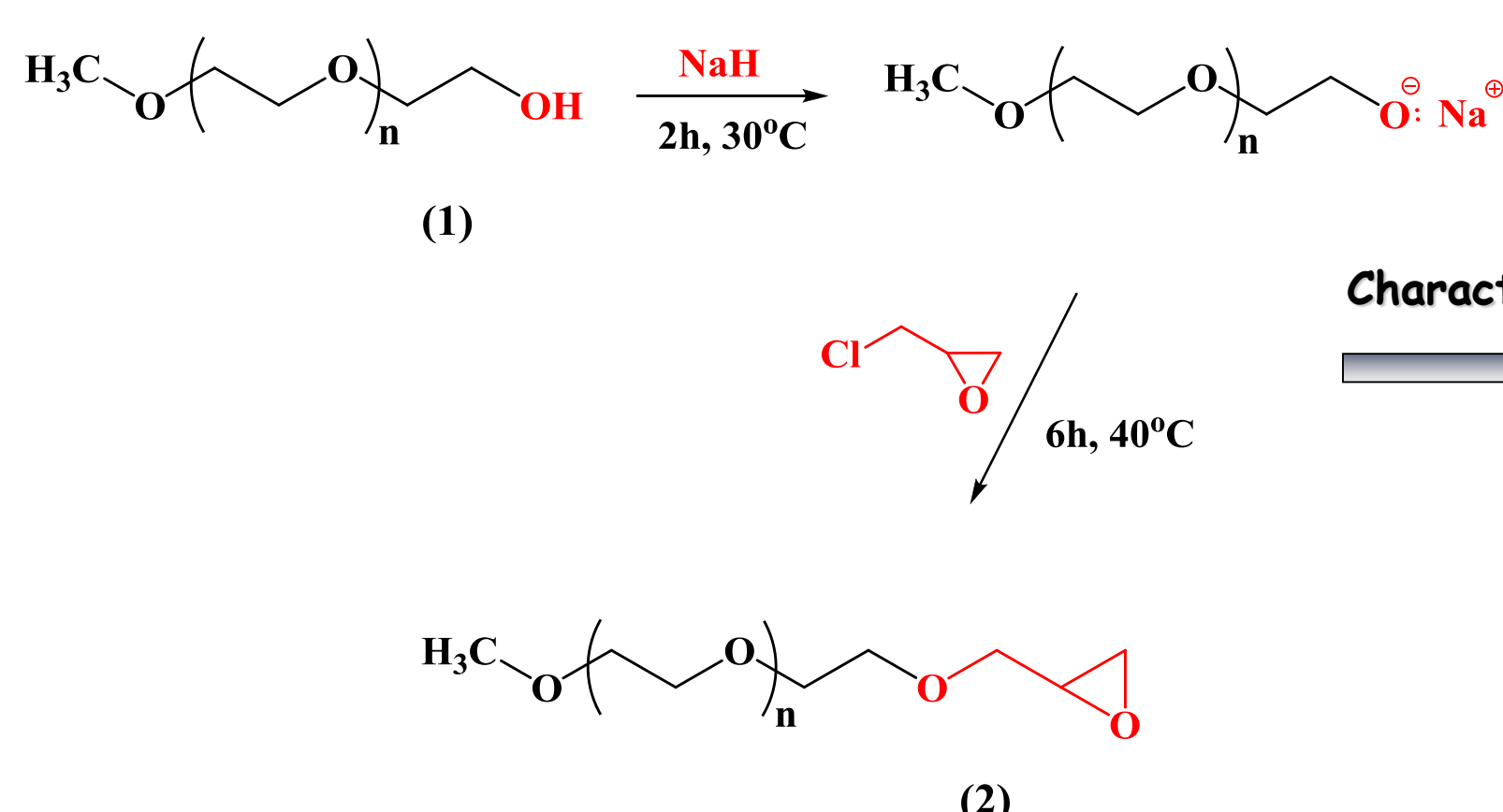
* E-mail address: s.petrova_81@yahoo.com

I. ABSTRACT

This work describes the synthesis of a novel amphiphilic AB₂ triarm star-shaped copolymers with A = non-toxic and biocompatible hydrophilic poly(ethylene oxide) (PEO) and B = biodegradable and hydrophobic poly(ε-caprolactone) (PCL). A series of AB₂ triarm star-shaped copolymers with different molecular weights for the PCL block were successfully synthesized by a three steps procedure. α-methoxy-ω-epoxy-poly(ethylene oxide) (PEO-epoxide) was first synthesized by nucleophilic substitution of α-methoxy-ω-hydroxy-poly(ethylene oxide) (MPEO) on epichlorohydrin. In a second step α-methoxy-ω,ω'-dihydroxy-poly(ethylene oxide) (PEO(OH)₂) macroinitiator was prepared by selective hydrolysis of the ω-epoxy end group of PEO-epoxide chain. Finally, PEO(OH)₂ was used as a macroinitiator for the ring-opening polymerization (ROP) of ε-caprolactone (ε-CL) catalyzed by tin octoate (Sn(Oct)₂). PEO-epoxide, PEO(OH)₂ and AB₂ triarm star-shaped copolymers were assessed by ¹H NMR spectroscopy, size exclusion chromatography (SEC) and MALDI-TOF. The behavior of the AB₂ triarm star-shaped copolymer in aqueous solution was studied by dynamic light scattering (DLS) and transmission electron microscopy (TEM).

II. SYNTHESIS AND CHARACTERIZATION OF THE AMPHIPHILIC TRIARM STAR-SHAPED BLOCK COPOLYMERS BASED ON PEO AND PCL

Synthesis of α-methoxy-ω-epoxy-poly(ethylene oxide) (2)



Characterization Techniques

$$M_n(\text{NMR}) = [(I_B/4)/I_A] \times 44 + 31 + 57 \quad (1)$$

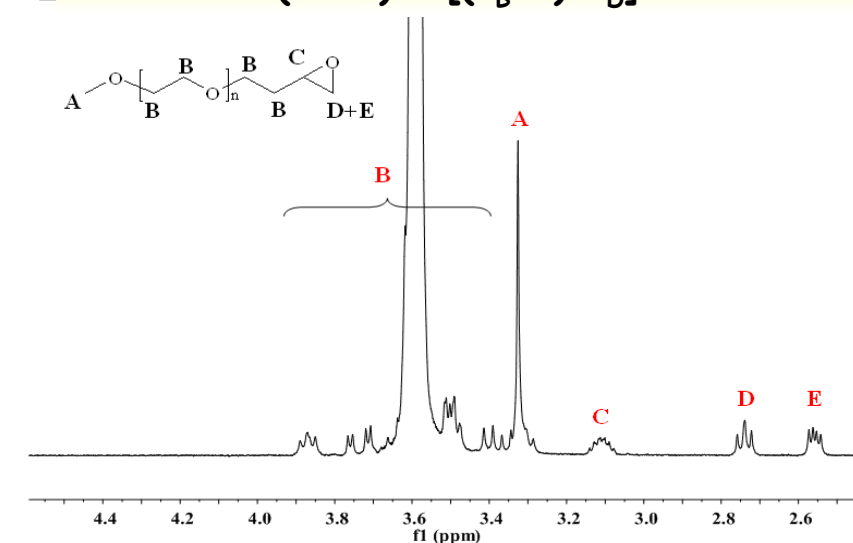


Figure 1. ¹H NMR spectrum of PEO-epoxide

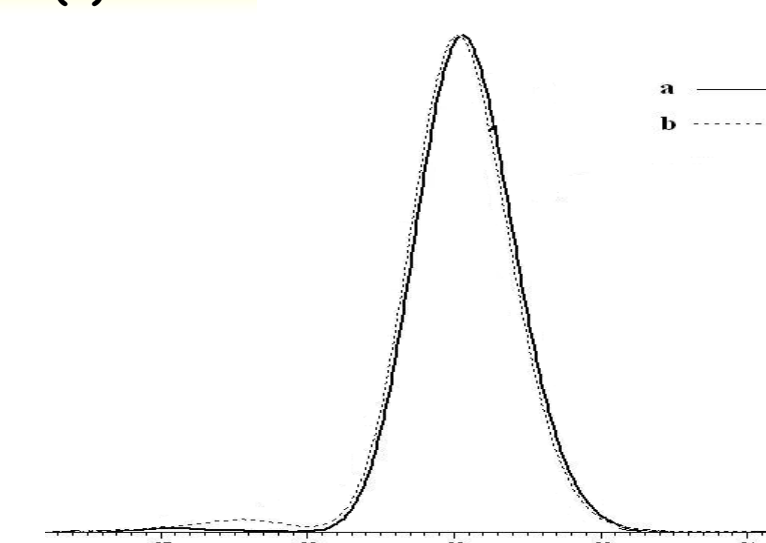


Figure 2. SEC curves of (a) MPEO (1a, in Table 1), (b) PEO-epoxide (1b, in Table 1)

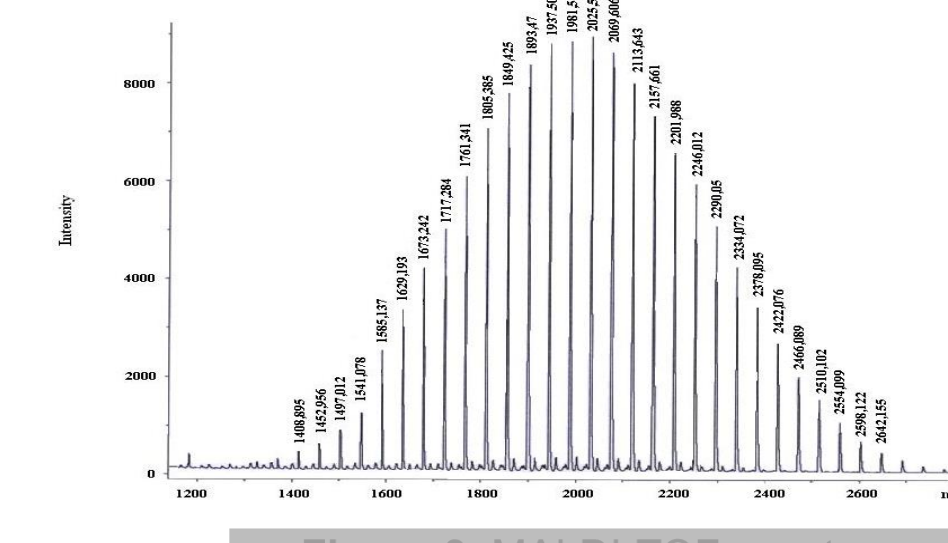
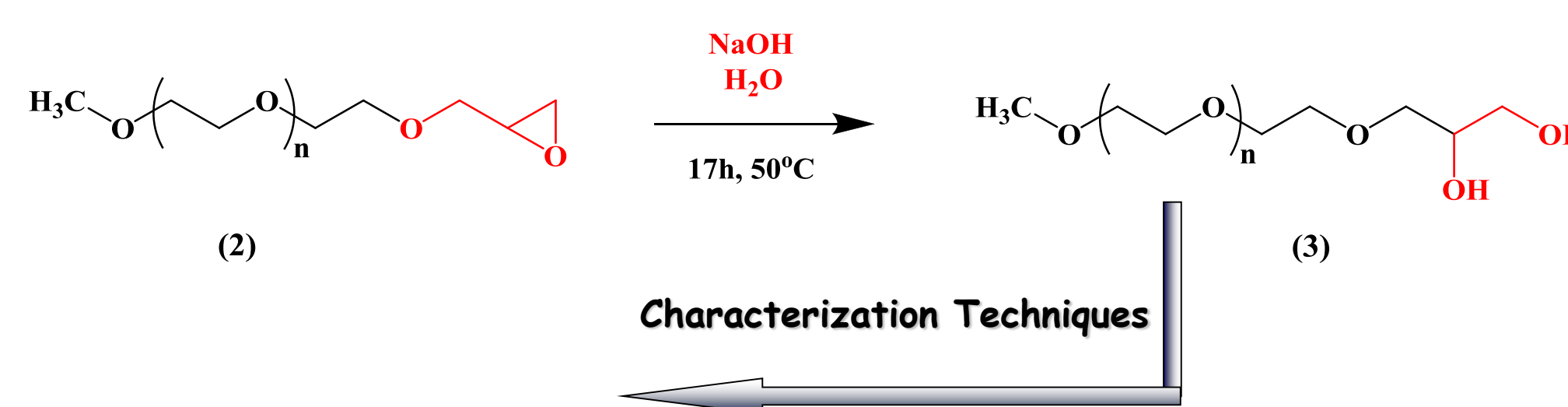


Figure 3. MALDI-TOF spectrum (linear mode) for PEO-epoxide

Synthesis of α-methoxy-ω,ω'-dihydroxypoly(ethylene oxide) macroinitiator (3)



Characterization Techniques

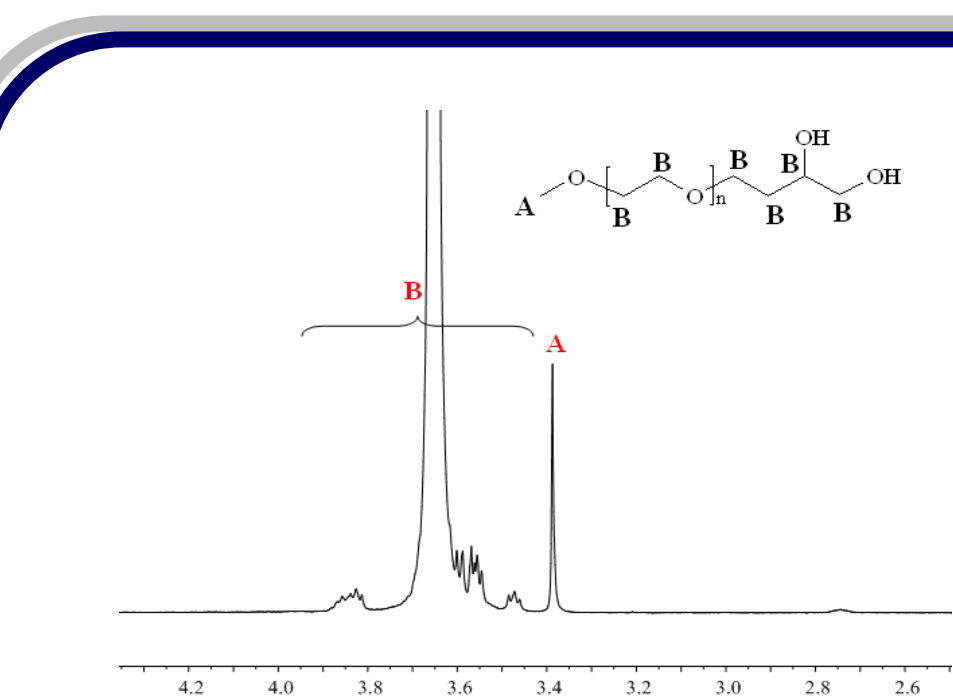


Figure 4. ¹H NMR spectrum of PEO(OH)₂

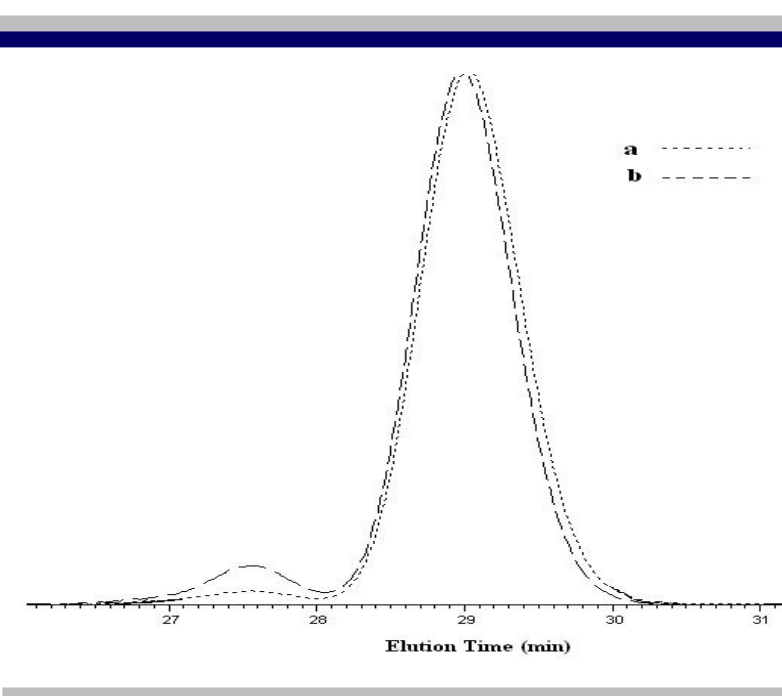


Figure 5. SEC curves of (a) PEO-epoxide and (b) PEO(OH)₂ (1b and 1c, in Table 1)

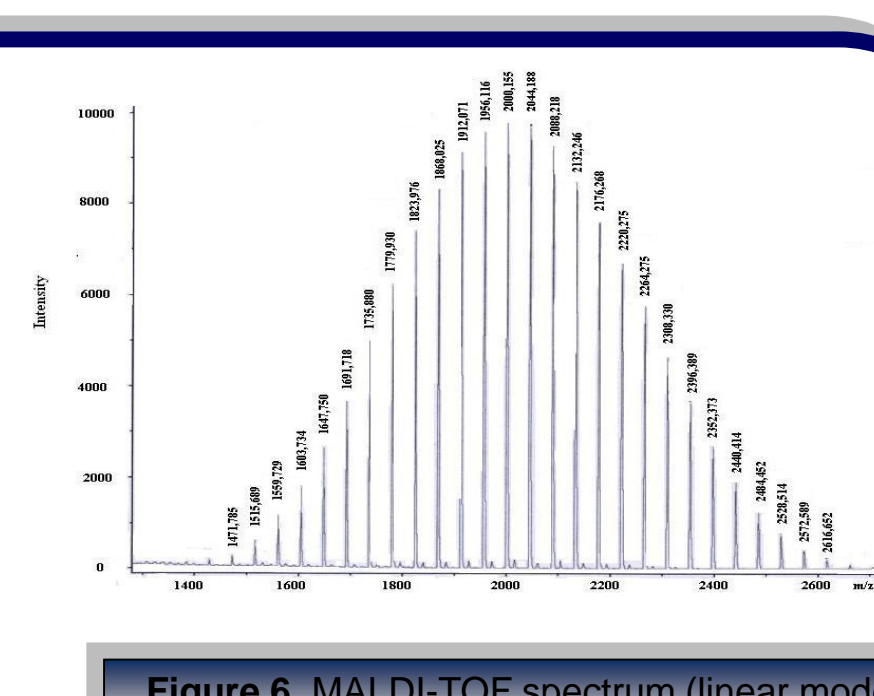
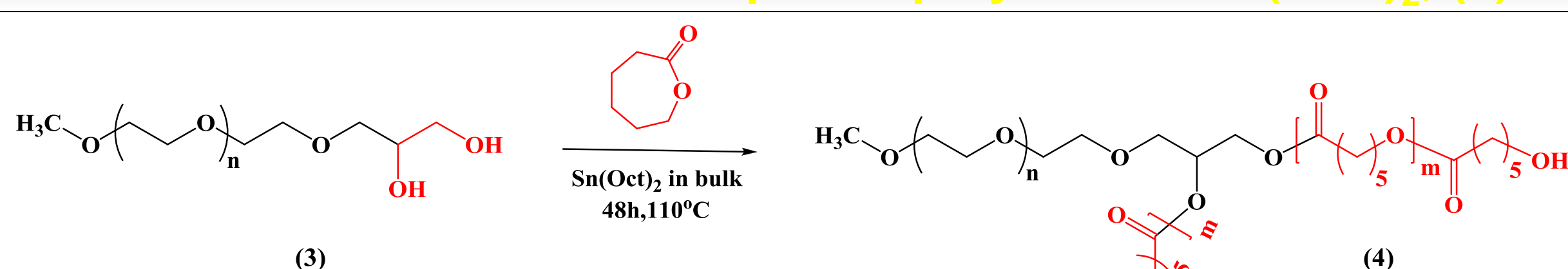


Figure 6. MALDI-TOF spectrum (linear mode) for PEO(OH)₂ macroinitiator

Synthesis of AB₂ triarm star-shaped copolymers PEO(PCL)₂ (4)



$$M_n(\text{NMR}) [\text{PEO}(\text{PCL})_2] = (I_A/2)/(I_B/4) \times dP_{\text{PEO}} \times 114.14 + M_n(\text{NMR}) \text{ PEO}(\text{OH})_2 \quad (2)$$

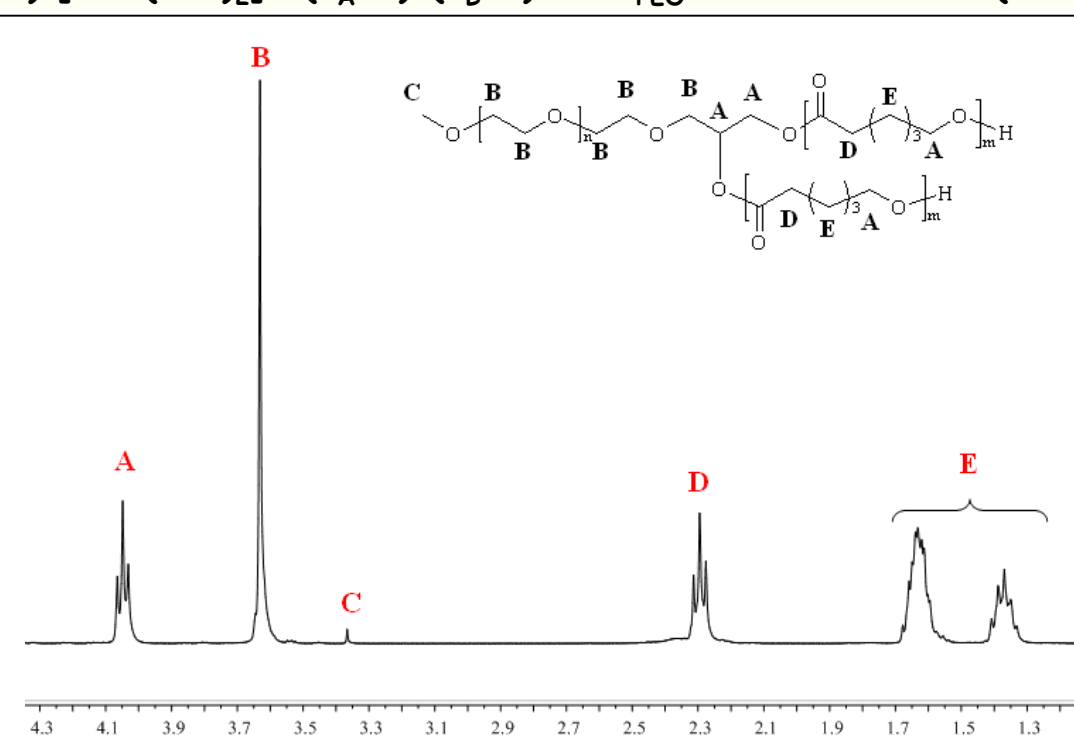


Figure 7. ¹H NMR spectrum for the [PEO(PCL)₂] star-shaped copolymer

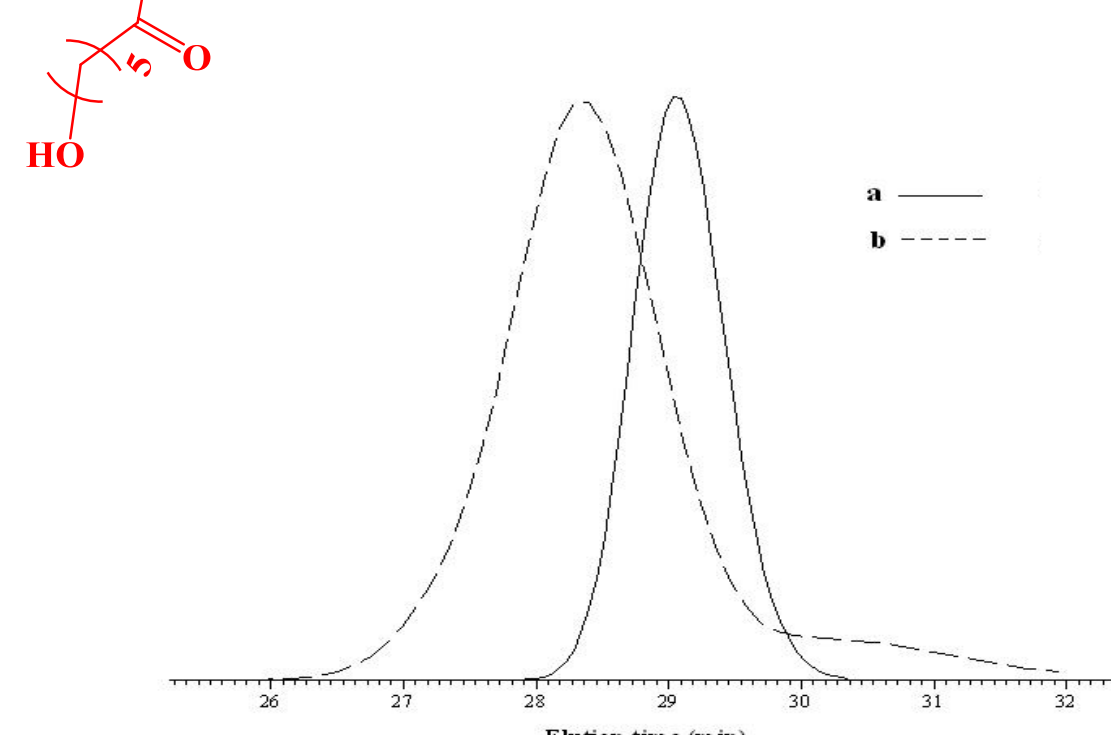


Figure 8. SEC curves of (a) [PEO(OH)₂] (1a, in Table 1), (b) [PEO(PCL)₂] triarm star-shaped copolymer (2a, in Table 2)

Table 1. Macromolecular characteristics of functional PEO

N ^o	Sample	Conv ^a , (%)	M _n ^b , (NMR)	M _n ^c , (MALDI-TOF)	M _n ^d , (SEC)	M _w /M _n ^e , (SEC)
1a	MPEO	/	2000	n.d.	1800	1.05
1b	PEO-epoxide	97	2100	2000	1900	1.05
1c	[PEO(OH) ₂]	97	1800	2000	2000	1.10

^a Conversion was calculated by ¹H NMR spectroscopy (Fig.1).

^b M_n was calculated by ¹H NMR spectroscopy according to Eq. 1.

^c M_n was determined by MALDI-TOF.

^d M_n and ^e M_w/M_n were determined by SEC calibrated with PEO standards.

Table 2. Characteristics of the AB₂ triarm star-shaped copolymers

N ^o	Sample	[M] ₀ /[I] ₀	M _n ^a (th)	M _n ^b (NMR)	M _w /M _n ^c (SEC)
2a	PEO(PCL) ₂ 1	4	3000	2700	1.10
2b	PEO(PCL) ₂ 2	8	4000	3700	1.35
2c	PEO(PCL) ₂ 3	17	6000	5700	1.10
2d	PEO(PCL) ₂ 4	26	8000	7500	1.30

^a M_n (th) = [M]₀/[I]₀ × M_{w,εCL} + M_n[MPEO(OH)₂]

^b M_n was calculated by ¹H NMR spectroscopy according to Eq. 2.

^c M_w/M_n was determined by SEC calibrated by PS standards.

III. MICELLIZATION

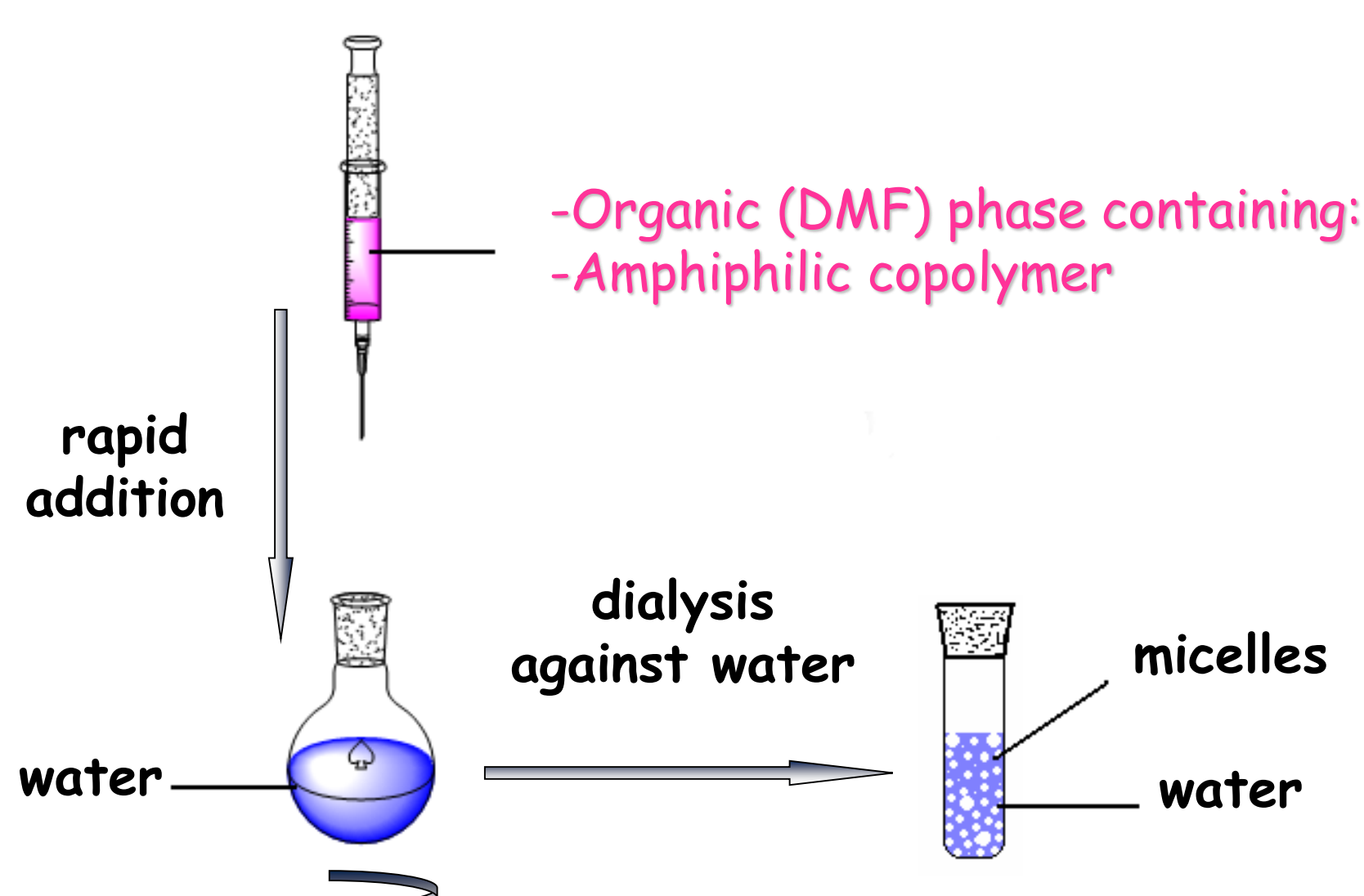
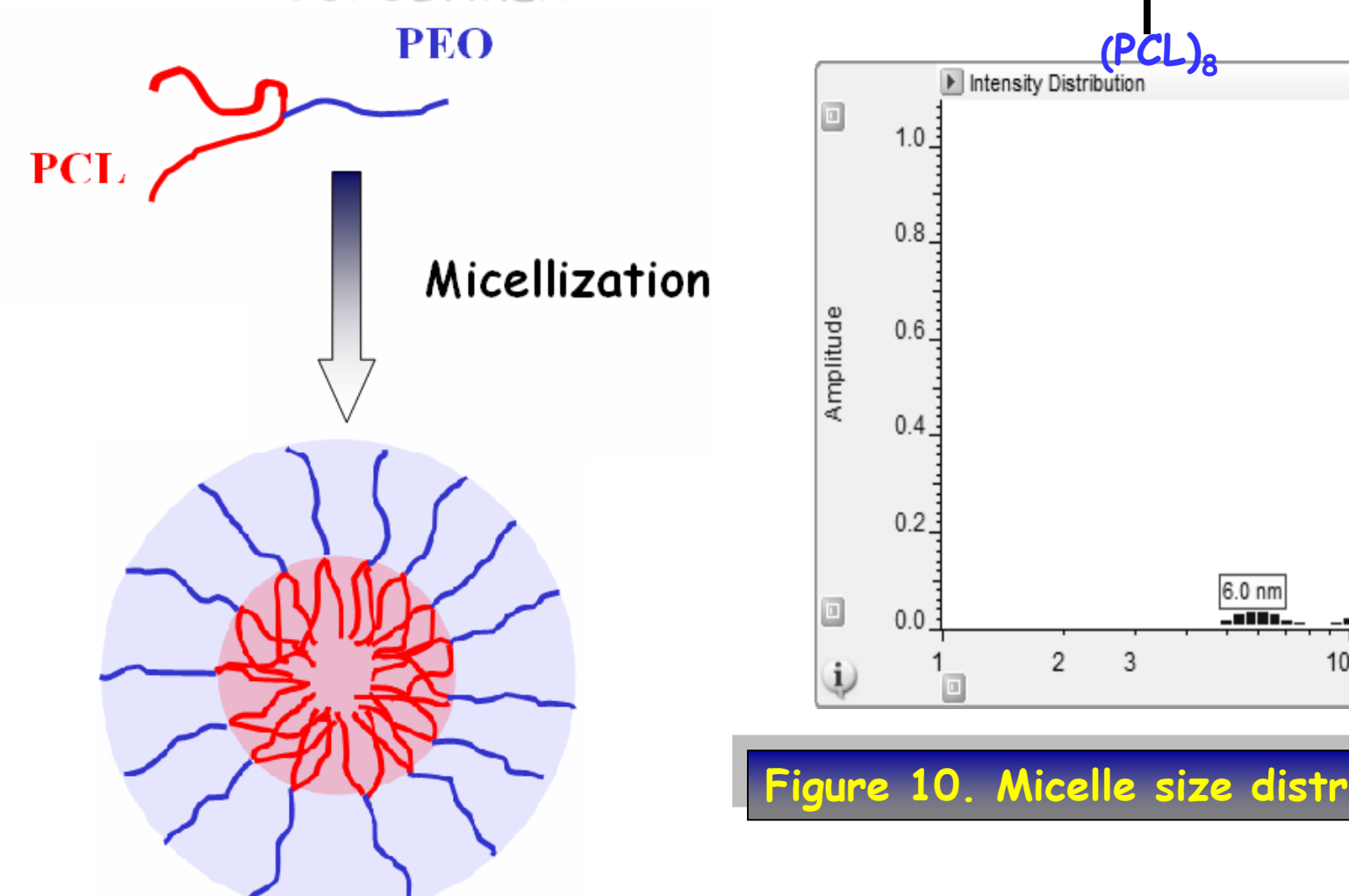


Figure 9. Schematic representation of micelles preparation by a dialysis against water

AB₂ TRIARM STAR-SHAPED BLOCK COPOLYMER



Petrova S, Riva R, Jérôme C, Lecomte Ph, Mateva R. Euro Polym Jnl 2009;45(12): 3442-3450.

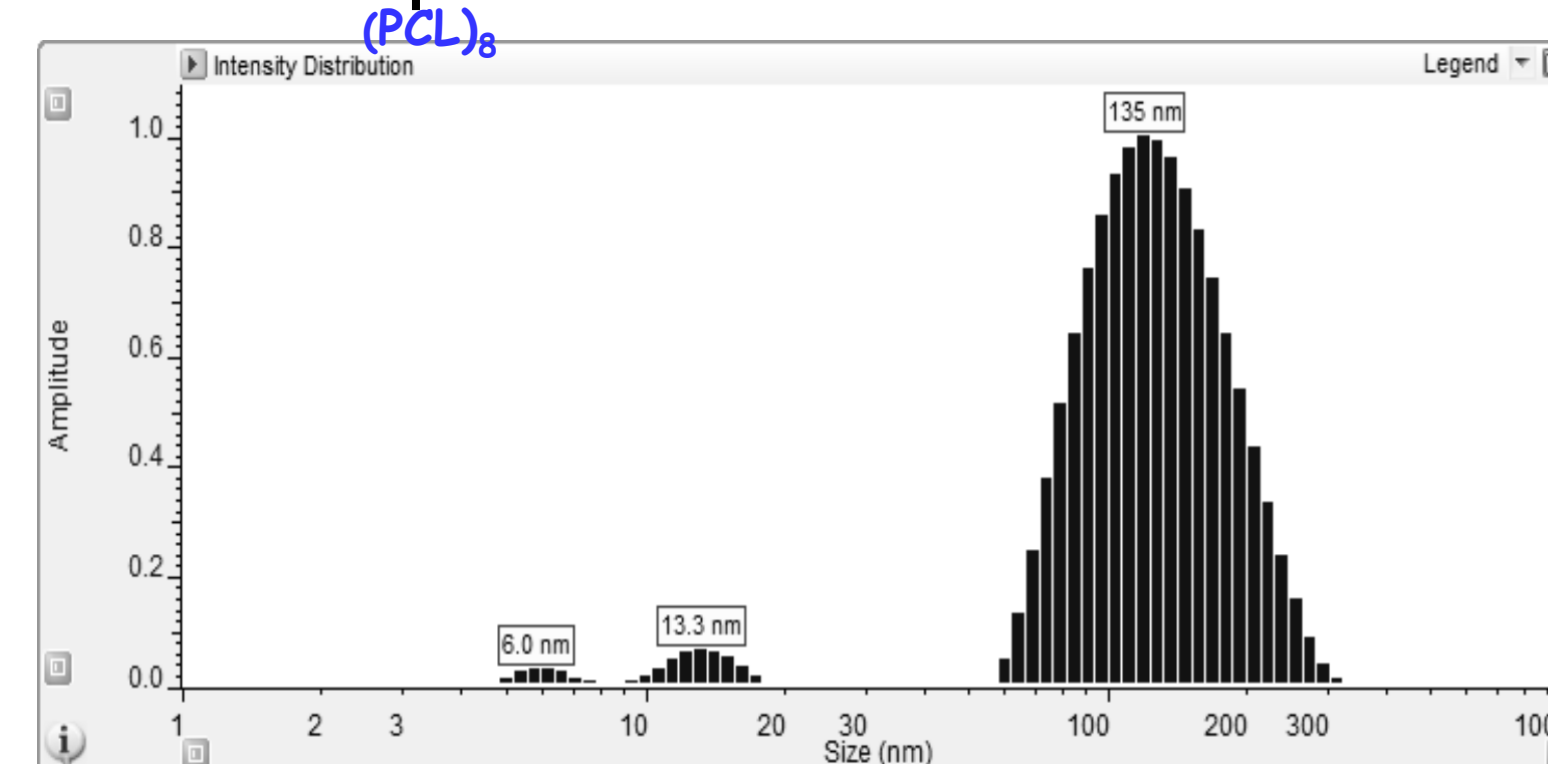


Figure 10. Micelle size distribution of [PEO(PCL)₂] (2b in Table 2)

Spherical Micelles

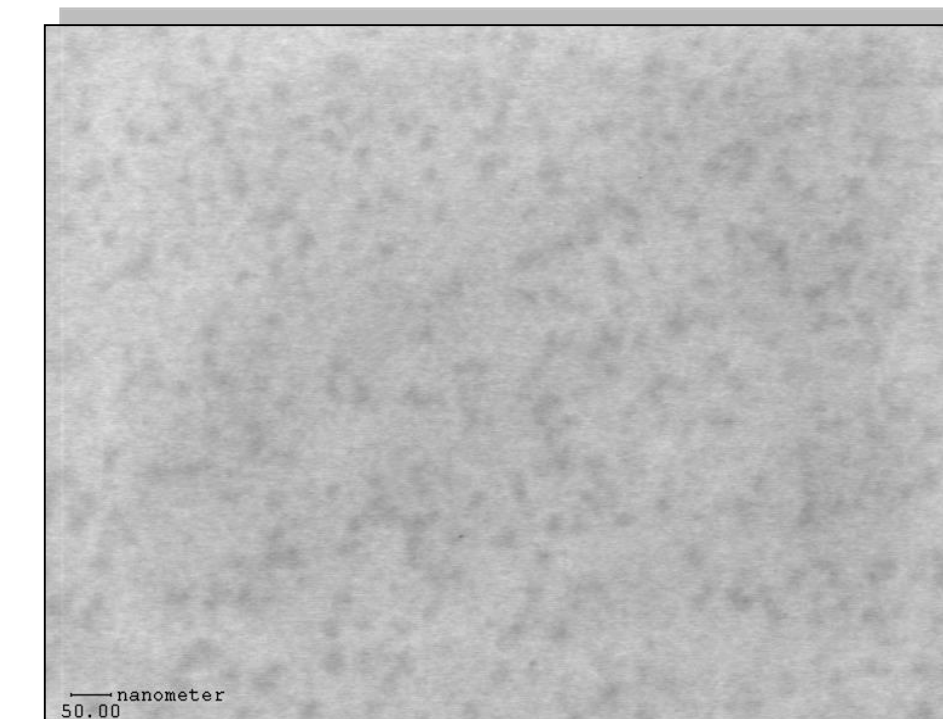


Figure 11. TEM image of micelle sample from [PEO(PCL)₂] star block copolymer solution (2b in Table 2)